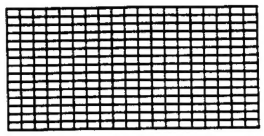

Materials Systems Inc.

MANUFACTURING DEMONSTRATION OF LARGE 1-3 PIEZOELECTRIC CERAMIC/POLYMER COMPOSITE PANELS USING CERAMIC INJECTION MOLDING

FINAL TECHNICAL REPORT

Office of Naval Research

Contract No. N00014-93-C-0104

Period of Performance

April 29, 1993 - September 30, 1994

Contractor:

Materials Systems Inc.

53 Hillcrest Road
Concord, MA 01742

TABLE OF CONTENTS

LIST OF FIGURES

LIST OF TABLES

ACKNOWLEDGMENTS

The successes achieved in this program are due in large measure to the skills, innovations, and enthusiasm of the Materials Systems technical team, which included Dan Fiore, Hong Pham, Bill Serwatka, Ken French, Rick Gentilman, and Les Bowen. The able support of our colleagues at the UMass-Lowell Department of Plastics engineering, Prof. Ross Stacer, Jan Andrusaitis, and Sandep Mehta, is greatly acknowledged.

Transducer testing, provided at no charge to the program, by Tony Medeiros of Raytheon and Fred Geil of Westinghouse is appreciated.

Our on-going collaborations with Bob Corsaro, Brian Houston, Bob Ting, and Tom Howarth of the Naval Research Laboratory were a major benefit to this program.

Finally, support and encouragement from Steve Newfield, Dick Vogelsong, and Wally Smith of the Office of Naval Research are greatly appreciated.

1.0 EXECUTIVE SUMMARY

The objective of this program was to manufacture a large area 1–3 piezo-electric composite transducer array for test and evaluation using the Materials Systems Inc. (MSI) ceramics injection molding technology. This program built upon the results of ONR Contract N00014-92-C-0010, in which a ceramics injection molding process and tooling for fabricating net shape 1-3 composite lead zirconate titanate (PZT) preforms was developed (Ref.1).

In this program, the PZT ceramic preform manufacturing process was scaled up and fabrication processes for 1-3 PZT-polymer composites and transducers were established and optimized. More than 1400 PZT preforms, such as that shown in Figure 1, were produced with a high overall process yield.

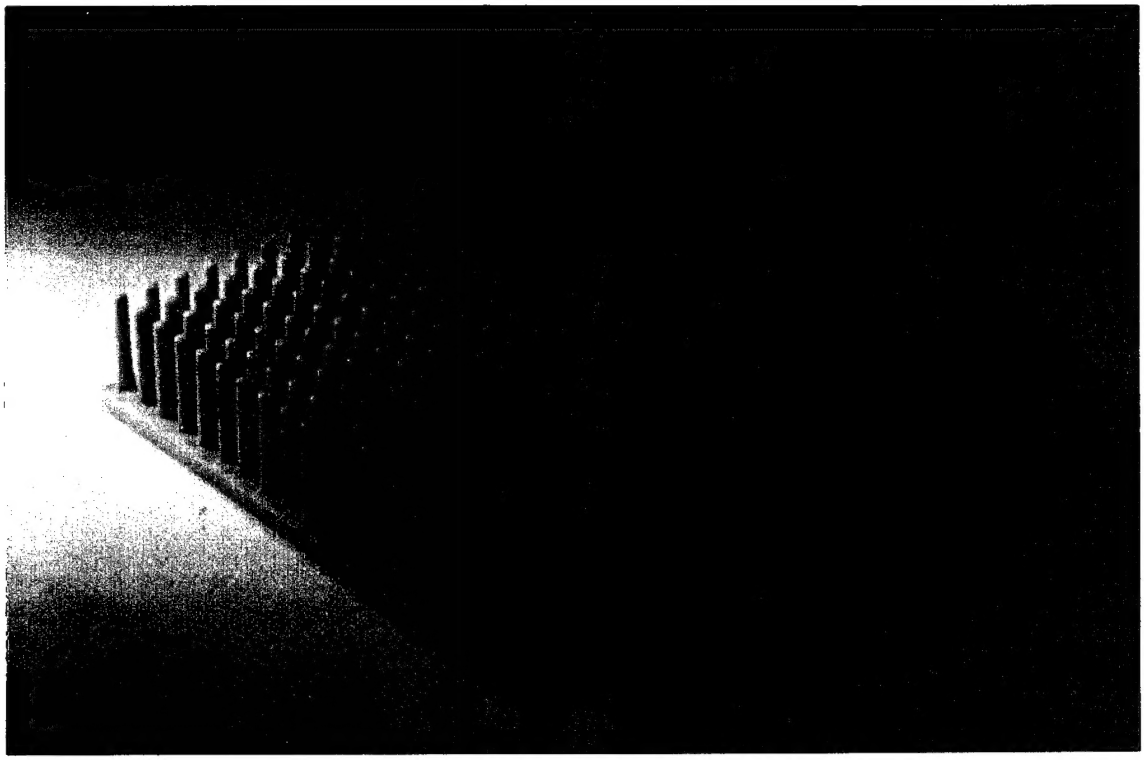

Figure 1. Sintered net-shape PZT preform, consisting of 361 PZT rods, each measuring 1.1 mm diameter and 7.9 mm long, on an integral base plate. More than 1400 identical injection-molded ceramic preforms were manufactured.

Cost-effective PZT-polymer composite material fabrication processes were developed and thirty-six (36) 250 x 250 x 6.3 mm composite sheets were manufactured. Thirty-two (32) 250 mm transducers, such as those shown in Figure 2, were made from the composite sheets. The detailed design of the transducers was optimized through an iterative collaboration with the Naval Research Laboratory.

Twenty-one final-design transducers were delivered to NRL for test and evaluation. Fifteen of these transducers were incorporated into a 3 x 5 array (Figure 3) as part of a system demonstration under ONR's ABC program.

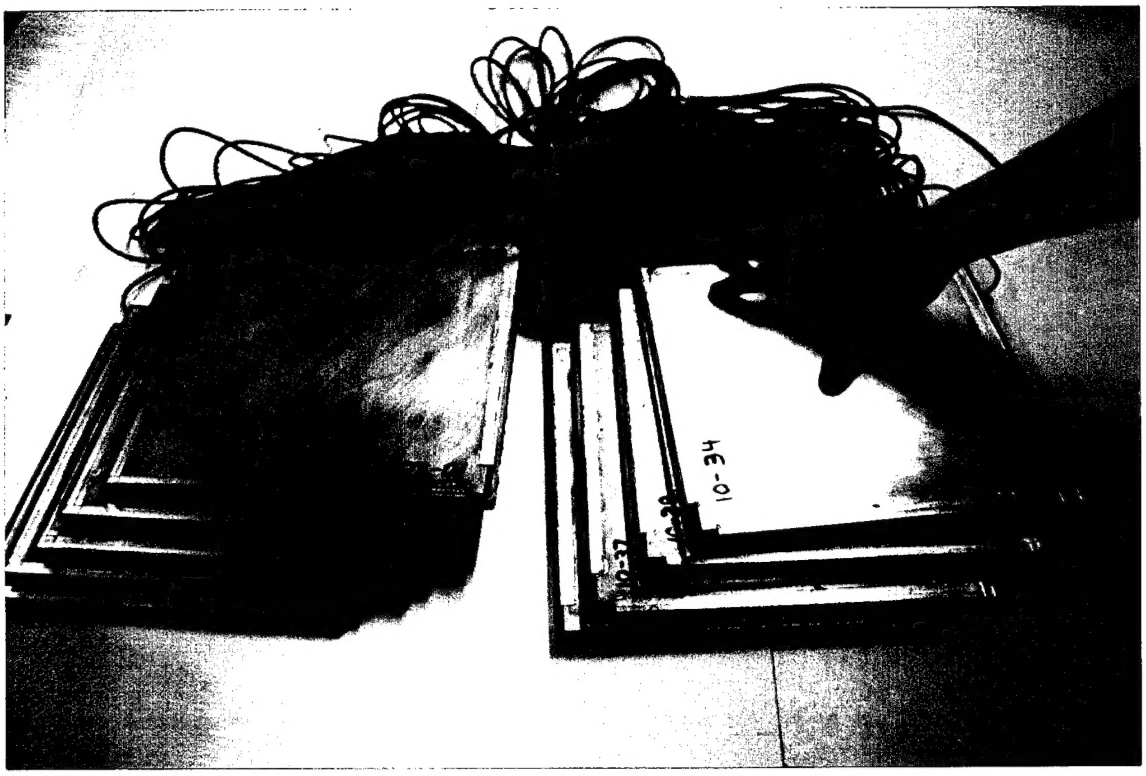

Figure 2. Several finished 250 mm SonoPanel transducers manufactured by MSI in this program.

For commercial purposes, MSI has designated this 1-3 transducer configuration as "SonoPanel"™ and is actively marketing this product for hydrophones, actuators, and undersea acoustic imaging applications.

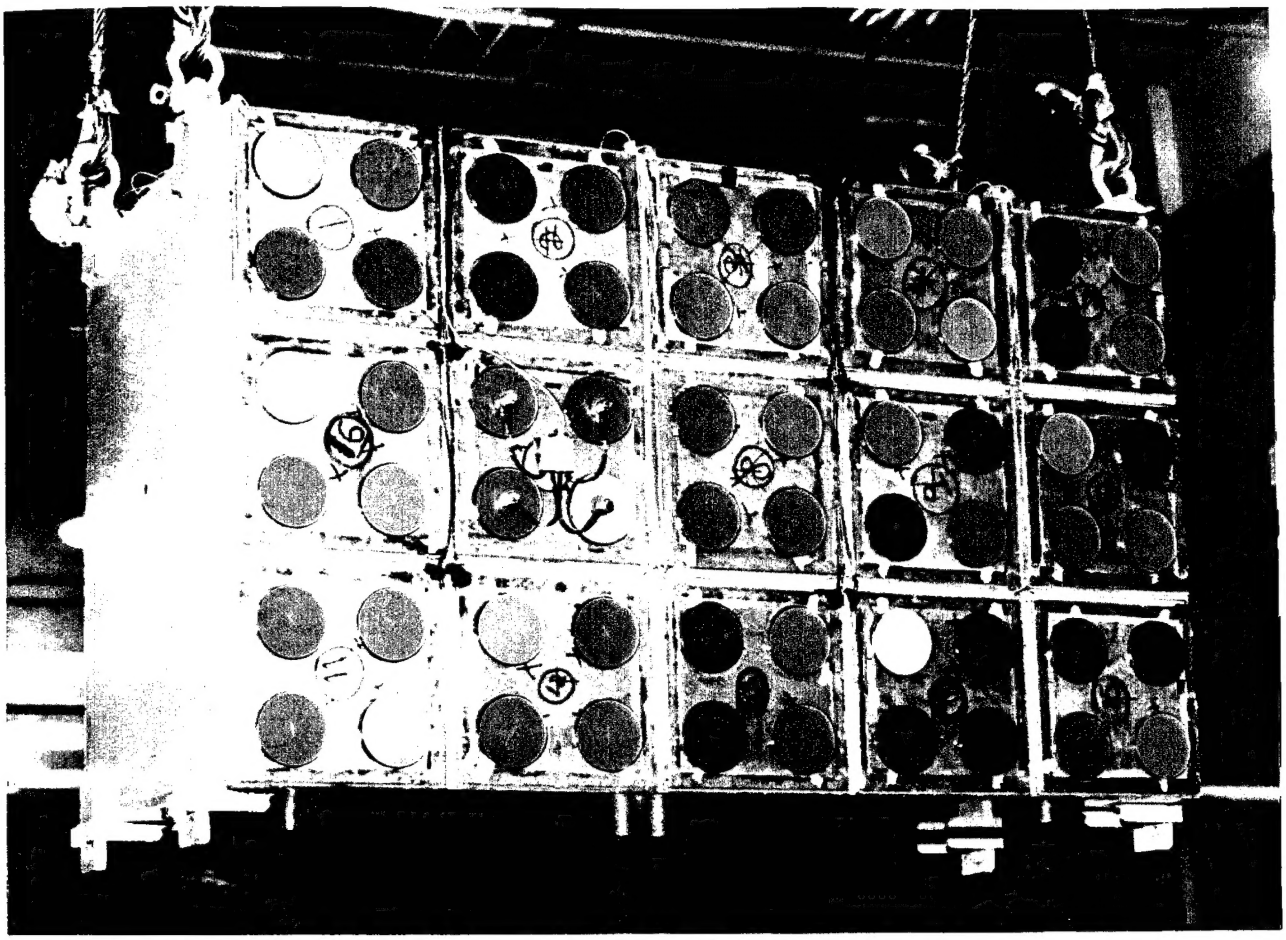

Figure 3. 3 x 5 array of SonoPanel transducers, integrated with pressure and acceleration sensors, on a steel backing structure prior to testing under the ONR ABC program. Assembly and testing of the array was carried out by the Naval Research Laboratory, Washington, DC.

2.0 TECHNICAL APPROACH

The manufacture of large area 1-3 PZT-polymer piezoelectric composite transducers at Materials Systems Inc. (MSI) consists of three major operations:

(1) PZT preform manufacture
(2) 1-3 composite fabrication
(3) transducer assembly.

Each major operation consists of a number of process steps, as shown in Figure 4.

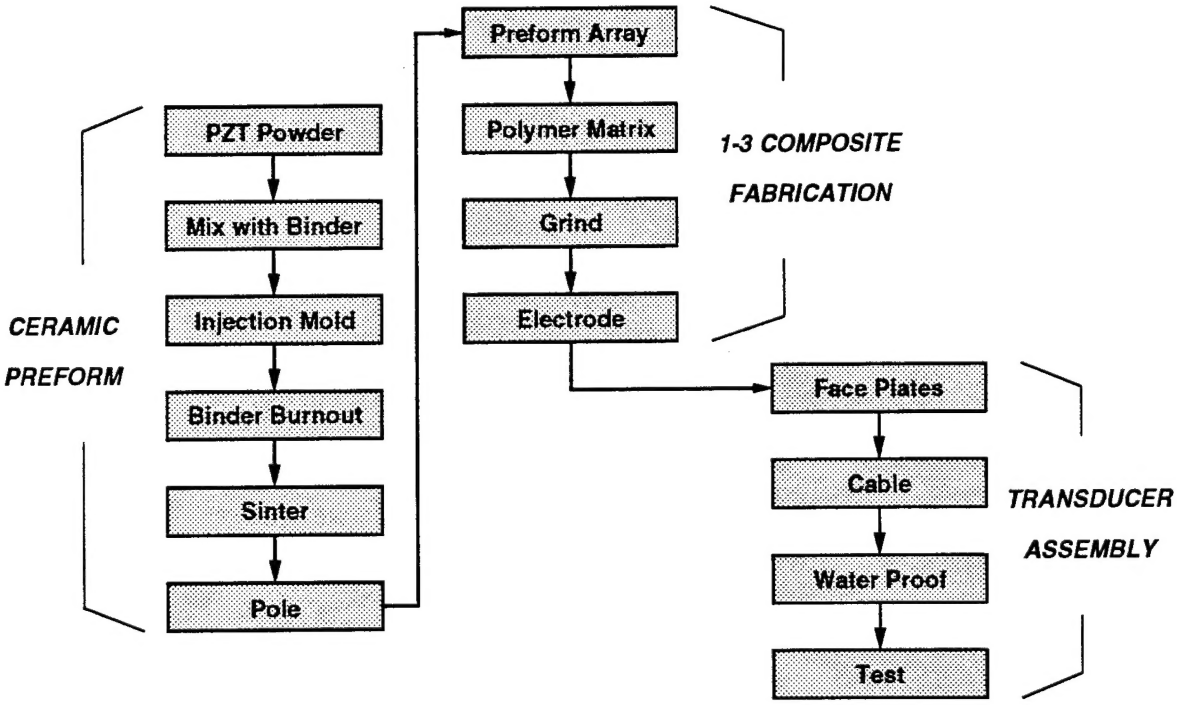

Figure 4. Process steps for manufacture of 1-3 composite transducers at Materials Systems Inc.

2.1 Ceramic Preform Manufacturing

Ceramics injection molding is the key technology for the PZT preform manufacturing operation. Commercially available PZT ceramic powder (Morgan Matroc PZT-5H, lot 128) was milled to adjust the powder properties for subsequent injection molding. The milled powder was then mixed (compounded) with a wax-based organic binder to form a homogeneous thermoplastic mixture. After compounding, the mix was granulated to a free-flowing state suitable for loading into the feed hopper of the injection molding machine. Thirty identical batches of compounded material, each containing approximately 4 kg of PZT powder, were prepared during this program.

Injection molding was accomplished using equipment and tooling similar to that used in the plastics industry. MSI's 15 ton, 1 ounce shot size Boy 15S injection molder was utilized for the program. This machine was adapted for ceramics injection molding by hard-facing the internal surfaces to avoid excessive wear and material contamination due to the abrasive nature of the PZT-wax mixture. The steel mold developed by MSI under Contract N00014-92-C-0010 was used to form the green net shape 1-3 preforms. Molding was accomplished in the semi-automatic mode, producing parts at a rate of approximately 1 per minute. Approximately 72 green parts were obtained from each batch of compounded material. A schematic description of the injection molding process used in this program is shown in Figure 5.

After forming, the green parts were fired in air to burn out the organic binder and then sintered at 1250°C for 1 hour in a PbO-rich atmosphere. The PbO-rich atmosphere controls the weight change of the parts during sintering, which has previously been shown to be correlated to the resulting piezoelectric coefficients. The sintered parts had a density of 7.51 ($\pm$0.02) g/cc. The dimensions of the sintered parts are given in Table 1.

Table 1: Dimensions of Sintered Injection-Molded PZT-5H Preform

Base plate	49.15 x 49.15 (±0.05) mm
Fiber length	7.9 mm
Fiber mid-point diameter	1.15 mm
Fiber spacing (center-to-center)	2.59 mm
Fibers per preform	361
PZT volume fraction	15%

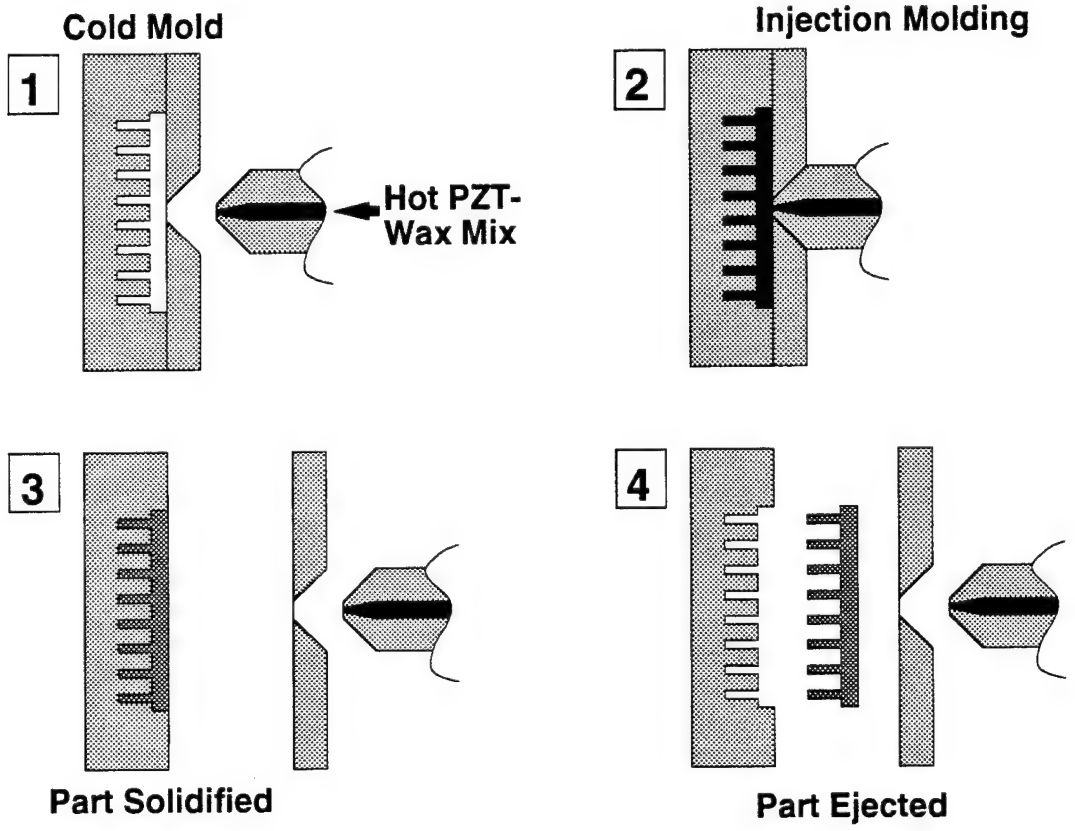

Figure 5. Schematic description of injection molding process used by MSI to produce net shape 1-3 ceramic preforms. (1) Hot wax-ceramic mixture in nozzle. (2) Injection of mix into mold. (3) Mix cools and forms solid part. (4) Net shape 1-3 preform is ejected from mold. This process is ideally suited for producing thousands of identical components.

Sintered injection-molded parts were provided by MSI to NRL-DC for microstructural examination (Ref.2). Microstructures were compared to those of other PZT-5H rods from other suppliers. The MSI material was observed to be free of macro and microscale voids and other defects and was found to have a uniform and fine grain microstructure. The absence of macro defects is due to the fact that injection molding is a "wet" process that results in a consistent and reproducible green microstructure, which converts to a high quality microstructure upon sintering.

The sintered parts were subsequently contact poled in oil at room temperature using flexible, temporary electrodes by applying a voltage of 11 kV for 5 minutes. This corresponds to a poling field of approximately 1.2 kV/mm (or 30 V/mil). Poling was performed on the sintered ceramic preforms to avoid risking dielectric breakdown in the finished 1-3 composite. Electrical breakdown during poling occurred in less than 0.2 percent of the preforms, attesting to the quality and uniformity of the injection molded material.

As a quality check, the d_{33} coefficient of randomly selected individual PZT ceramic rods was measured on ground and electroded 1-3 composite sheets. A Pennebaker model 8000 d_{33} meter was modified by MSI so that individual rods at any point on composite sheets as large as 300 mm square could be measured. The d_{33} values measured on finished composite sheets averaged 657 $x10^{-12}$ m/V with a standard deviation of 9.6 percent. Towards the end of the program, systematic variations in the d_{33} values were discovered and subsequently traced to the specific geometry and ceramic preform arrangement used during sintering. As a result of this discovery, a sintering study was performed and minor process changes made, yielding an average d_{33} coefficient of 659 $x10^{-12}$ m/V with the standard deviation reduced to 5.3 percent. In addition, the systematic variations were largely eliminated. PZT preforms made with the improved sintering process were used in the final four 250 mm transducers delivered in this program (10-40 through 10-43).

In order to meet the manufacturing demonstration requirements of this program, MSI successfully scaled-up several aspects of the preform manufacturing process by putting new and/or additional equipment and fixturing into service. The initial and final scale of each process step, expressed in terms of parts per batch, are given in Table 2.

Table 2: Number of Parts Produced per Batch in Various Steps of Preform Manufacturing

Step	Prior to Scale-Up	After Scale-Up
Milling	8	160
Compounding	80	80
Binder Burn-Out	8	60
Sintering	4	24

After the scaled-up equipment and procedures were put in place, MSI began its ceramic production run for this program in August 1993 and achieved the planned production rate of 120 sintered parts per week within 4 weeks time. More than 1400 finished PZT preforms were produced Several hundred of the preforms are shown in Figure 6. A unique identification code was assigned to each PZT preform and written on the bottom of the part. The code provides full tracibility of each part, including powder batch, molding run, and sintering run, for quality control purposes.

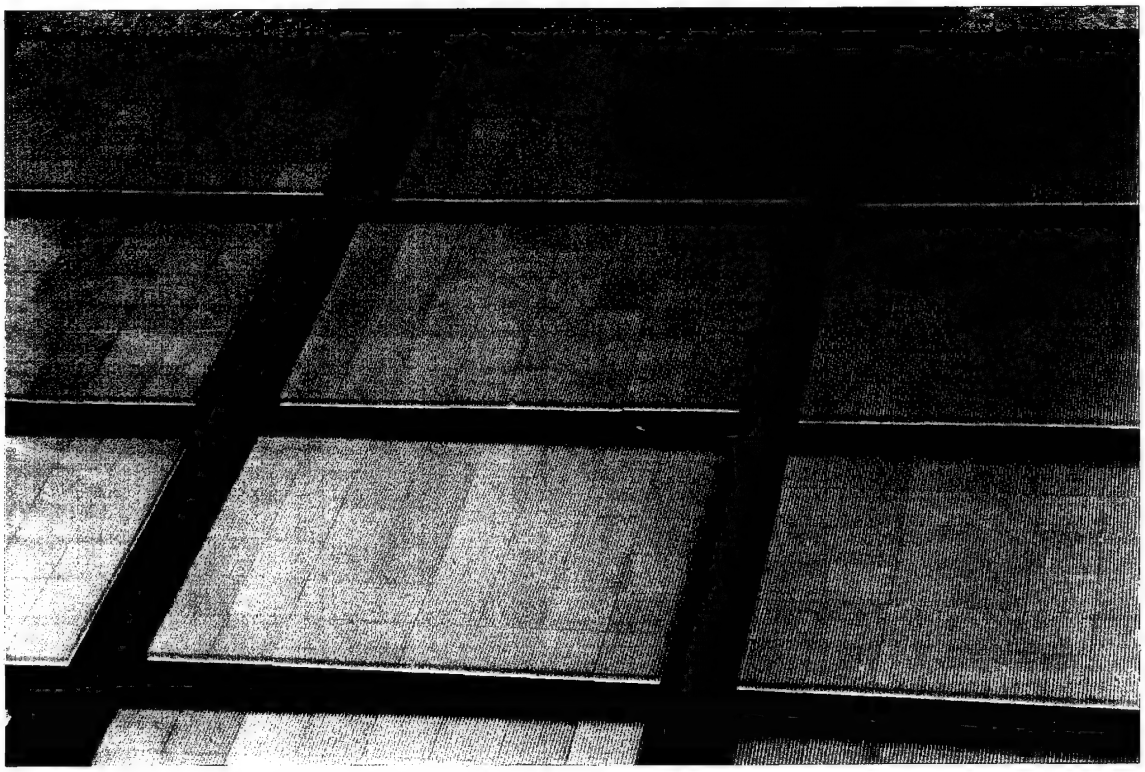

Figure 6. Approximately 300 identical sintered net-shape PZT preforms produced by Materials Systems Inc.

2.2 1-3 PZT-Polymer Composite Fabrication

PZT-polymer composite sheets were fabricated by laying out a square array of poled PZT preforms, typically 25 preforms to make a 250 mm square sheet of composite, as shown in Figure 7. The locations of the preforms in the layout were recorded with their identification numbers to maintain tracibility for quality control purposes.

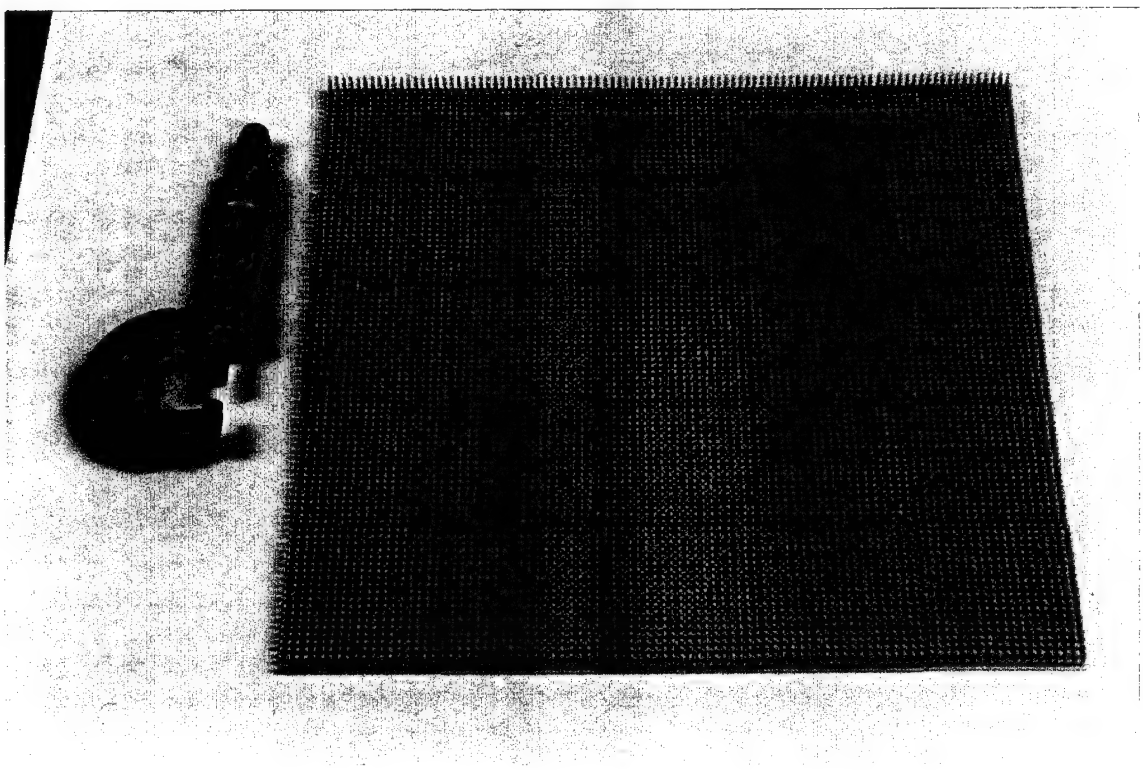

Figure 7. Twenty-five sintered and poled PZT preforms arranged in a square array ready for incorporation into a 250 mm 1-3 composite sheet.

The preform array was then covered with castable polymer as shown schematically in Figure 8. The polymer selected by ONR to be used for this program was EN-2 two-part polyurethane (Conap Inc, Olean, NY) containing 40 volume percent (approximately 3 wt.%) Expancel 551 DE polymer microspheres (Expancel, Marietta, GA). The microspheres were uniformly mixed with the polyurethane. The mixture was then de-aired and poured over the ceramic preforms until they were completely submerged. The voided polyurethane was allowed to cure overnight before the composite was de-molded.

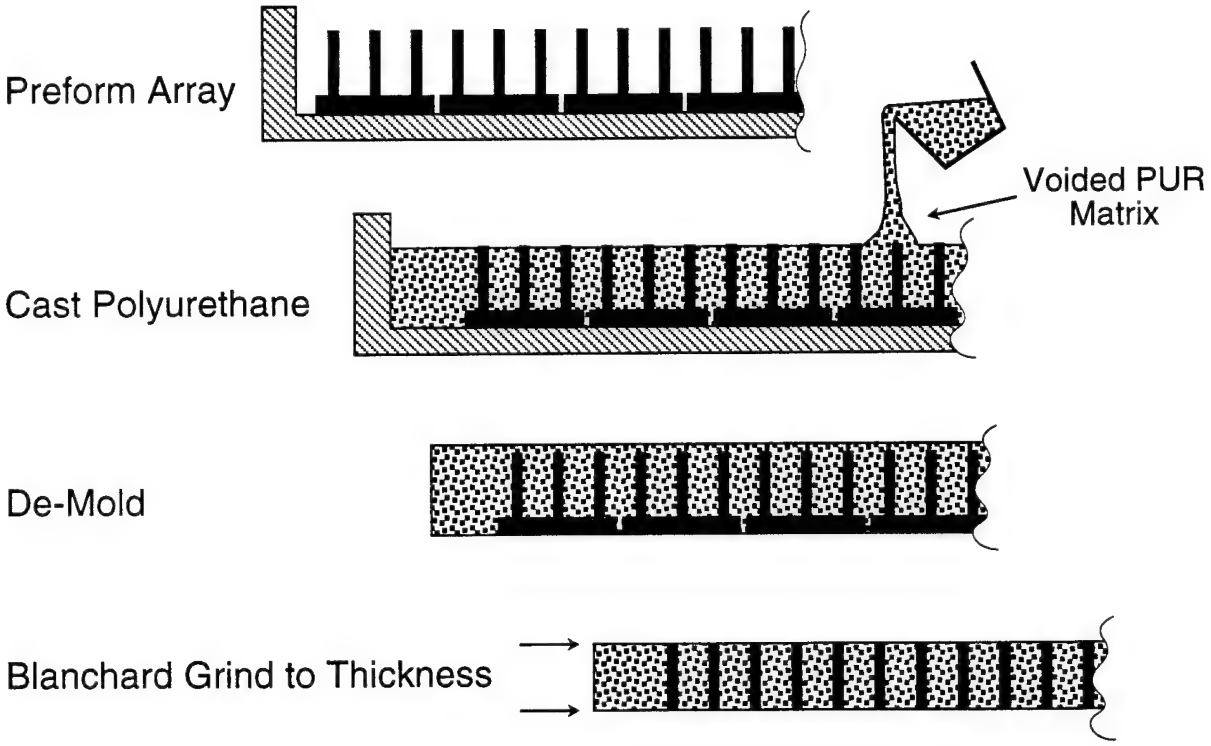

Figure 8. Schematic description of the 1-3 composite fabrication technique utilized by MSI.

Figures 9 and 10 show the top and bottom of an as-cast 250 mm square composite. A permanent reference mark was applied at the edge of the composite to indicate preform location and poling direction. Each composite sheet was also assigned a unique serial number.

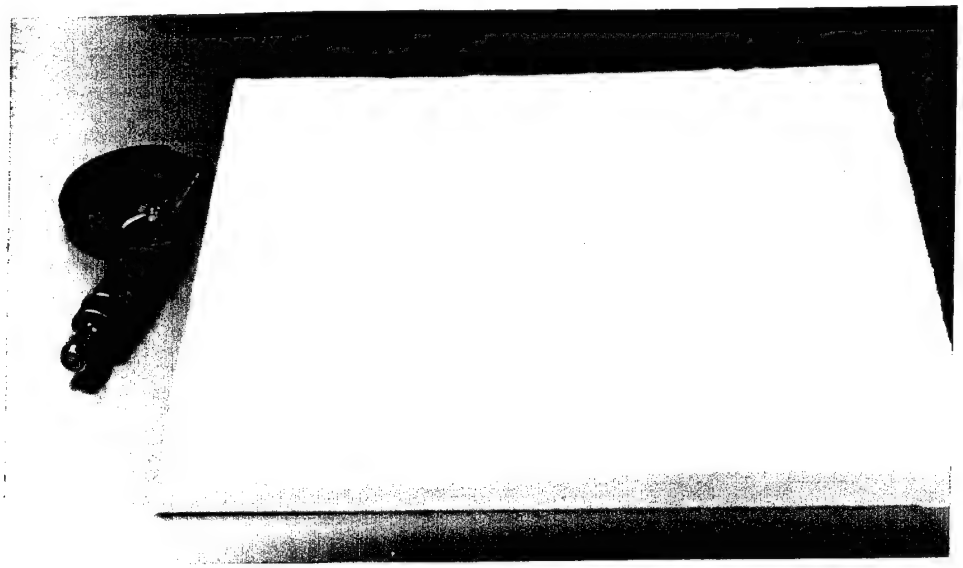

Figure 9. As-cast 250 mm 1-3 PZT-polymer composite sheet - top surface.

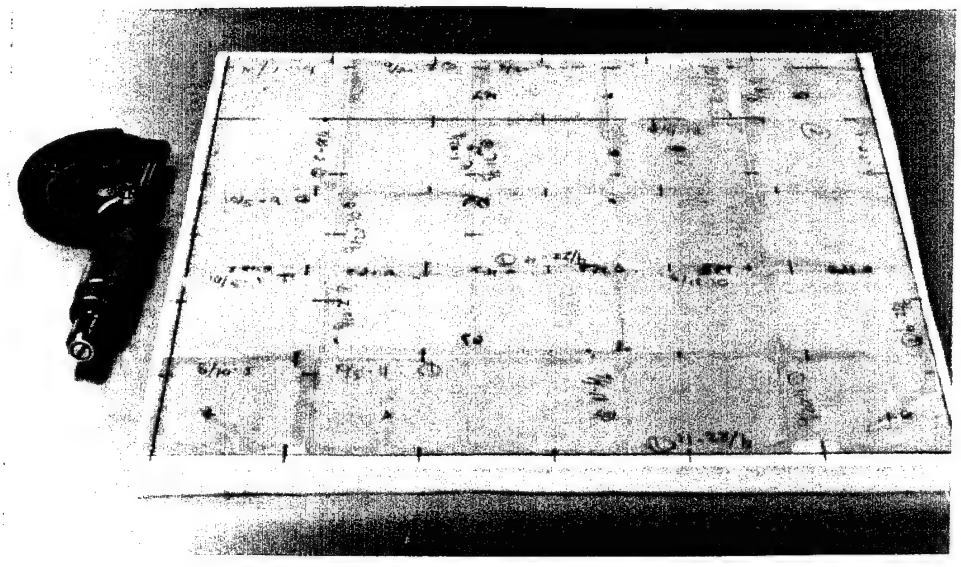

Figure 10. Bottom surface of as-cast 250 mm 1-3 PZT-polymer composite sheet, showing the ceramic base plates each marked with its unique identification number.

The cast composite was ground flat and parallel to a thickness of 6.38 ($\pm$0.15) mm by Blanchard grinding. This operation removes the ceramic base plates and exposes the ends of the 9025 PZT rods on both surfaces. Blanchard grinding was performed as an outside service at one of two local vendors qualified by MSI. All ground composite sheets were then carefully inspected by MSI for proper dimensions and surface finish prior to further processing. Figure 11 shows a close-up photograph of a portion of the ground composite sheet.

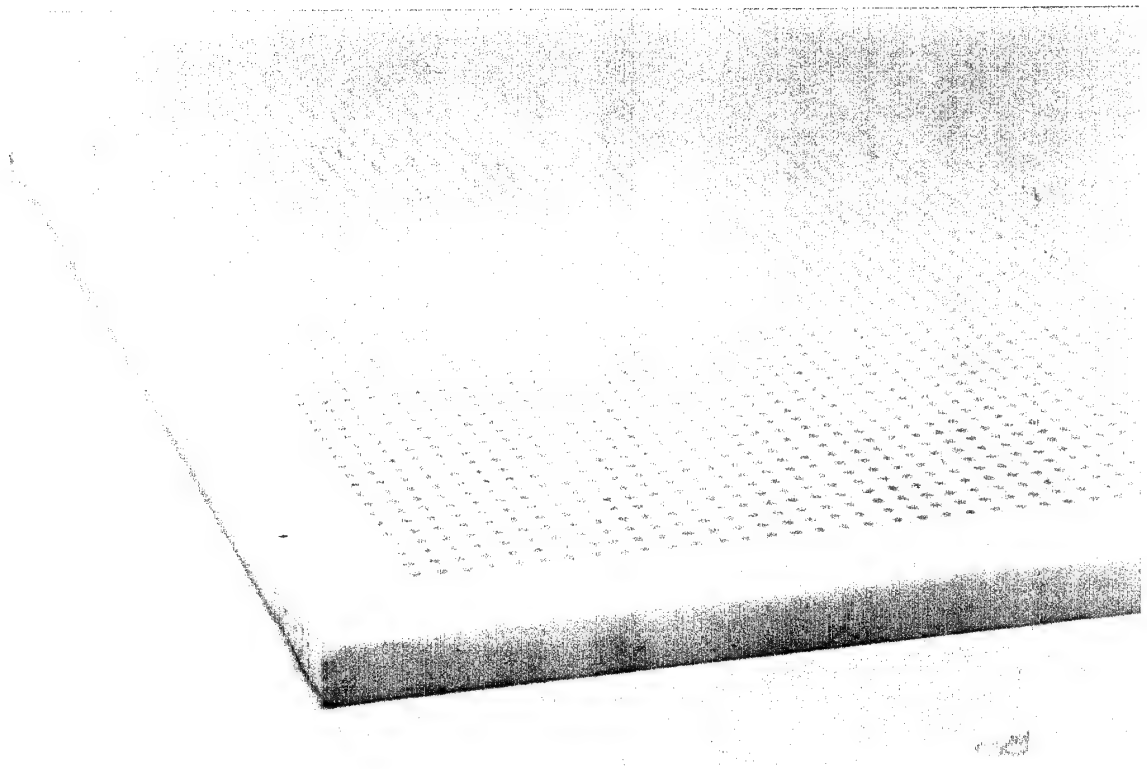

Figure 11. Close-up view of Blanchard-ground surface of 1-3 composite sheet.

A total of thirty-six (36) 250 mm 1-3 composite sheets were manufactured during the present program. In addition, one 250 mm composite sample was made as a demonstration with the ceramic preform base plates still attached.

The static and dynamic mechanical properties of the voided polyurethane were measured in a research program at the Department of Plastics Engineering of the University of Massachusetts Lowell (Ref.3). The static tensile modulus and Poisson's ratio were measured using an Instron tester on rectangular bar shaped samples of EN-2 polyurethane containing various amounts of Expancel microspheres. The static modulus and Poisson's ratio as a function of microsphere content are shown in Figure 12. It is seen that the Poisson's ratio decreases from 0.43 to 0.37 and the modulus increases by approximately 50 percent as the microsphere content increases from 0 to 50 volume percent. These measurements, as well as other polymer materials support activities carried out by UMass-Lowell under subcontract, are described in more detail in Appendix A.

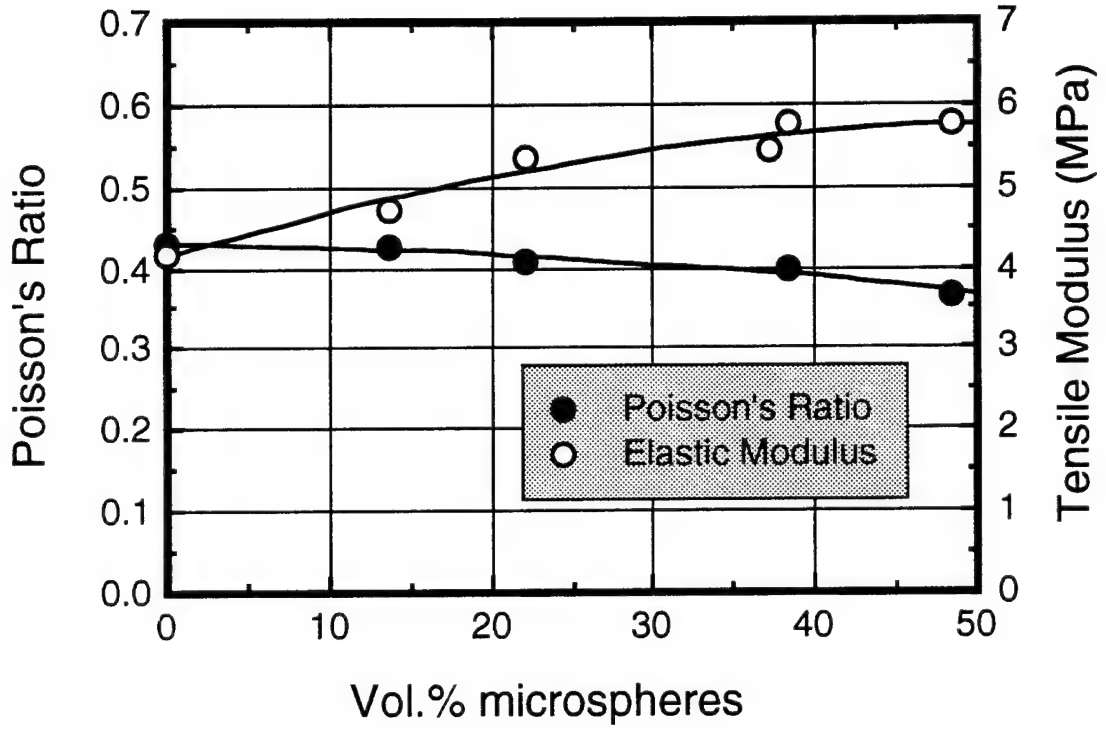

Figure 12. Static tensile modulus and Poisson's ratio as a function of microsphere content in EN-2 polyurethane.

2.3 SonoPanel Transducer Design and Assembly

The initial design for the 1-3 composite transducers, as developed for ONR by Vector Research (Ref.4), is shown in Figure 13.

The transducers were assembled by bonding the GRP face plates to both surfaces of the 1-3 composite sheet, attaching and securing the coaxial cable, shielding, and water-proofing. The face plates were bonded with conductive epoxy applied by a screening technique and clamped overnight for curing. The epoxy bond-line final thickness was approximately 0.08 mm. After curing, the excess epoxy was cleaned from the edges prior to cabling and shielding. The transducer was then encapsulated with (unvoided) EN-2 polyurethane and allowed to cure overnight.

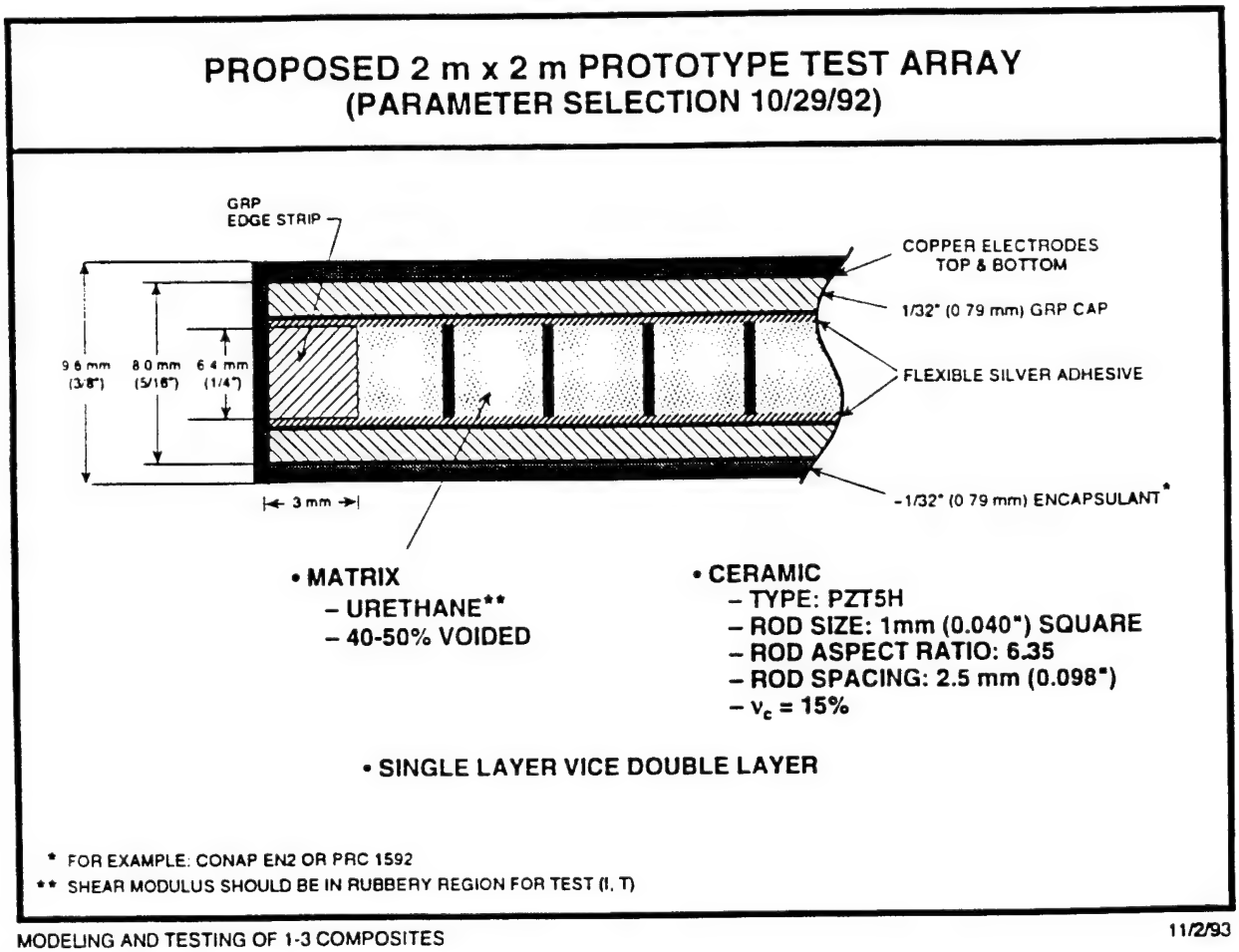

Figure 13. Initial 1-3 composite transducer design.

During the course of this program, these design parameters and the associated assembly processes were modified based on the following inputs:

(1) initial assembly experience and performance of subscale transducers,
(2) additional finite element analysis by Vector Research,
(3) requirements for subsequent transducer array testing (ABC program),
(4) iterative collaboration with the Naval Research Laboratory to optimize spatial uniformity of the transducer response.

Each of these factors and the resulting design changes are discussed in the following sections.

2.3.1 Subscale Transducers

Several subscale 100 mm square transducers were assembled by MSI and delivered to ONR for comparative evaluation (Figure 14). In addition, underwater TVR and RVS measurements were made on some of these transducers by Raytheon and Westinghouse. These test results are presented in Appendix B. A listing of the 100 mm transducers and their distinguishing characteristics is given in Table 3.

Table 3: Subscale 100 mm 1-3 Composite Transducers Delivered by MSI

Transducer	Matrix	Edge Strips	Comment
A	Voided EN-2	Yes	ONR Baseline
B	Voided EN-2	No	
C	Voided EN-2	No	
E	Voided EN-2 + Air Gaps	No	Bonding Problem

MSI's initial experience with assembly of the 100 mm transducers indicated that the flexible silver adhesive produced bonds between the 1-3 composite and the copper-plated GRP face plate of marginal mechanical integrity.

Figure 14. Two of the 100 mm sub-scale 1-3 composite transducers fabricated by MSI.

There was particular concern for bond line integrity in larger size transducers. Therefore, a study was undertaken in conjunction with UMass Lowell to determine the integrity of bonds between 1-3 composite and GRP face plates. For this purpose, 25 mm square coupons of actual 1-3 composite were bonded to faceplates using four different candidate conductive adhesives, each of which exhibited good electrical conductivity. Four coupons of each adhesive were prepared, and tested in tension at UMass-Lowell. To facilitate testing, 25 mm square plates of 6.3 mm thick PMMA with a steel bolt attached were bonded to outer surface of the face plates with a high strength commercial epoxy adhesive. The failure strength and mode of failure were determined. Several failure modes were

observed. Data from the few samples that failed at the commercial epoxy bond line were not included in the analysis. Representative tested coupons are shown in Figure 15.

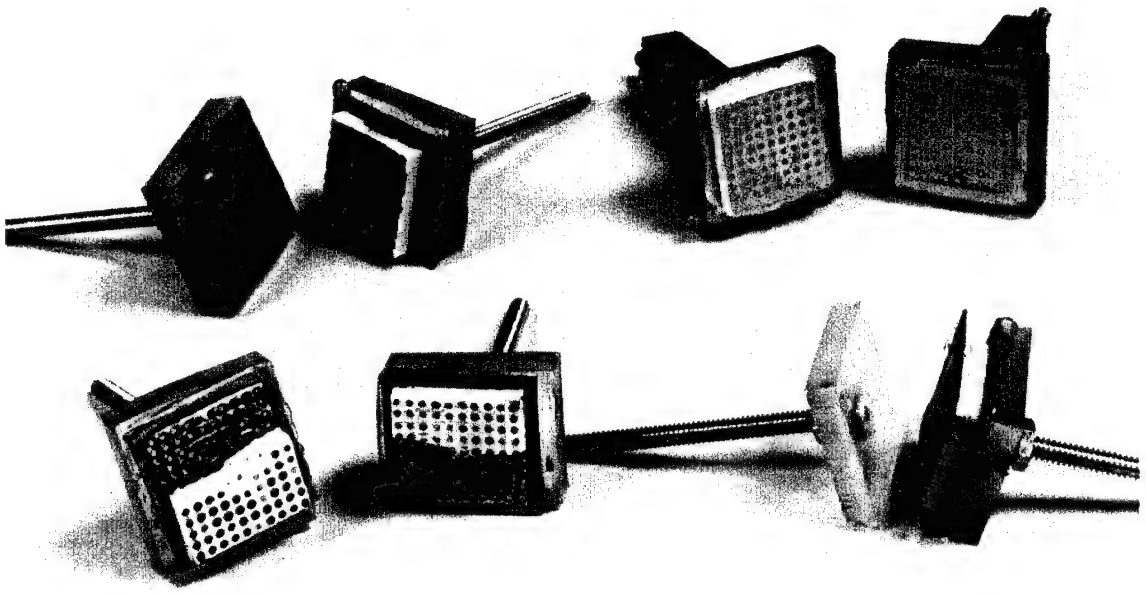

Figure 15. Photograph of several 1-3 composite test coupons after tensile testing to determine adhesive bond strength. Several different failure modes were observed.

The average bond strengths for the four adhesive types are plotted in Figure 16. Adhesive C was found to have significantly higher strength than the other candidates tested. As a result, this adhesive was used for all subsequent transducer assembly in this program.

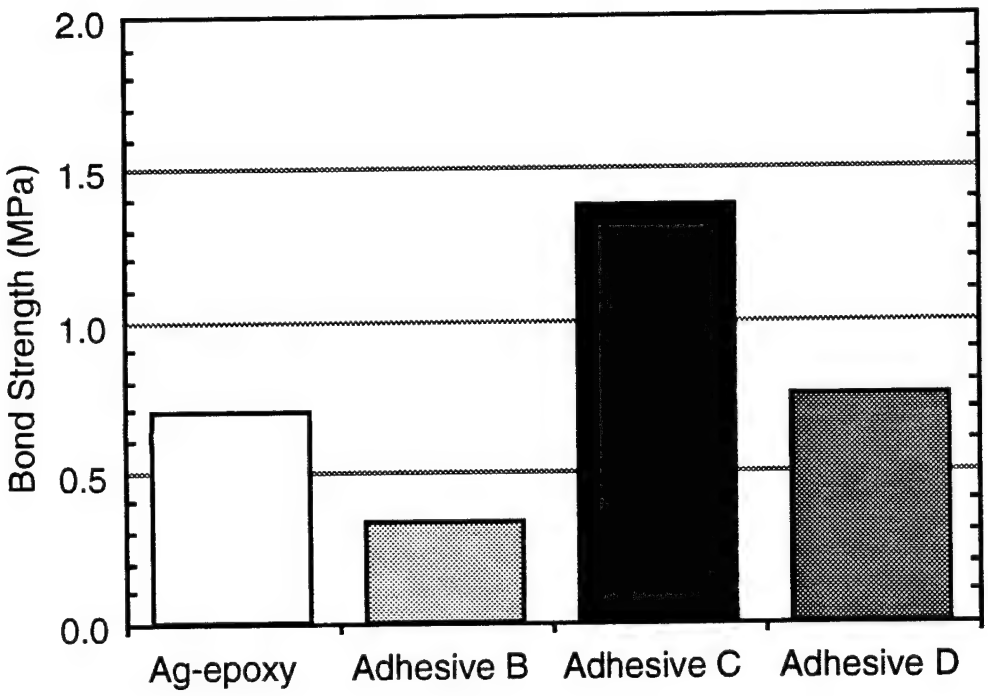

Figure 16. Bond strength for four types of conductive adhesives.

For MSI's initial subscale 100 mm transducers, the electrical cable was simply attached at the mid-point of one edge, with a relatively short length of cable contained within the outer polyurethane encapsulation. It was immediately obvious that this method would not provide adequate mechanical support for the cable or sufficient path length to prevent water penetration. As a result, for the 250 mm transducers, the cable was attached at one corner (Figure 17), and then run along one edge of the transducer before emerging from the outer polyurethane (Figure 18). A groove was machined in the edge of the composite to provide additional mechanical protection for the cable. Type N21-44B-503 (New England Electric Wire Corp., Lisbon, NH) shielded coaxial cable was specified by ONR to be used for this program. This cable contains two 22-gauge conductors, has a PVC outer jacket, and is 3.61 mm O.D.

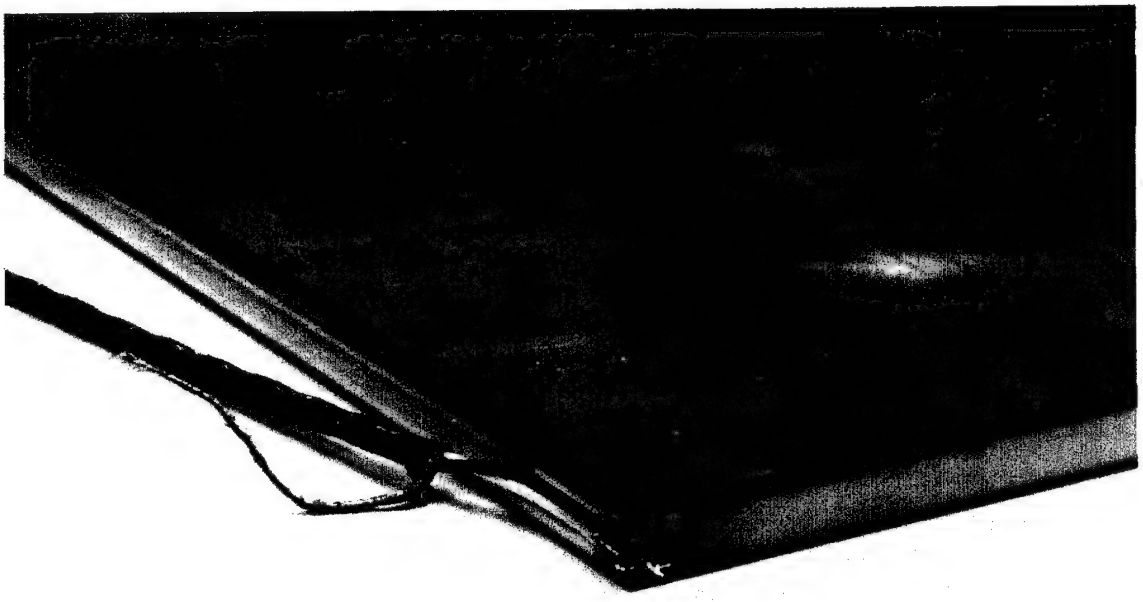

Figure 17. Photo showing cable attachment on the SonoPanel transducers.

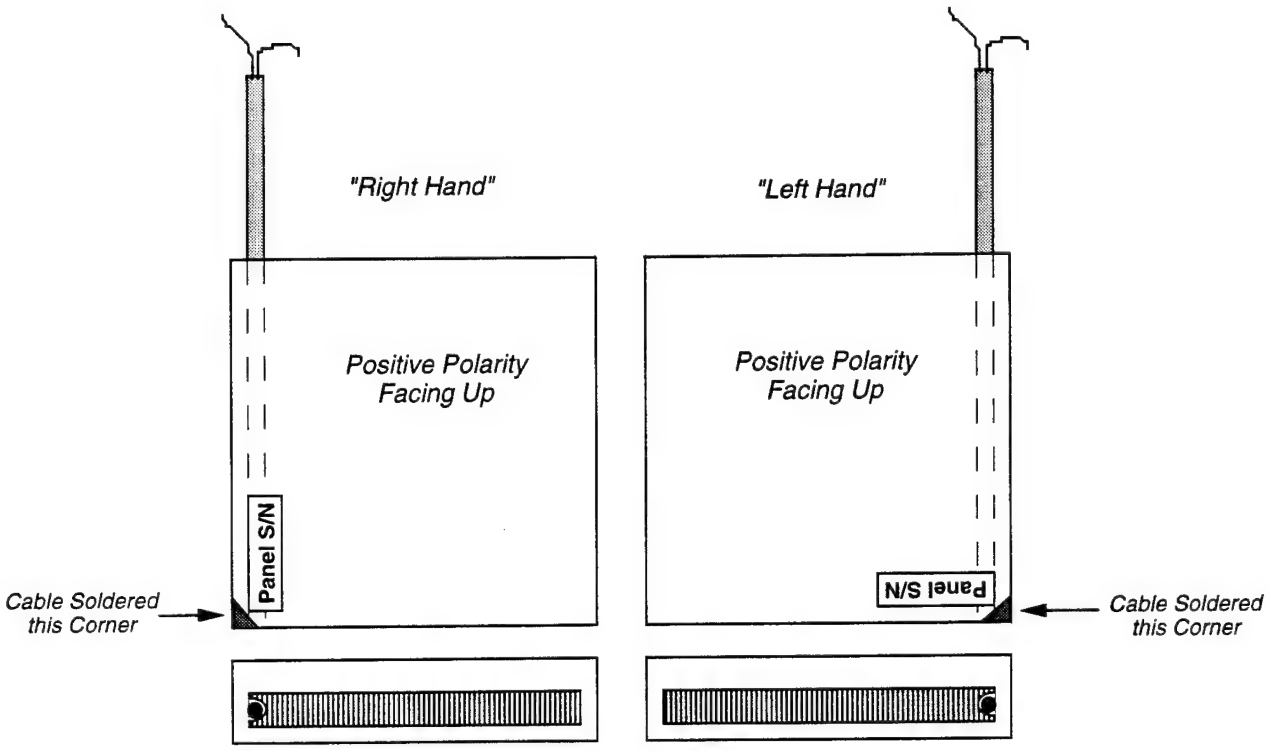

Figure 18. Cable path used for the 250 mm SonoPanel transducers. Both right-hand (RH) and left-hand (LH) cable configurations were used for the SonoPanels delivered to NRL-DC.

2.3.2 Additional Finite Element Analysis

As part of its modeling activities under the ONR Transduction Materials Program, Vector Research undertook additional finite element analyses to predict the performance of larger area 1-3 composite transducers, with and without stiff edge strips. This analysis (Ref.5) predicted that the edge strips would, in fact, have a negative effect on transducer performance because they would restrain the transducer at and near the edges. However, the predicted negative effect became insignificant when the active area was large compared to the edge area of the transducer. As a result of this analysis, ONR decided that edge strips could be eliminated from the transducer design.

2.3.3 Transducer Array Testing (ABC Program)

In late 1993, ONR decided to utilize several of the 250 mm SonoPanel transducers produced in this program as an actuator array in a system demonstration of the ONR ABC program. This application dictated some additional design changes. Two different cable routings were required to accommodate the array layout, as shown in Figure 18. These were designated "right-hand" (RH) and "left-hand" (LH) configurations.

In addition, it was determined that electromagnetic interference (EMI) might interfere with nearby sensors. Therefore, a shielding approach was implemented, which involved electrically connecting the cable shield to the outer copper layers of the GRP face plates and copper foil tape applied to edges. The outer copper layers and the edge foil form a nearly complete grounded enclosure for the transducers. The edge foil was soldered to the two outer copper sheets at several spots along each edge to ensure electrical continuity.

Two measures were taken to avoid shorting the outer shield to the electrodes. First, the copper was etched away from the edge area of the face plates. In addition, a strip of electrical insulation was applied to the edges prior to application of the copper foil tape.

Finally, for the deliverable 250-mm transducers for the array demonstration, NRL-DC requested that the outer polyurethane encapsulant on the back side be reduced to the minimum possible thickness, while still providing a continuous seal. A thickness of 0.5 mm was agreed to for the backside, with encapsulant thickness on the edges and front side maintained at approximately 3 mm.

2.3.4 Iterative Collaboration with the Naval Research Laboratory

Prior to finalizing the design for the panels to be used in the ABC program, NRL-DC conducted laser vibrometer measurements to determine the spatial uniformity of selected 250 mm panels. The actual displacement of the panel surface was measured at 1089 points in a 33 x 33 array while the panel was actuated at frequencies from 350 to 10,000 Hz. Low spatial variability, ideally less than 10% (~0.5 dB), is desired for future active control applications.

The 250 mm transducers measured as part of the final design determination are listed in Table 4, along with a summary of the magnitude and uniformity of the surface displacement. Initially, an encapsulated panel with the baseline design (10-12) was measured and found to have significantly greater spatial variation than desired. Subsequently, an unencapsulated by otherwise identical panel (10-11) was checked and found to be improved but still short of the desired spatial uniformity.

Table 4: Summary of Spatial Uniformity Laser Vibrometer Measurements of Selected Transducer Panels by NRL-DC (Mean + Std.Dev.)

Panel	Description	Displacement per Volt (dB, re: 1 m/V) 1000 Hz	3000 Hz
10-12	Baseline - Encapsulated	-192.5 ± 7.5	-196 ± 4
10-11	Baseline	-192 ± 5	-196 ± 3.5
10-21	3X thicker Faceplates	-187 ± 3	-196 ± 3.5
10-16	Modified Electrode	-192 ± 3	-193 ± 1.5
10-X	Improved Sintering	-187 ± 3	-192 ± 2

(Panels not encapsulated except as noted.)

To explore alternate transducer designs and manufacturing process changes that could lead to improved spatial uniformity, three modified panels were assembled and provided unencapsulated to NRL for evaluation. These changes included thicker GRP face plates and modified electroding, as well as a panel made from PZT preforms sintered with the improved process, discussed previously in Section 2.1. As seen in Table 4, improved sintering and modified electroding gave more uniform response at both 1000 and 3000 Hz.

As a result of these measurements, the modified electroding process was implemented for the final transducer design. Because most of the 1-3 composite sheets had already been fabricated, the improved sintering process was utilized only for the final four transducers delivered (to NRL-USRD in July 1994).

2.4 Final Transducer Design and Deliverables

Figure 19 shows the detailed final design for the sixteen (16) 250 mm SonoPanel transducers delivered to NRL-DC under this program. The four transducers delivered to NRL-USRD were identical, except that the outer polyurethane encapsulation layer was kept at approximately 3 mm on all surfaces. A log of the 250 mm SonoPanel transducers produced in this program is given in Table 5.

The transducer serial number was printed on the positive polarity surface with permanent marker in the same corner as the original reference mark for the composite sheet (see Figure 18). A 15 meter length of cable was used for the deliverable transducers. Finished transducers were then given a final inspection and electrical characterization. Electrical measurements included capacitance, dissipation, and impedance and phase as a function of frequency. Typical impedance spectra for finished 250 mm SonoPanel transducer 10-40, before and after final encapsulation, are shown in Figure 20. This primary thickness mode resonance occurs at 248 kHz. A lower frequency resonance, the source of which has not been definitively determined, occurs at approximately 90 kHz in the unencapsulated panel and shifts to approximately 70 kHz after encapsulation. After encapsulation, a third resonance feature appears at approximately 160 kHz. This is believed to be a secondary thickness mode resonance, associated with increased total thickness of the transducer.

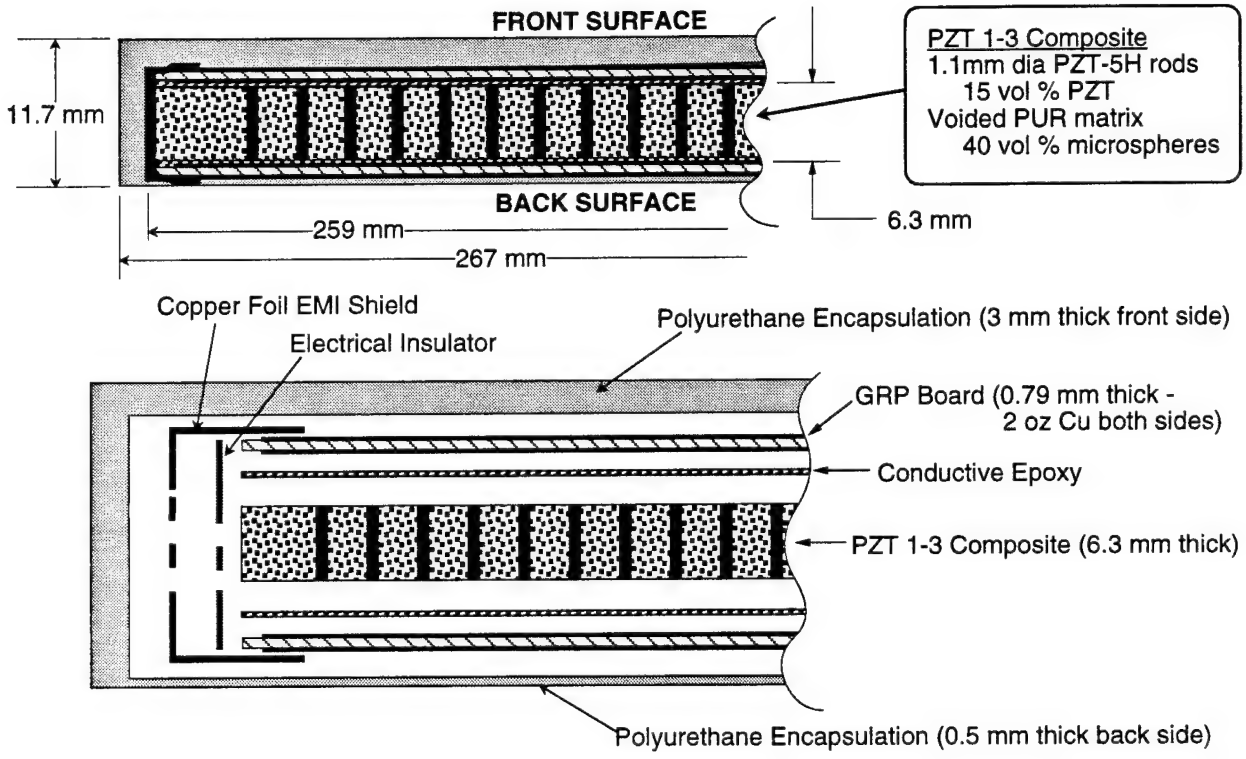

Figure 19. Final design for the 250 mm SonoPanel transducers delivered to NRL-DC.

Table 5. 250 mm SonoPanel Transducers Produced in this Program

Panel #	Encap-sulated	Modified Electrodes	Cable Path	Delivered	To	Comments
10-1	X		RH	Feb-94	NRL-DC	
10-2	X	X	RH	16-Jun-94	ABC	
10-6	X		RH	Jan-94	NRL-DC	
10-9	X	X	RH	16-Jun-94	ABC	
10-11			RH	Feb-94	Laser	
10-12	X		RH	Feb-94	Laser	
10-13	X		RH	21-Apr-94	USRD	Also tested by Raytheon
10-15	X		RH	Jan-94	NRL-DC	
10-16		X	RH	Mar-94	Laser	
10-17	X	X	RH	21-Apr-94	NRL-DC	
10-18	X	X	RH	21-Apr-94	NRL-DC	
10-19	X	X	LH	20-Jun-94	ABC	
10-20	X	X	LH	23-Jun-94	ABC	
10-21			RH	Mar-94	Laser	3x thicker faceplates
10-22	X	X	LH	16-Jun-94	ABC	
10-23	X	X	LH	20-Jun-94	ABC	
10-25	X	X	LH	23-Jun-94	ABC	
10-26	X	X	LH	13-Jun-94	ABC	
10-28	X	X	RH	13-Jun-94	ABC	
10-29	X	X	RH	16-Jun-94	ABC	
10-31	X	X	RH	21-Apr-94	NRL-DC	
10-32	X	X	RH	7-Jul-94	ABC	
10-34	X	X	RH	23-Jun-94	ABC	
10-35	X	X	RH	23-Jun-94	ABC	
10-37	X	X	RH	20-Jun-94	ABC	
10-38	X	X	RH	20-Jun-94	ABC	
10-39	X	X	RH	23-Jun-94	ABC	
10-40	X	X	RH	14-Jul-94	USRD	Improved sintering process
10-41	X	X	RH	14-Jul-94	USRD	Improved sintering process
10-42	X	X	RH	14-Jul-94	USRD	Improved sintering process
10-43	X	X	RH	14-Jul-94	USRD	Improved sintering process
10-X			RH	Apr-94	Laser	Improved sintering process

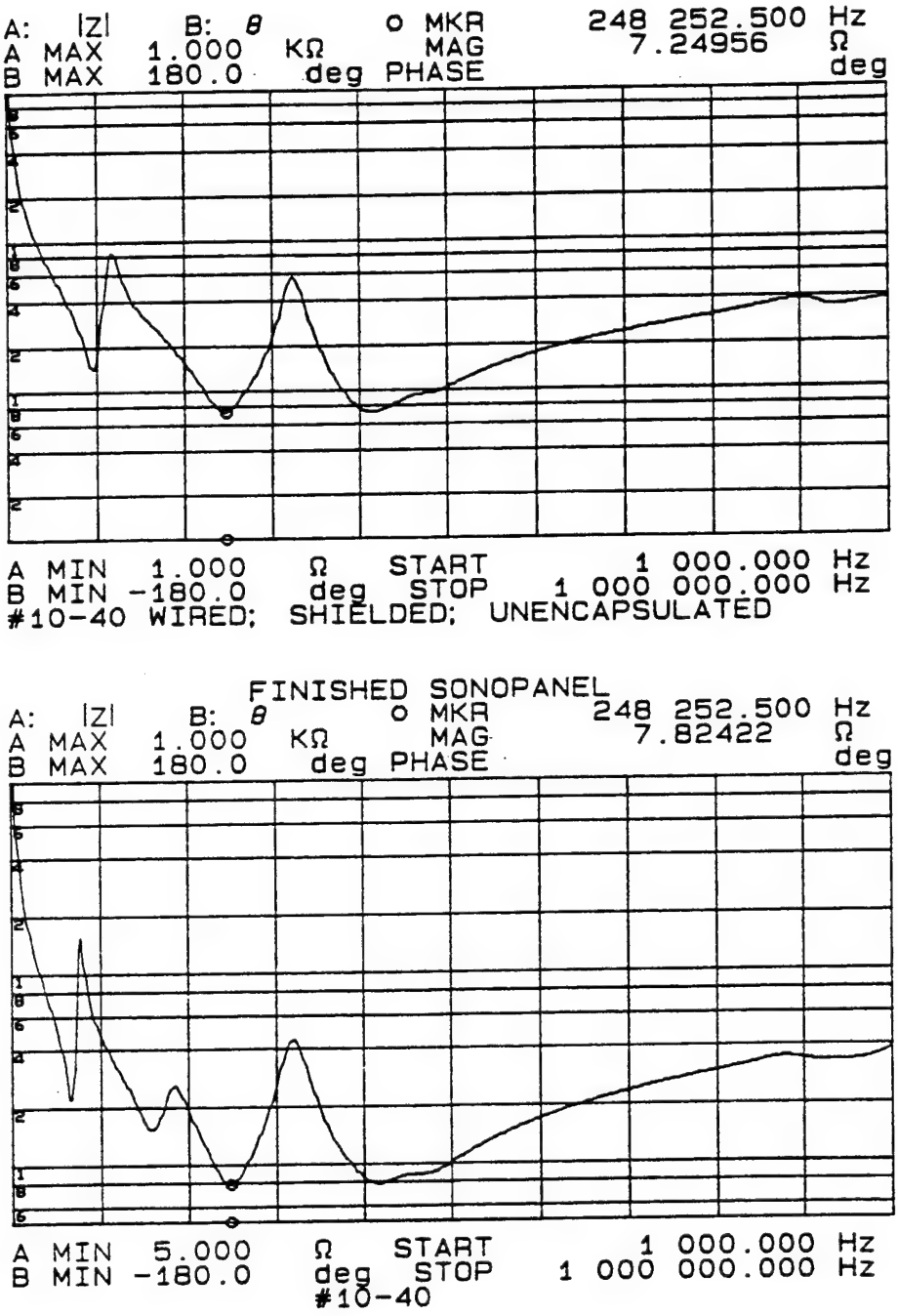

Figure 20. Impedance plot for 250 mm SonoPanel transducer #10-40. Top: Before final encapsulation. Bottom: After encapsulation. This transducer was encapsulted on all sides with 3 mm of polyurethane.

2.5 Transducer Test Data

In-water receiving voltage sensitivity and receive beam patterns of SonoPanel transducer 10-13 were measured by Raytheon in March 1994. The measured RVS was $-187(\pm 3)$ dB re: 1 V/μPa over the entire band from 1 to 100 kHz. The RVS data and receive beam patterns at 1, 10, 25, 50, and 100 kHz are presented in Appendix C.

Two of the 250 mm transducer panels delivered to NRL-USRD were tested in August 1994. Free-field voltage sensitivity, transmitting voltage response, and sound pressure level were measured for panel 10-43 at the USRD Lake Facility. Receive beam patterns at 5,10, 30, 50, 100, and 200 kHz were measured for panels 10-40 and 10-43. In addition, the free-field voltage sensitivity of panel 10-40 was measured at various pressures up to 6890 kPa in the Anechoic Tank Facility. The test data and related briefing charts from NRL-USRD are presented in Appendix D.

The average FFVS of the panels was –185 dB re: 1 V/μPa from 1 to 200 kHz. The TVR results showed theoretically predicted behavior from 1 to 200 kHz, increasing linearly at approximately 40 dB per decade. The SPL measurements showed linear response without breakdown at drive voltages up to 900 V (142 V/mm), the highest level tested. The FFVS measurements as a function of pressure showed no discontinuous effects. Within experimental limits, the sensitivity returned to initial levels after the pressure cycle.

3.0 REFERENCES

1. Materials Systems Inc., Fabrication of Piezoelectric Ceramic/Polymer Composites by Injection Molding, Final Report Contract N00014-92-C-0010, April 15, 1993

2. C. Kim, M. Springer, M. Kahn, PZT Rod Evaluation, ONR Transduction Materials Program Review, Nov.2, 1993

3. J. Andrusaitis, Dielectric and Mechanical Properties of Syntactic Polyurethane Foam, M.S. Thesis, Plastics Engineering, UMass-Lowell, May 1994

4. W. Reader, Modeling and Testing of 1-3 Composites, ONR Transduction Materials Program Review, Dec.7, 1992

5. D. Sauter, Analysis and Testing of 1-3 Composites, ONR Transduction Materials Program Review, April 21, 1994

APPENDIX A

MATERIALS SUPPORT FOR THE DEVELOPMENT OF A PIEZOELECTRIC CERAMIC/POLYMER COMPOSITE

R.G. Stacer, J.A. Andrusaitis and S. Mehta
Department of Plastics Engineering
University of Massachusetts Lowell

Final Report
To Materials Systems Inc.
September, 1994

SUMMARY

During the past fifteen months, the Plastics Engineering Department at UMass Lowell has supported under contract the efforts of Materials Systems Incorporated to demonstrate a novel approach for producing ceramic fiber/polymer composites which are piezoelectrically active for use in naval underwater applications. Basically, these composite structures consist of an array of PZT ceramic fibers imbedded in a syntactic polyurethane foam which provides an organic isolation barrier between the poled fibers. Individual fibers are bonded using a conductive epoxy structural adhesive to copper transducer plates. The final structure is encapsulated by a polyurethane resin which protects against shock and vibration, as well as serving as a moisture barrier.

As part of this effort, evaluation and characterization testing was accomplished on the various polymeric components used in the prototype demonstration arrays. Bond-in-tension tests were employed to evaluate candidate adhesives for the fiber/conductive plate interface. The bond region is a critical feature of the design since it must provide both a conductive interface between the fibers and the transducer plates, as well as maintaining this bond under complex structural loading conditions. Results included in this report show that an increase in bond strength from 0.7 to 1.4 MPa can be achieved via a simple adhesive substitution. Future work is planned to optimize adhesive bonding, bondline processing, and interface surface preparation to provide superior strengths and reduced costs.

Also included in this report are the results of an experimental investigation to determine the effect of volume percent microsphere content on the dielectric and mechanical properties of the syntactic foam. Complete documentation of this portion of the effect is to be found in Reference 1. Briefly summarized, the dielectric permittivity was found to behave similarly to the mechanical moduli in that it increased with microsphere content and testing frequency, and decreased when temperature was increased. The glass transition temperature was unaffected by percent microspheres within experimental error. Both tensile modulus and Poisson's ratio were measured under static conditions.

Modulus increased by a factor of two while Poisson's ratio dropped from 0.43 to 0.36 for volume fractions up to 48 percent. Experiments conducted using both forced dynamic shear and forced dynamic tensile deformations showed similar results while also quantifying the effects of temperature and frequency.

Finally, rheological properties and potlives of various polyurethane resins were evaluated. These data showed that potlife could be extended from 25 minutes to three hours for the matrix material used in the syntactic foam. Additionally, suitable candidates were investigated in the preliminary fashion to develop an encapsulating resin capable of providing extended underwater life.

1.0 Density Measurements

Mechanical, rheological and electrical properties of polymers as functions of additive concentrations are more appropriately viewed as volume rather than weight fractions. This is especially true for solid fillers such as the hollow microspheres used in preparing the syntactic foams for this investigation. Additionally, samples in this study were prepared by hand mixing and some microspheres were lost to the surrounding environment after weighing because of their low densities.

After uniformity of filler distribution within the test specimens was verified using a Shore A hardness tester, the total volume percent of microspheres was determined using densimeter measurements. The density of the unfilled polyurethane was found to be 1.0572 g/cm^3. Similar measurements were made as weight fraction of microspheres was increased to 0.0375. Density of the 0.0300 weight fraction sample, which is the baseline syntactic foam, was 0.672 g/cm^3. Mass determinations were also made using an analytical balance. From the measured mass and density values, the microsphere volume fractions shown in Table I were calculated.

Table I. Weight and Volume Fractions of Microspheres

Weight Fractions	Volume Fractions
0.0000	0.00
0.0075	0.14
0.0150	0.22
0.0225	0.37
0.0300	0.38
0.0375	0.48

2.0 Cure Studies and Alternative Polyurethane Chemistry

A Brookfield viscometer was used to measure end-of-mix (EOM) viscosity and potlife for the various polyurethane resins investigated as part of this effort. These tests were conducted at a rotational rate of 12 rev/min. Figure 1 shows end-of-mix viscosity as a function of volume fraction microspheres in the EN-2 system. As can be seen, viscosity increases up to 40 percent microspheres in a manner describable by the Smallwood Equation:

$$\eta = \eta_o (1 + 2.5V + 14.1V^2) \qquad (1)$$

where η is the viscosity, η_o is the viscosity of the EN-2 material without microspheres, and V is the volume fraction of microspheres. Above 40 percent, viscosity increases dramatically and deviates from Equation (1). This indicates that processing of syntactic foams above the 40 percent level in the subject application would be difficult and perhaps impossible.

Figure 2 illustrates the effect of microsphere fraction on cure time. Potlife in this situation was defined a doubling on the EOM viscosity. Using this definition, the potlife of the unfilled EN-2 material was 25 minutes, while the presence of the microspheres act as apparent catalysts and decrease this to 20 minutes. Lowering of the cure temperature from ambient to 0 °C

only increased potlife by approximately five minutes. A longer potlife of nearly three hours was observed from similar experiments carried out on the EN-3 material. This longer potlife is obtained by lowering the levels of organometallic cure catalysts. It should be possible to vary the potlife anywhere between these limits by adding additional catalyst to the EN-3 material. Ferric acetylacetonate is believed to be the principal catalyst used in the EN series (Ref.3). The main disadvantage to increasing potlife is a corresponding increase in cure time.

In addition to the above effort, work was begun as part of this contract to investigate alternatives to EN-2 and -3. Both of these polyurethanes use a polyether backbone which is known to experience hydrolytic instability when aged in water for prolonged periods. For this reason, an alternative polyurethane utilizing a polybutadiene (Ref.4) backbone was investigated. The specific prepolymers considered were R45-M and -HT from Elf Atochem. The HT prepolymer is approximately 1/10 the price of EN-2, has similar mechanical properties (although somewhat higher EOM viscosity), and ages well underwater. Underwater aging at 80 °C was started near the end of the contractual period to evaluate the various candidates and is continuing.

3.0 Adhesive Bond Strength

Bond strengths of several conductive adhesives used to bond the PZT fibers to the copper transducer plate were evaluated by bond-in-tension testing. Figure 3 shows the bond-in-tension test specimen employed. This specimen consisted of a 2.5 cm square sample of the polyurethane/ceramic composite bonded to the copper plate using four candidate adhesives, including the silver/epoxy baseline. Specimens were bonded to a piece of plexiglas to distribute the loads during testing using a two-part epoxy purchased at a local hardware store. Tests were conducted in an INSTRON 1137 universal test machine at a crosshead rate of 5 cm/min. Data were reduced by dividing the measured breaking force by the sample cross-sectional area. Replicates were tested for each adhesive and the average fracture stress reported.

Table II presents the results for the four adhesive formulations investigated.

Table II. Adhesive Bond Strengths

Material	Strength (MPa)	Fracture Mode
Ag/Epoxy	0.7	Cohesive in polyurethane/ceramic
Adhesive B	0.3	Adhesive at interface
Adhesive C	1.4	Cohesive in polyurethane/ceramic
Adhesive D	0.7	Adhesive at interface

The weaker materials, Adhesives B and D, failed at the adhesive interface with very clean fracture surfaces for the weakest samples. The stronger materials, Ag/Epoxy and Adhesive C, failed cohesively in the polyurethane/ceramic composite with rough fracture surfaces. For the strongest bonds, those obtained using Adhesive C, cracks propagated deep into the composite. Clearly, increases in strength from the Ag/Epoxy baseline are possible. Other variables to be investigated as part of the follow-on effort include: adhesive thickness, copper surface preparation, influence of conductive fillers, and specific epoxy chemistry.

4.0 Thermal Properties

Thermal properties of the syntactic polyurethane foams were measured using a TA Instruments' Differential Scanning Calorimeter (DSC). This instrument measures heat capacity C_p of a material in comparison to an inert reference material during a programmed heating cycle. In this case, samples were cooled rapidly to -120 °C then heated slowly to 200 °C at a rate of 10 °C/min. Figures 4 and 5 present typical

results for sample containing 48 percent by volume (3.75 percent by weight) and 38 percent by volume (3.00 percent by weight) microspheres, respectively. The only thermal event observed over this temperature range is the rubber-to-glass transition. The temperature at which this transition occurs is designated T_g and is associated with the onset of long-range molecular motions. Table III gives the measured T_g values for each of the volume fractions of microspheres considered.

Table III. Glass Transition Temperatures from DSC

Volume Percent Filler	T_g (°C)
0	- 9
14	- 8
22	-10
37	- 7
38	-10
48	- 7

These values range from -7 to -10 °C, independent of filler fraction. This is somewhat surprising since several earlier investigators (Ref.4-8) have reported that T_g should increase with the addition of filler, although not all investigations (Ref.9) agree. In terms of the specific application under consideration, these data indicate that at very high strain rates or frequencies, the polyurethane material will behave more like a brittle plastic rather than a flexible rubber. More will be said in this regard after the mechanical properties data have been discussed.

5.0 Dielectric Properties

Dielectric analysis refers to the measurement of two fundamental characteristics of polymers, capacitance and conductance, with respect to time, temperature and frequency. Capacitance is the ability of a material to

store charge. Conductance is the ability of a material to transfer charge. The quantitative properties that are usually reported in dielectric analysis of polymers are permittivity, loss factor and the dissipation factor. The permittivity e' is proportional to the capacitance and is a measure of dipole alignment. The amount of energy it takes to align the dipoles is noted by the loss factor e" which is proportional to the conductance. The dissipation factor is the amount of energy generated in an insulating material when the material is experiencing an electric field (Ref.10). Mathematically, the dielectric properties e' and e" are analogous to the mechanical properties E' and E" (Ref.11).

Dielectric analysis (DEA) of the syntactic foams was accomplished using a TA Instruments' DEA. An initial compressive force of 100 N was applied to insure the surface of the test specimen was between the sensor wires. A nitrogen purge was used to remove moisture from the chamber throughout the test. The specimen was quickly cooled to -100 °C and then slowly heated to 100 °C at a rate of 1 °C/min. Excitation frequencies were varied from between 1 and 300,000 Hz. Figures 6 and 7 show typical curves thus produced. A single peak is apparent in each set of relaxation data. These peaks can be used to quantify the frequency dependence of T_g as shown in Figure 8. Included in this figure are data for both the unfilled polyurethane and the formulation containing 38 percent volume fraction microspheres. As can be seen, T_g decreased with log frequency by 70 °C over the range of frequencies investigated. These data can be compared with the DSC values obtained under static conditions which are also shown in the figure. These data suggest that if the experiments were conducted with the DEA at even lower frequencies, the two measurement systems would have provided identical results. Similar results have been previously reported (Ref.12)

6.0 Static Modulus/Poisson's Ratio

Tensile stress relaxation modulus and Poisson's ratio were measured using rectangular test specimen of known cross-sectional area. These were tested in an INSTRON 1137 universal test machine. Reported relaxation

moduli values represent equilibrium values at t = 1000 s and $\varepsilon = 0.2$. Poisson's ratio was calculated from the corresponding lateral contraction measured at 10 locations along the specimen's length using a pair of calipers. Figure 9 presents the results of these experiments on the five polyurethanes considered. Consistent with what would be expected from the literature (Ref.2,13), these data showed modulus increased with microsphere content while Poisson's ratio decreased. The increase in modulus might at first glance seem surprising since one would expect a foam to be "softer" than its unfoamed counterpart; however, it must be recognized that in this case the foam is created by incorporating microspheres with rigid walls of greater modulus than the surrounding matrix.

7.0 Dynamic Mechanical Properties

A Rheometrics Mechanical Spectrometer System Four was used to measure the dynamic moduli of the syntactic polyurethane foams in both tension and shear. The experiments were performed according to ASTM D5279 and ASTM D5026 for tension and shear, respectively. Rectangular specimens were placed within the grips of the instrument after all of the geometry measurements were taken. Separate fixtures were used depending on the mode of deformation. The instrument was programmed for various temperature and frequency ranges. Temperature sweeps covered the range from -75 to 30 °C at 3 °C/min with $\omega = 1$ Hz, and strain amplitude equal to 0.2 percent. The frequency sweep experiments were conducted from 0.1 to 100 Hz at the same strain amplitude over discrete temperature steps.

Figure 10 presents the results from the temperature sweep in tension for the material containing 38 percent by volume microspheres. The tensile storage modulus E' can be seen to drop a little more than two orders of magnitude (from around 1 GPa to under 10 MPa) as the glass transition region is traversed. At temperatures below T_g, the glassy plateau is observed, while the rubbery plateau can be seen at $T > T_g$. Also in the transition region both the tensile loss modulus E" and the loss factor, tan δ, experience local maximums. These peaks are also associated with T_g and

may be considered as mechanical measures thereof. The peak for tan δ is approximately five degrees lower than that for E" consistent with known literature phenomena (Ref.2). These data again indicate that the syntactic foam used in the composite structure is very close to the rubber-to-glass transition region. Figure 11 illustrates the effect volume fraction filler has on E' (approximately doubles from near 6 to 12 MPa) is similar to that previously noted for E.

Figure 12 presents the shear response properties that correspond to those given in Figure 10 for tensile. Values for shear storage G' and loss G" moduli are approximately one third of those observed for E' and E" as expected from the equations of linear elasticity. Peaks identical to the tensile counterparts are seen in both damping functions in the transition region. Finally, Figure 13 shows shear storage modulus increases from 2.3 to 4.9 MPa as filler is added up to 48 percent by volume.

8.0 References

1. J.A. Andrusaitis, "Dielectric and Mechanical Response Properties of Syntactic Polyurethane Foams," M.S. Thesis, University of Massachusetts Lowell, 1994.

2. L.E. Nielsen and R.F. Landel, "Mechanical Properties of Polymers and Composites, 2nd Edition," Dekker, New York, 1993.

3. C. Arnold, Rubber Chem. Technol. 47, 456 (1974).

4. D.M. French, Rubber Chem. Technol. 42, 71 (1969).

5. R.F. Landel, Trans. Soc. Rheol. 2, 53 (1958).

6. D.H. Droste and A.T. di Benedetto, J. Appl. Polym. Sci. 13, 2149 (1969).

7. G. Kraus and J.T. Gruver, J. Polym. Sci., Polym. Phy. Ed. 8, 571 (1970).

8. R.G. Stacer and D.M. Husband, Rheol. Acta, 29, 152 (1990).

9. C.W. Van der Waal, H. Bree and F.R. Schwarzl, J. Appl. Polym. Sci. 9, 2143 (1965).

10. G.R. Moore and D.E. Kline, "Properties and Processing of Polymers for Engineers," Prentice-Hall, New York, 1984.

11. N.W. Tschoegl, "The Phenomenological Theory of Linear Viscoelastic Behavior," Springer-Verlag, Berlin, 1989.

12. G. Ver Strate, in "Science and Technology of Rubber," F.R. Eirich, ed., Academic Press, New York, 1978.

13. J. Farber and R.J. Farris, J. Appl. Polym. Sci. 34, 2093 (1987).

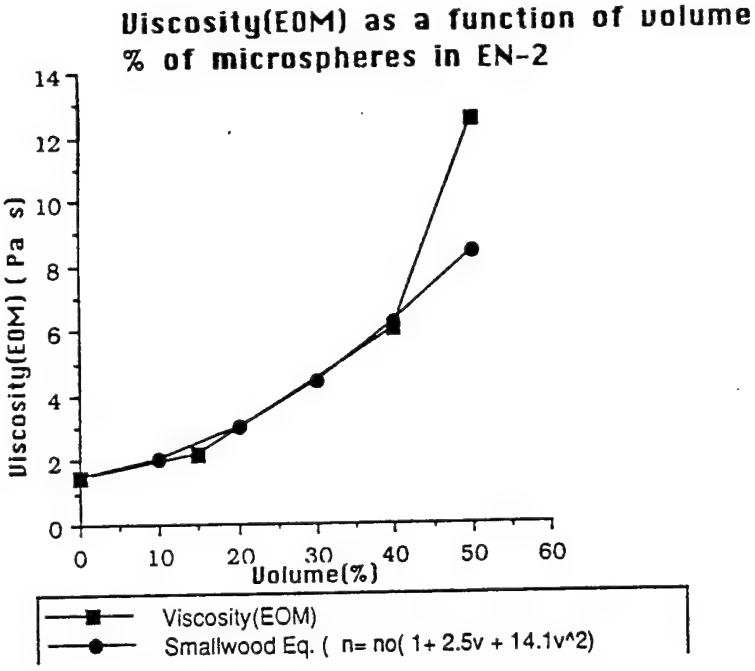

Figure 1. End-of-mix viscosity as a function of volume fraction microspheres in the EN-2 system.

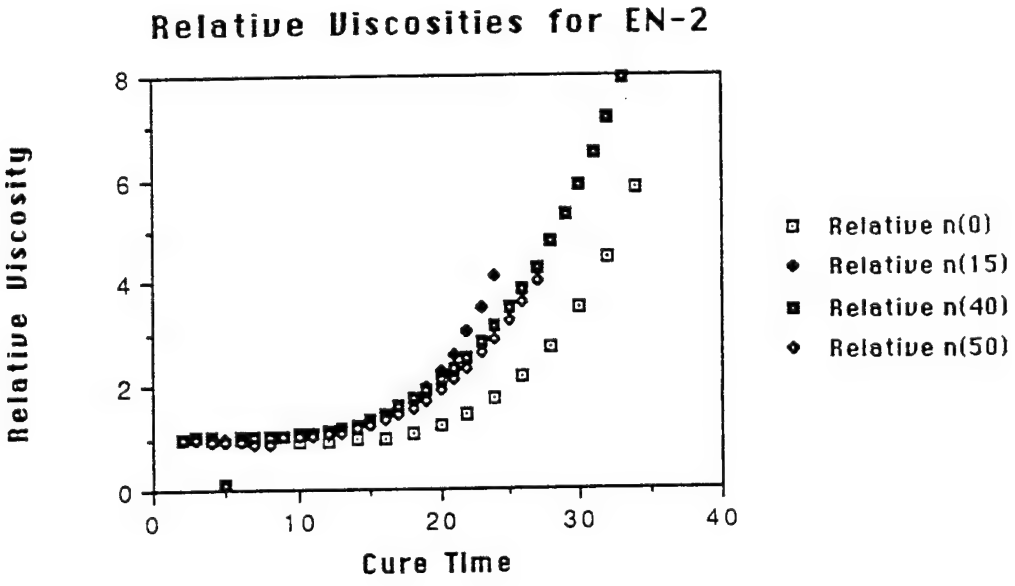

Figure 2. Effect of microsphere fraction on cure time in the EN-2 system.

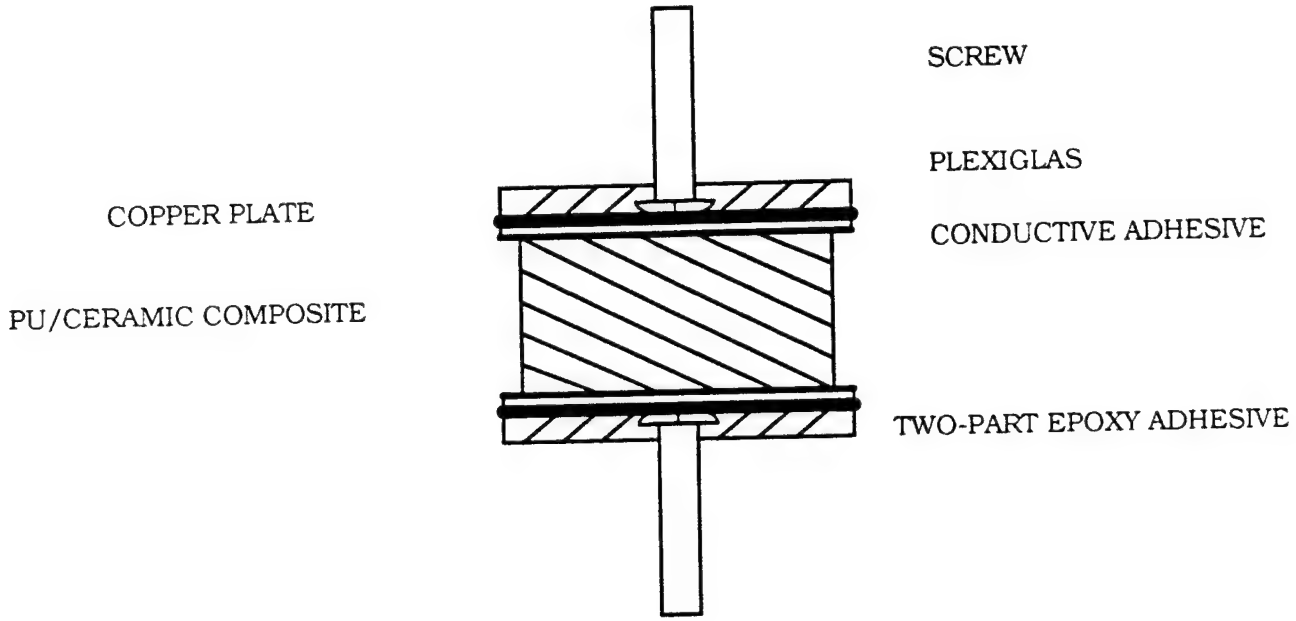

Figure 3. Bond-in-tension test specimen.

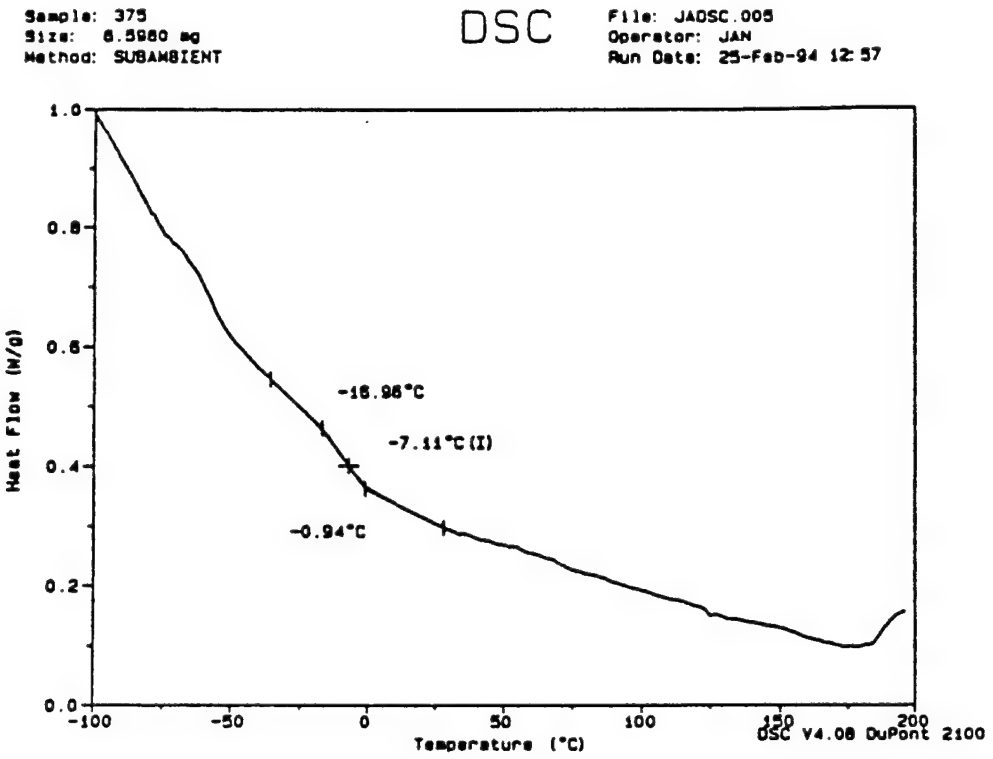

Figure 4. Differential scanning calorimeter (DSC) results for sample containing 48 percent by volume (3.75 percent by weight) microspheres.

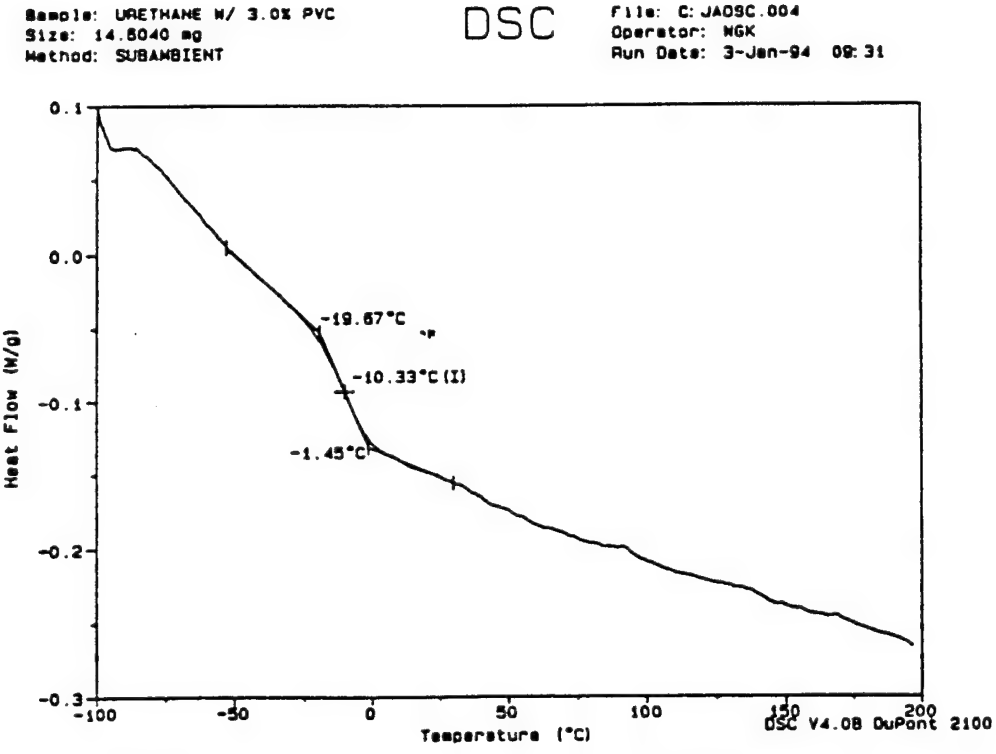

Figure 5. Differential scanning calorimeter (DSC) results for sample containing 38 percent by volume (3.00 percent by weight) microspheres.

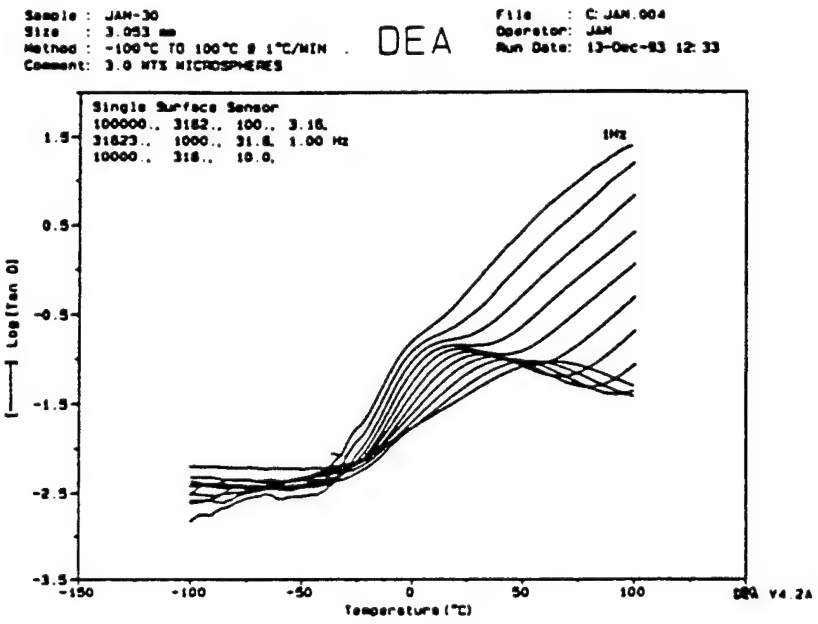

Figure 6. Dielectric analysis (DEA) results for sample containing 38 percent by volume (3.00 percent by weight) microspheres.

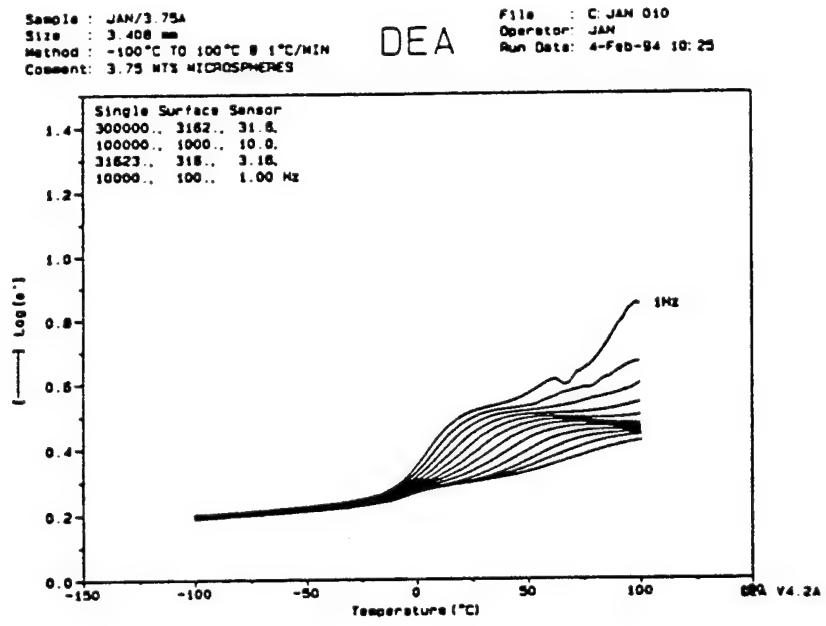

Figure 7. Dielectric analysis (DEA) results for sample containing 48 percent by volume (3.75 percent by weight) microspheres.

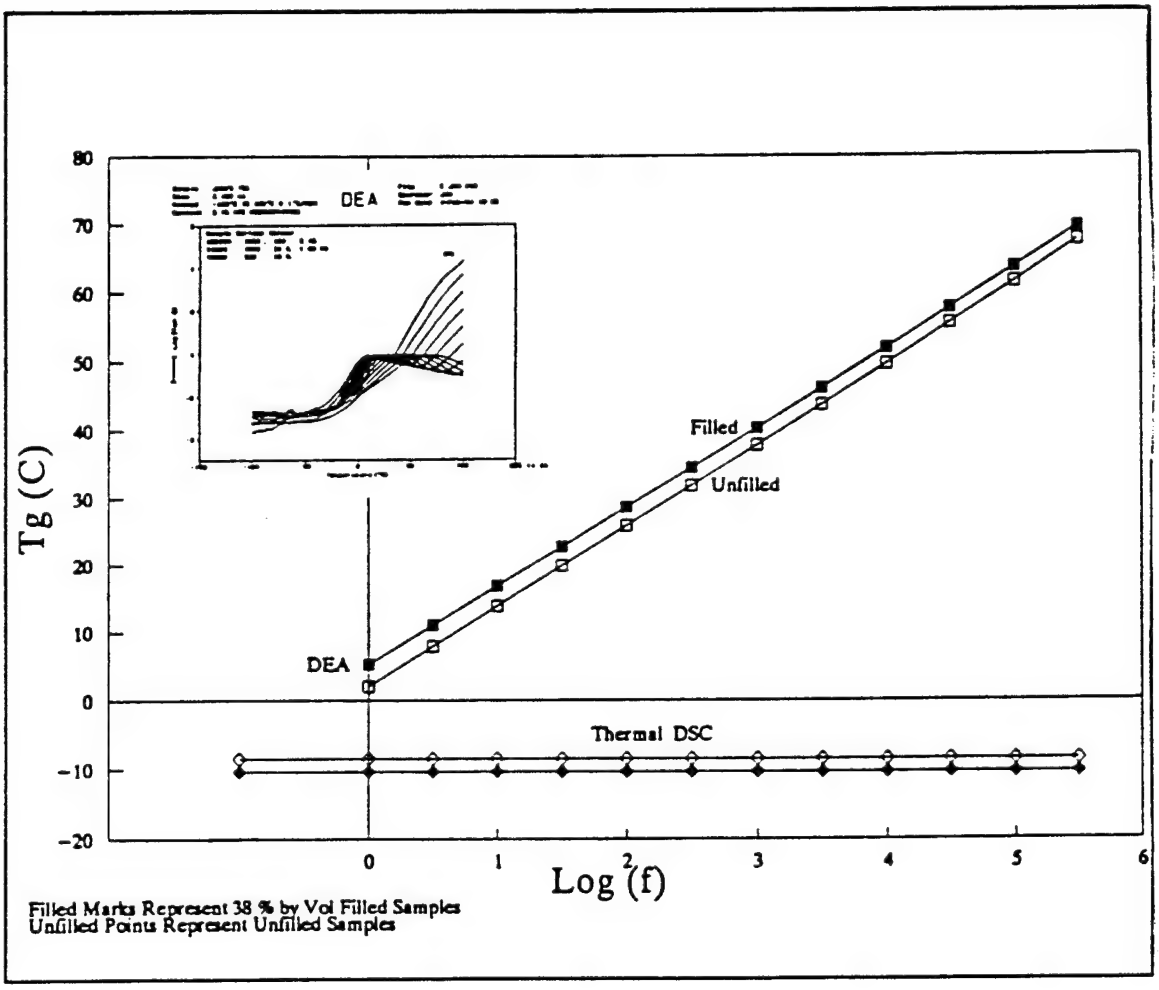

Figure 8. Effect of filler and testing frequency on T_g. Included in this figure are data for both the unfilled polyurethane and the formulation containing 38 percent volume fraction microspheres.

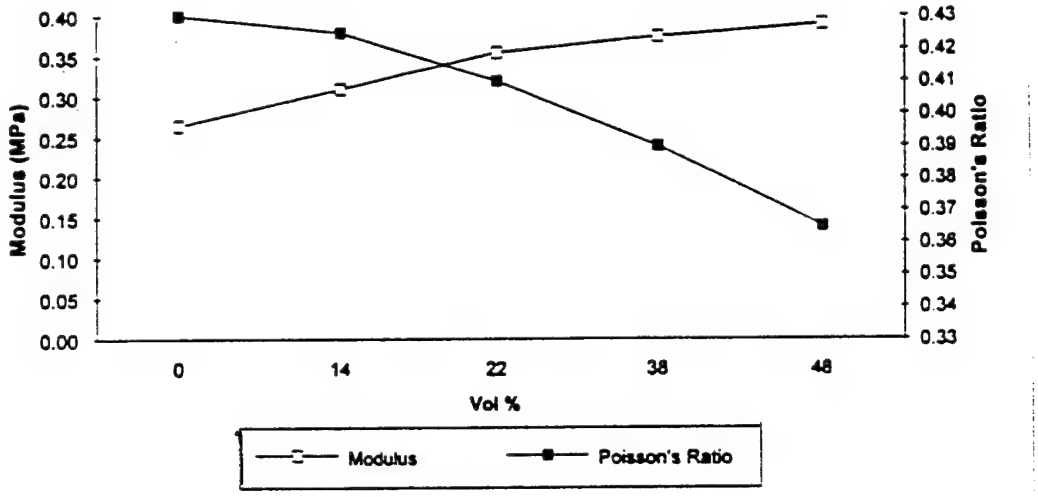

Figure 9. Effect of volume fraction filler content on tensile modulus and Poisson's ratio.

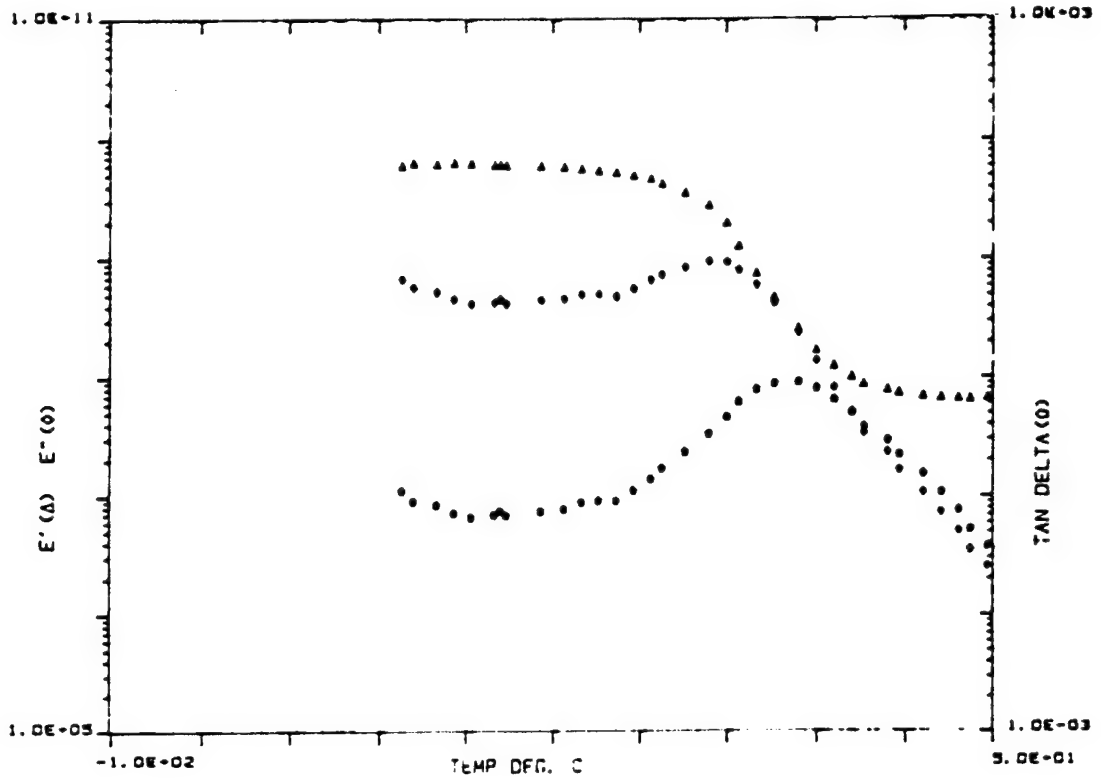

Figure 10. Effect of temperature on tensile storage modulus (E'), tensile loss modulus (E"), and the loss factor (tan δ) for EN-2 material containing 38 volume percent microspheres.

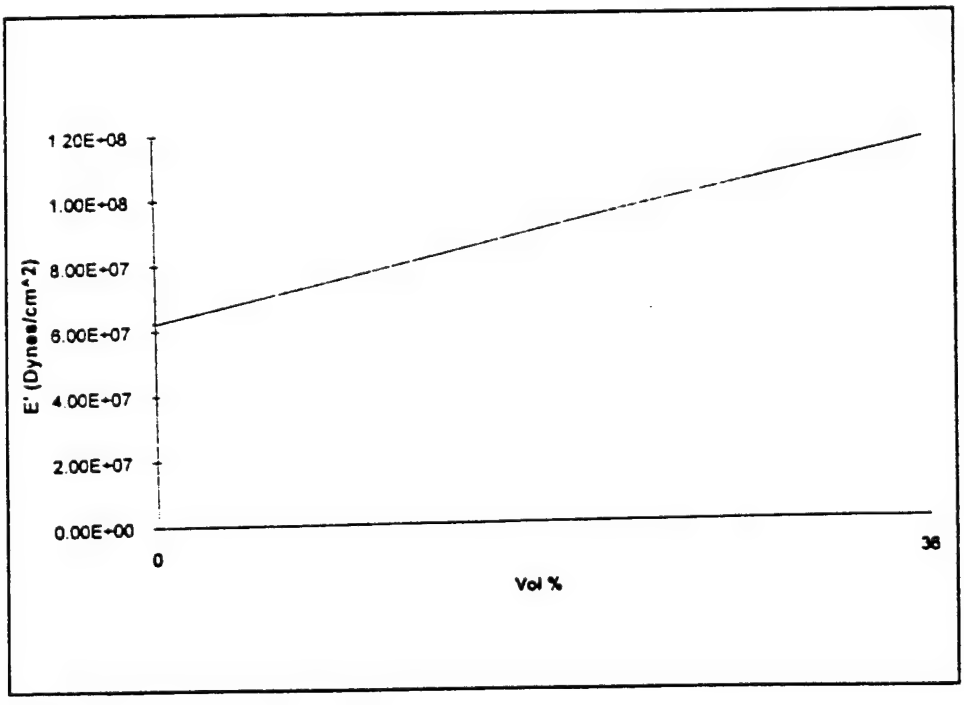

Figure 11. Effect of volume fraction filler on E'.

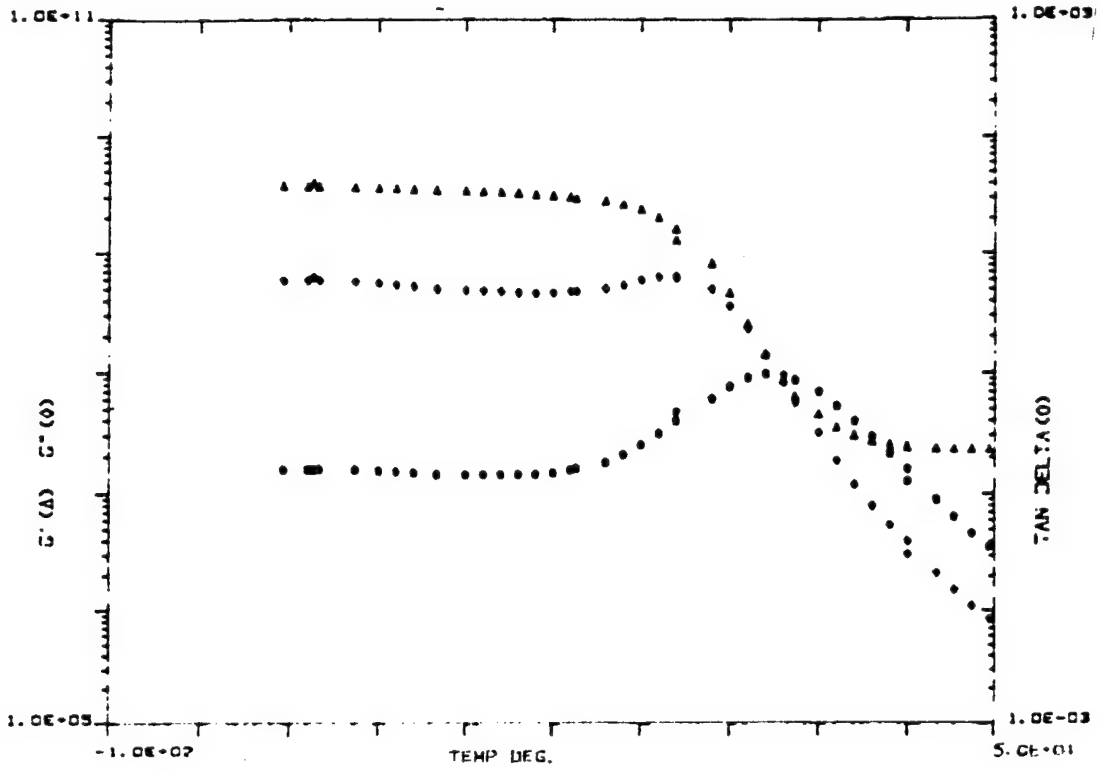

Figure 12. Shear response properties corresponding to those given in Figure 10 for tensile.

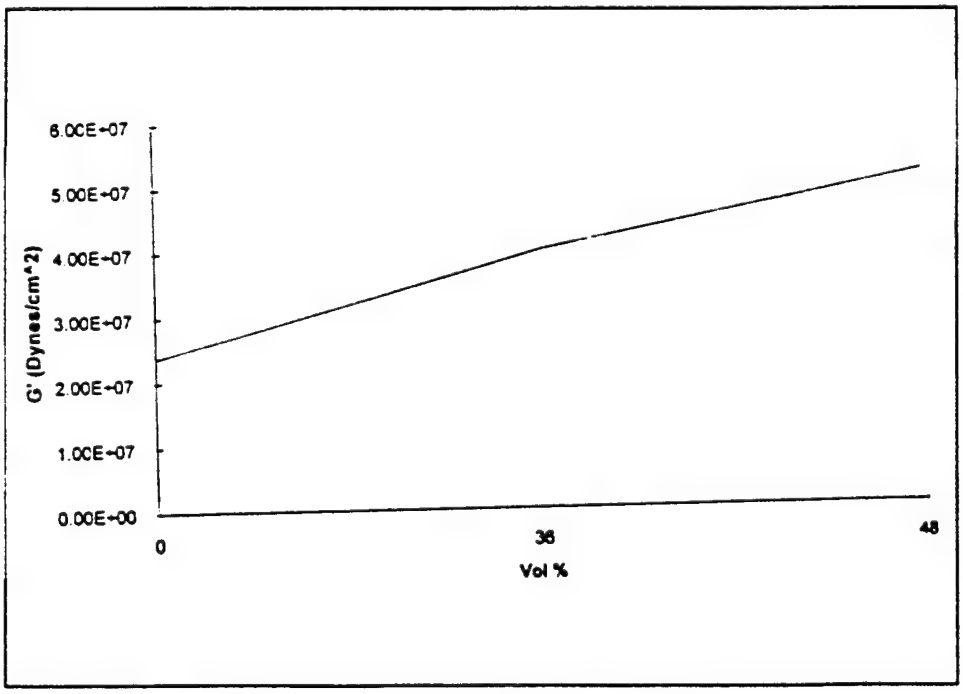

Figure 13. Effect of volume fraction filler on G'.

APPENDIX B

100 mm TRANSDUCER TEST DATA

Measurements made by:

Raytheon Company
Portsmouth, RI

and

Westinghouse Electric Corporation
Annapolis, MD

SUMMARY

Transmitting Voltage Response (TVR) and Receiving Voltage Sensitivity (RVS) of several 100 mm square SonoPanel™ transducers were measured underwater at Raytheon and Westinghouse during 1993. These tests were made by the respective systems companies at no cost to the program.

The test results are presented in this appendix. The following transducers were tested:

Company	Date	Transducer	Description	Test Data
Raytheon	Jul-93	B	100 x 100 mm Standard SonoPanel	RVS - Face RVS - Edge Beam Patterns
Raytheon	Jul-93	#1	100 x 100 mm 1-3 Composite Hard Epoxy Matrix No Face Plates	RVS - Face RVS - Edge Beam Patterns
Raytheon	Jul-93	F	100 x 100 mm MSI Proprietary Design	Transmit Response RVS - Face RVS - Edge Beam Patterns
Westinghouse	Sep-93	MSI-1	100 x 100 mm Standard SonoPanel	TVR RVS - Face Beam Patterns
Westinghouse	Sep-93	MSI-2	100 x 100 mm MSI Proprietary Design	TVR RVS - Face Beam Patterns

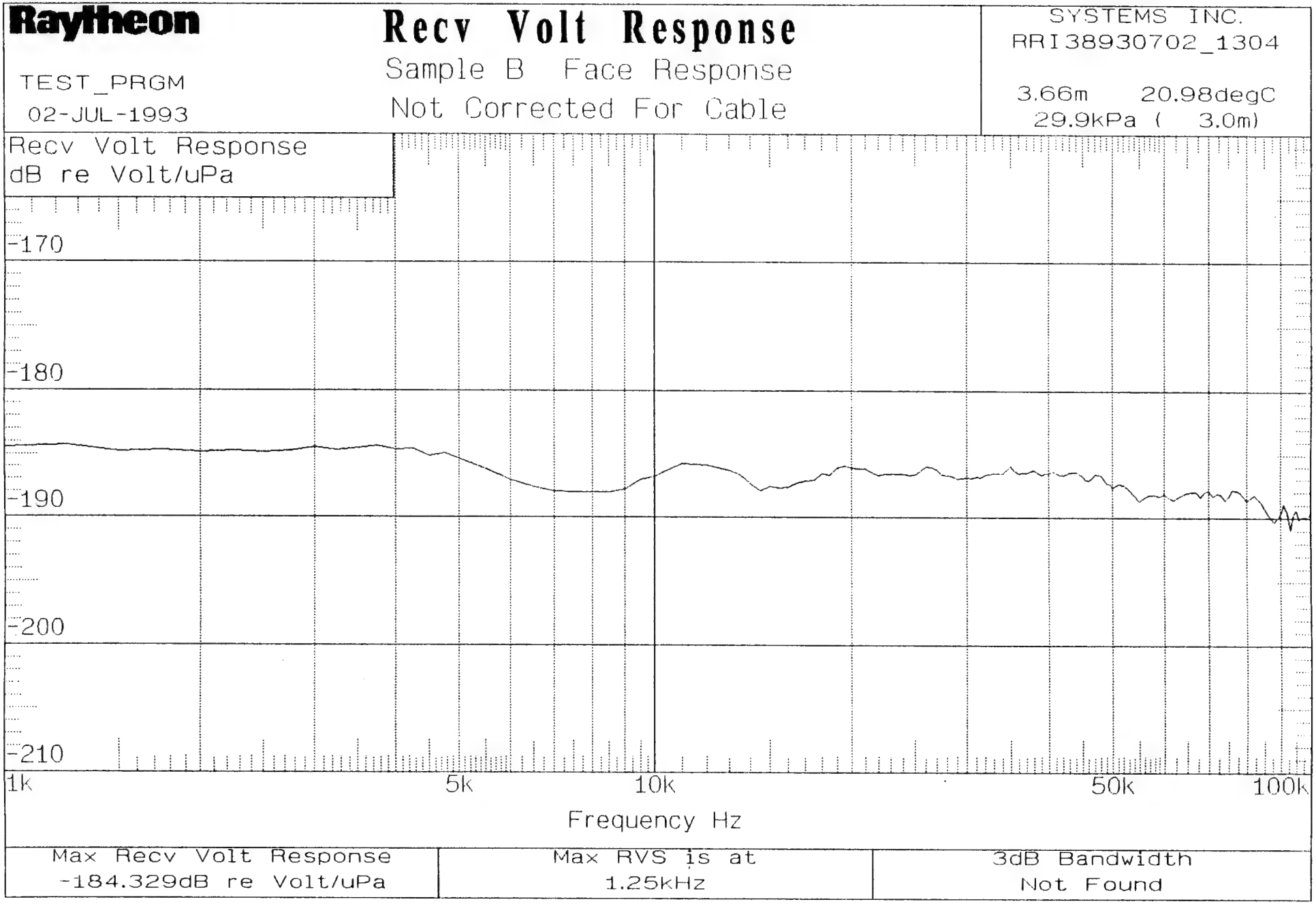
Raytheon
Recv Volt Response
Sample B Face Response
Not Corrected For Cable
SYSTEMS INC.
RRI38930702_1304
TEST_PRGM
02-JUL-1993
3.66m 20.98degC
29.9kPa (3.0m)
Recv Volt Response
dB re Volt/uPa
-170
-180
-190
-200
-210
1k
5k
10k
50k
100k
Frequency Hz
Max Recv Volt Response
-184.329dB re Volt/uPa
Max RVS is at
1.25kHz
3dB Bandwidth
Not Found

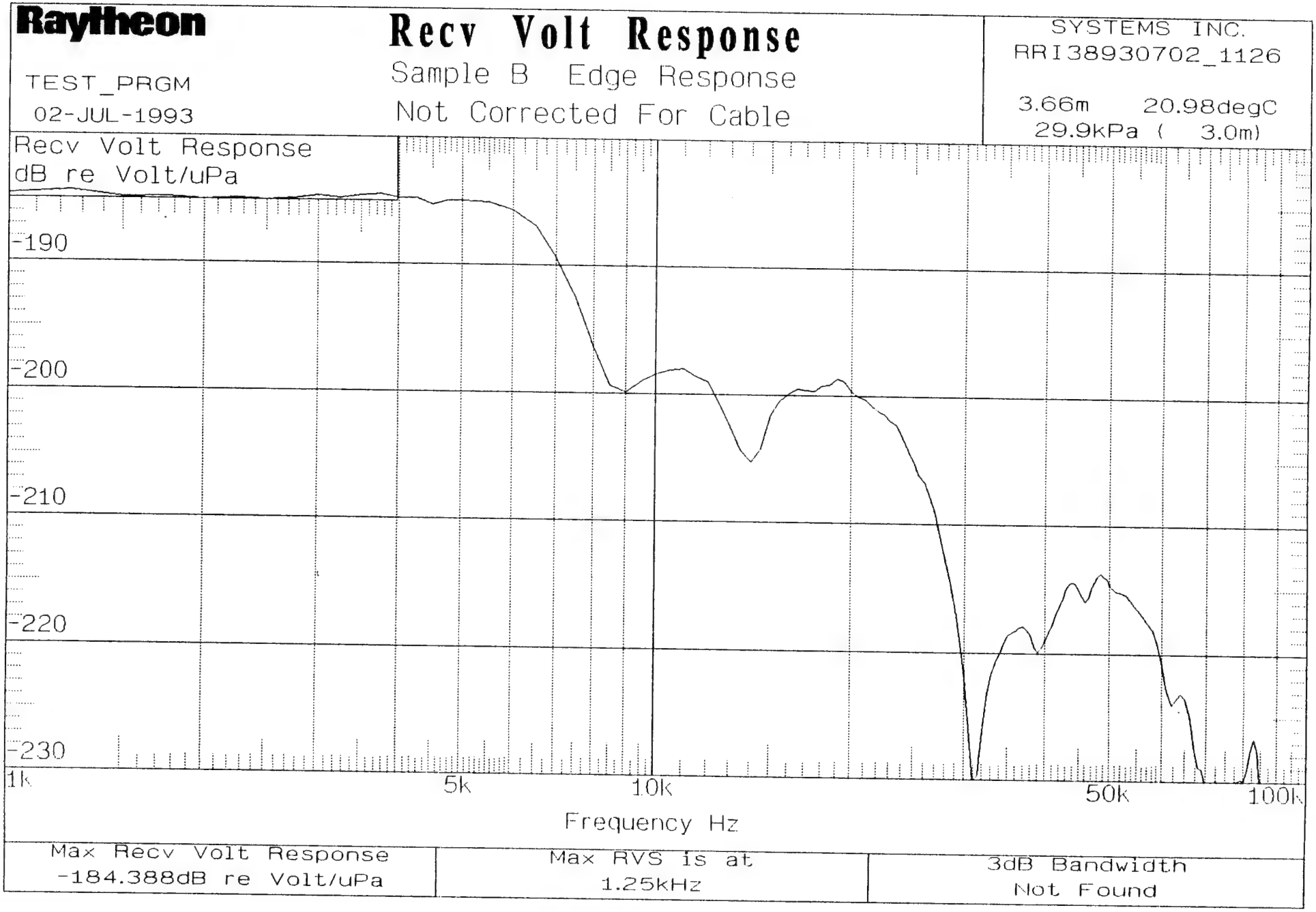
Raytheon
Recv Volt Response
Sample B Edge Response
Not Corrected For Cable
SYSTEMS INC.
RRI38930702_1126
3.66m 20.98degC
29.9kPa (3.0m)
TEST_PRGM
02-JUL-1993
Recv Volt Response
dB re Volt/uPa
-190
-200
-210
-220
-230
1k
5k
10k
50k
100k
Frequency Hz
Max Recv Volt Response
-184.388dB re Volt/uPa
Max RVS is at
1.25kHz
3dB Bandwidth
Not Found

Raytheon

RECEIVE PATTERN

Sample B

X/Y Plane

TEST_PRGM
02-JUL-1993

SYSTEMS INC.
RBI38930702_1319
Frequency 10k
3.66m 20.97degC
29.9kPa (3.0m)

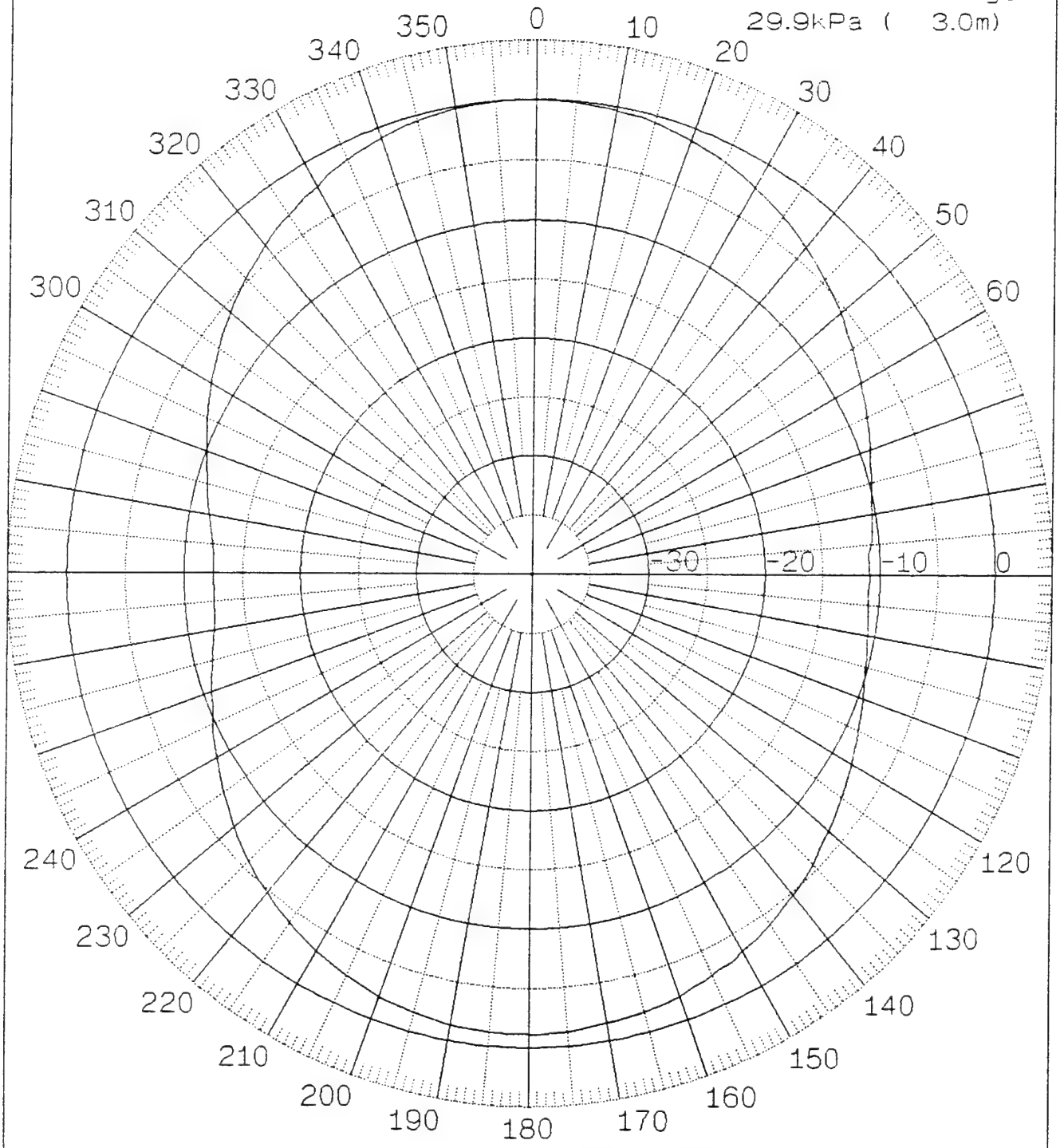

Relative Response in dB

Maximum Response Angle	Maximum Response Value	Beam Width	DI
.51 Degrees	-186.92 dB re V/uPa	70.59 Deg	6.06 dB

Raytheon

RECEIVE PATTERN

Sample B Edge Response

X/Y Plane

TEST_PRGM
02-JUL-1993

SYSTEMS INC.
RBI38930702_1135
Frequency 100k
3.66m 20.97degC
29.9kPa (3.0m)

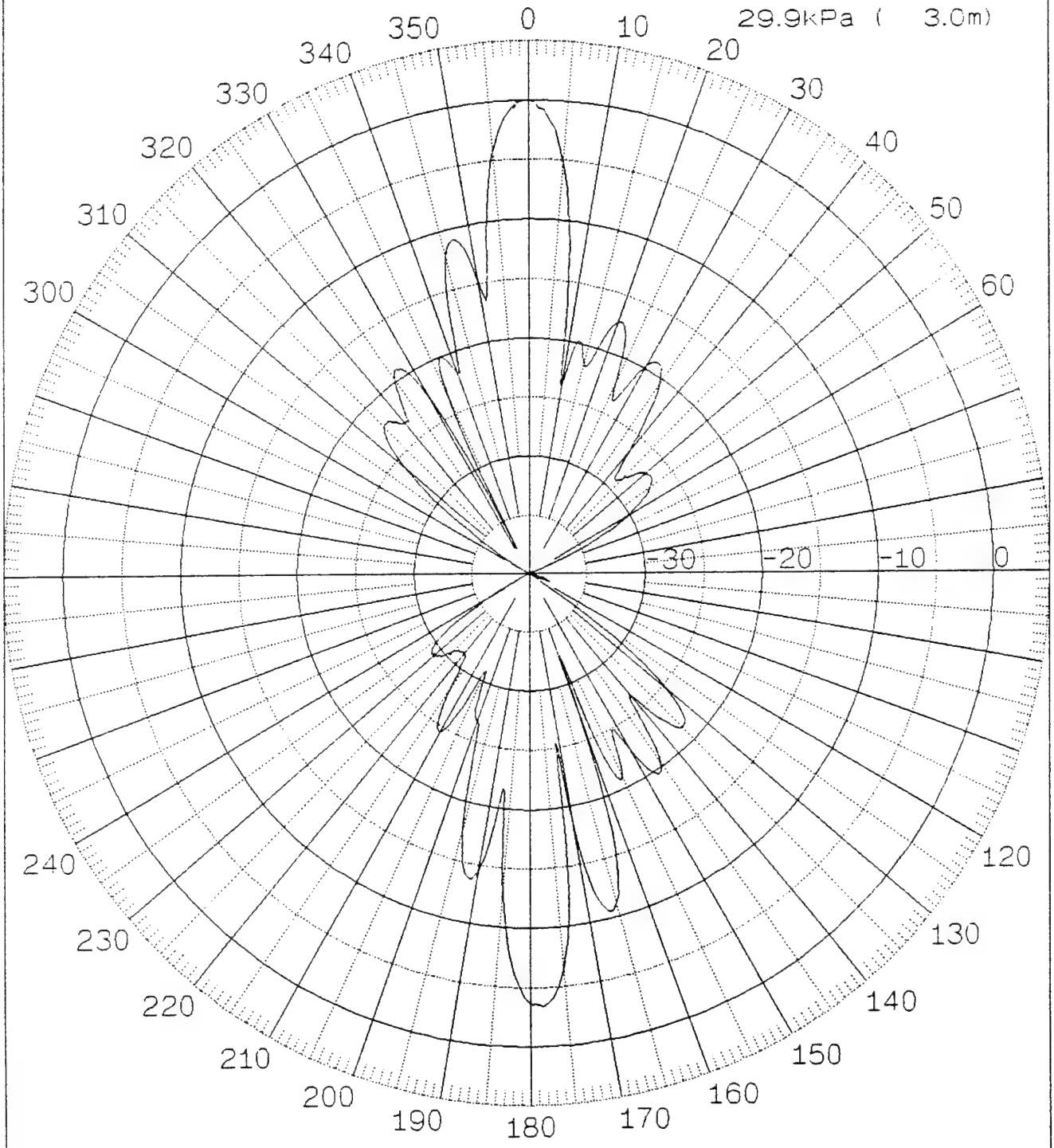

Relative Response in dB

Maximum Response Angle	Maximum Response Value	Beam Width	DI
180.01 Degrees	-189.73 dB re V/uPa	8.09 Deg	22.87 dB

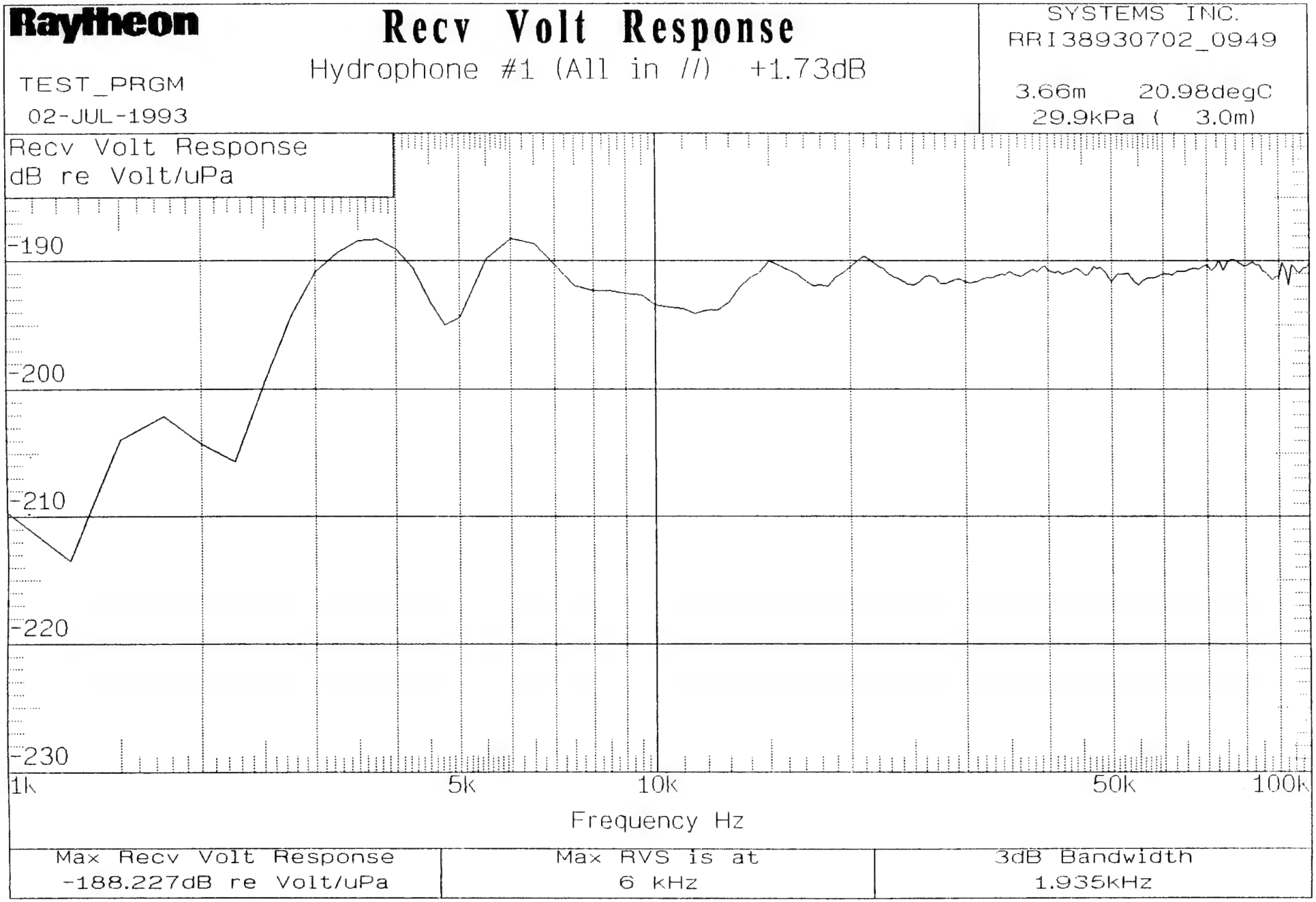
Raytheon
Recv Volt Response
Hydrophone #1 (All in //) +1.73dB
SYSTEMS INC.
RRI38930702_0949
TEST_PRGM
02-JUL-1993
3.66m 20.98degC
29.9kPa (3.0m)
Recv Volt Response
dB re Volt/uPa
-190
-200
-210
-220
-230
1k
5k
10k
50k
100k
Frequency Hz
Max Recv Volt Response
-188.227dB re Volt/uPa
Max RVS is at
6 kHz
3dB Bandwidth
1.935kHz

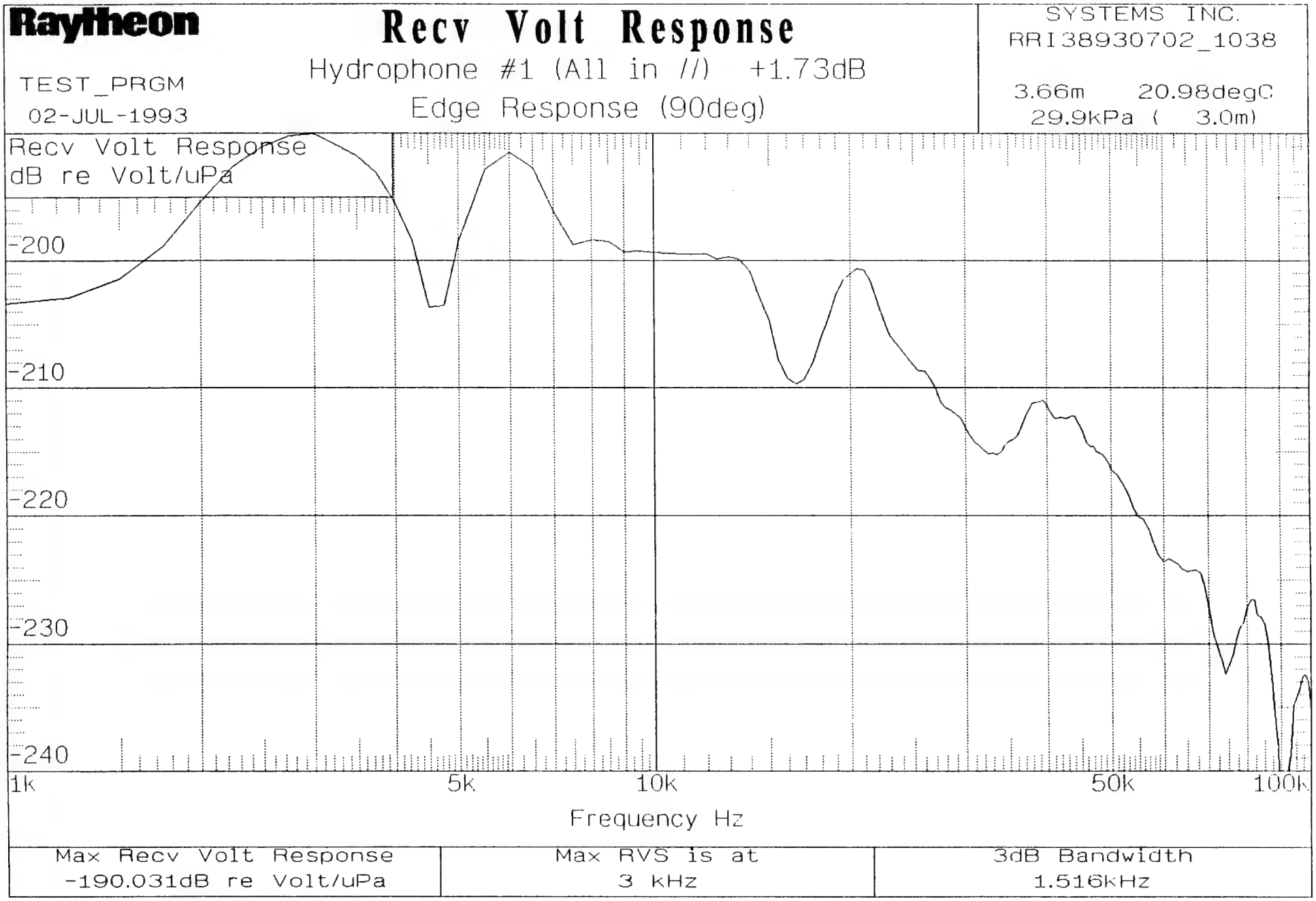
Raytheon
Recv Volt Response
Hydrophone #1 (All in //) +1.73dB
Edge Response (90deg)
TEST_PRGM
02-JUL-1993
SYSTEMS INC.
RRI38930702_1038
3.66m 20.98degC
29.9kPa (3.0m)
Recv Volt Response
dB re Volt/uPa
-200
-210
-220
-230
-240
1k
5k
10k
50k
100k
Frequency Hz
Max Recv Volt Response
-190.031dB re Volt/uPa
Max RVS is at
3 kHz
3dB Bandwidth
1.516kHz

Raytheon

RECEIVE PATTERN

Hydrophone #1 (All in //) +1.73dB

X/Y Plane

TEST_PRGM
02-JUL-1993

SYSTEMS INC.
RBI38930702_1014
Frequency 2k
3.66m 20.98degC
29.9kPa (3.0m)

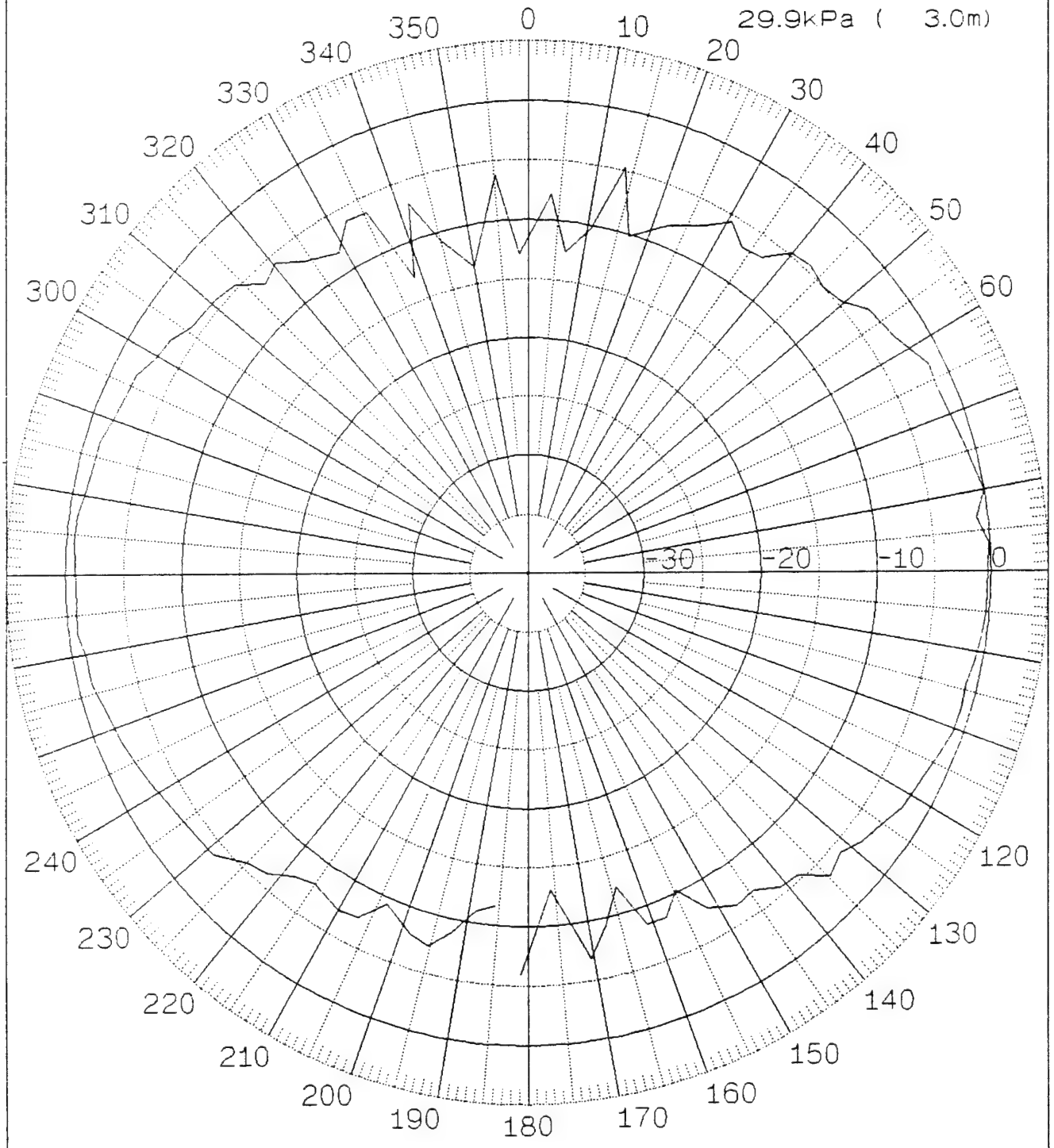

Relative Response in dB

Maximum Response Angle	Maximum Response Value	Beam Width	DI
80.08 Degrees	-195.15 dB re V/uPa	71.44 Deg	5.30 dB

Raytheon

RECEIVE PATTERN

Hydrophone #1 (All in //) +1.73dB

X/Y Plane

TEST_PRGM
02-JUL-1993

SYSTEMS INC.
RBI38930702_1007
Frequency 3.5k
3.66m 20.98degC
29.9kPa (3.0m)

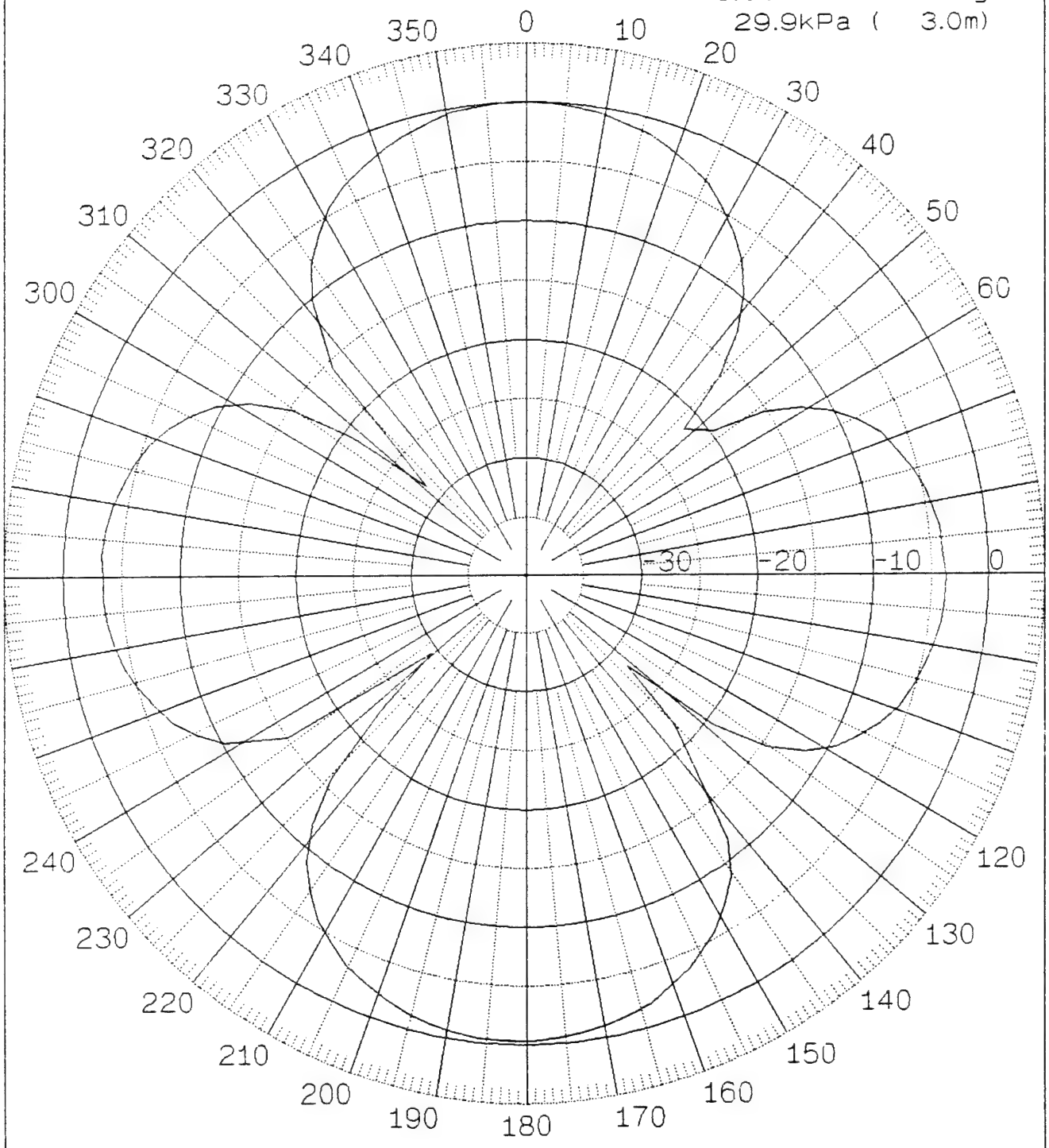

Relative Response in dB

Maximum Response Angle	Maximum Response Value	Beam Width	DI
.02 Degrees	-188.51 dB re V/uPa	47.58 Deg	5.91 dB

Raytheon

RECEIVE PATTERN

Hydrophone #1 (All in //) +1.73dB

X/Y Plane

TEST_PRGM
02-JUL-1993

SYSTEMS INC.
RBI38930702_1025
Frequency 5k
3.66m 20.98degC
29.9kPa (3.0m)

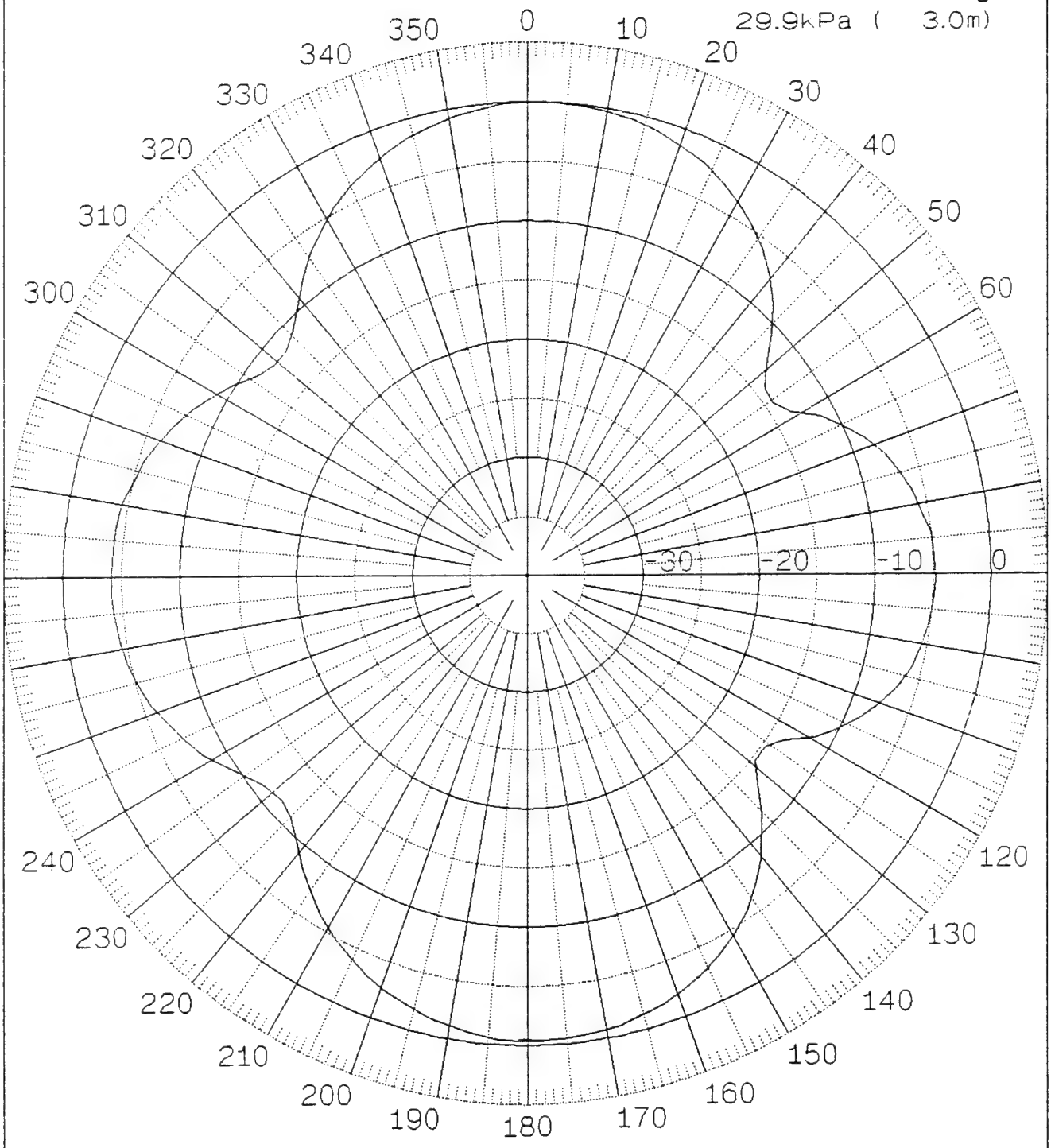

Relative Response in dB

Maximum Response Angle	Maximum Response Value	Beam Width	DI
.31 Degrees	-194.62 dB re V/uPa	50.05 Deg	6.11 dB

Raytheon

RECEIVE PATTERN

Hydrophone #1 (All in //) +1.73dB

X/Y Plane

TEST_PRGM
02-JUL-1993

SYSTEMS INC.
RBI38930702_0925
Frequency 100k
3.66m 20.98degC
29.9kPa (3.0m)

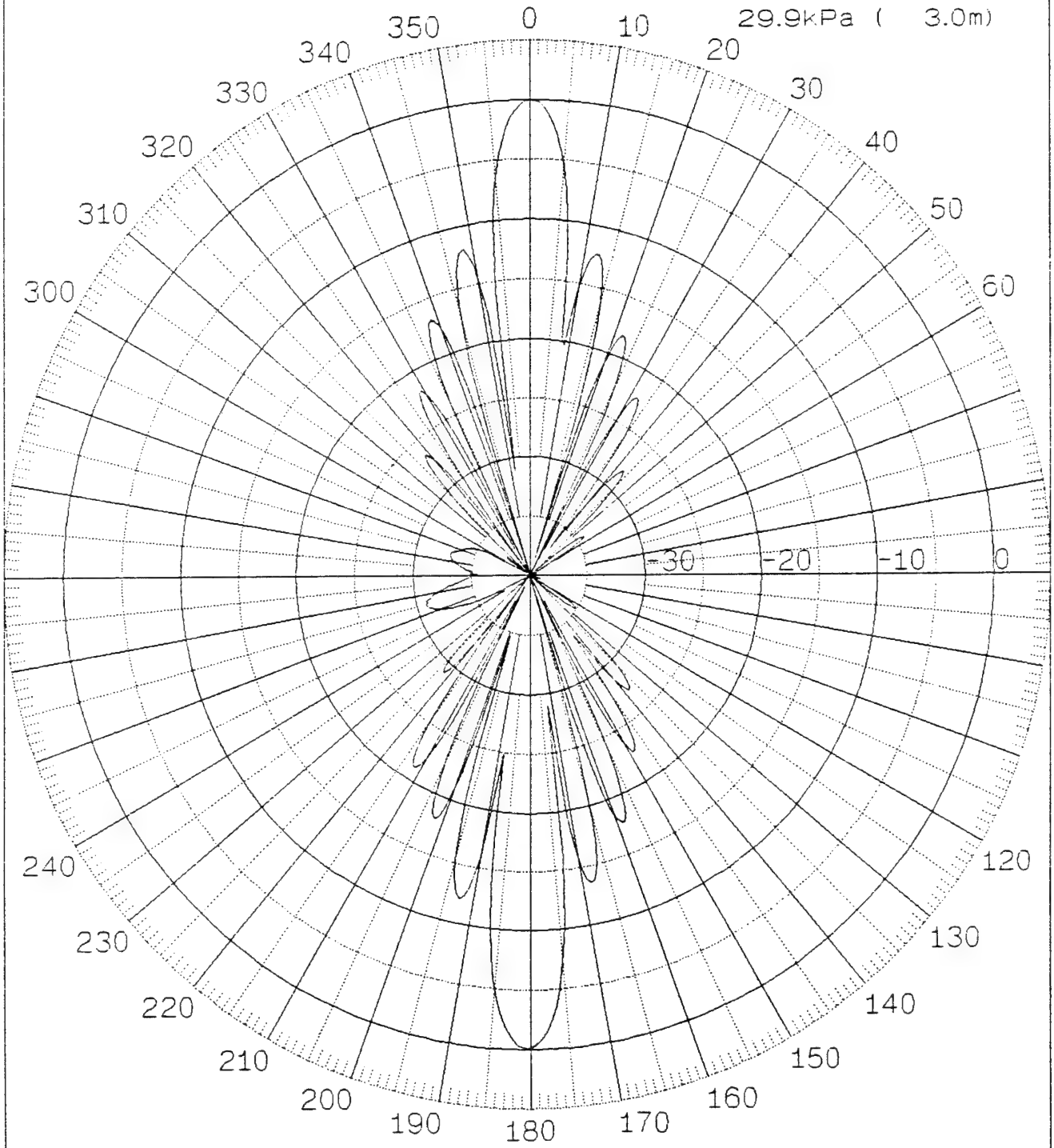

Relative Response in dB

Maximum Response Angle	Maximum Response Value	Beam Width	DI
.05 Degrees	-190.13 dB re V/uPa	7.37 Deg	23.31 dB

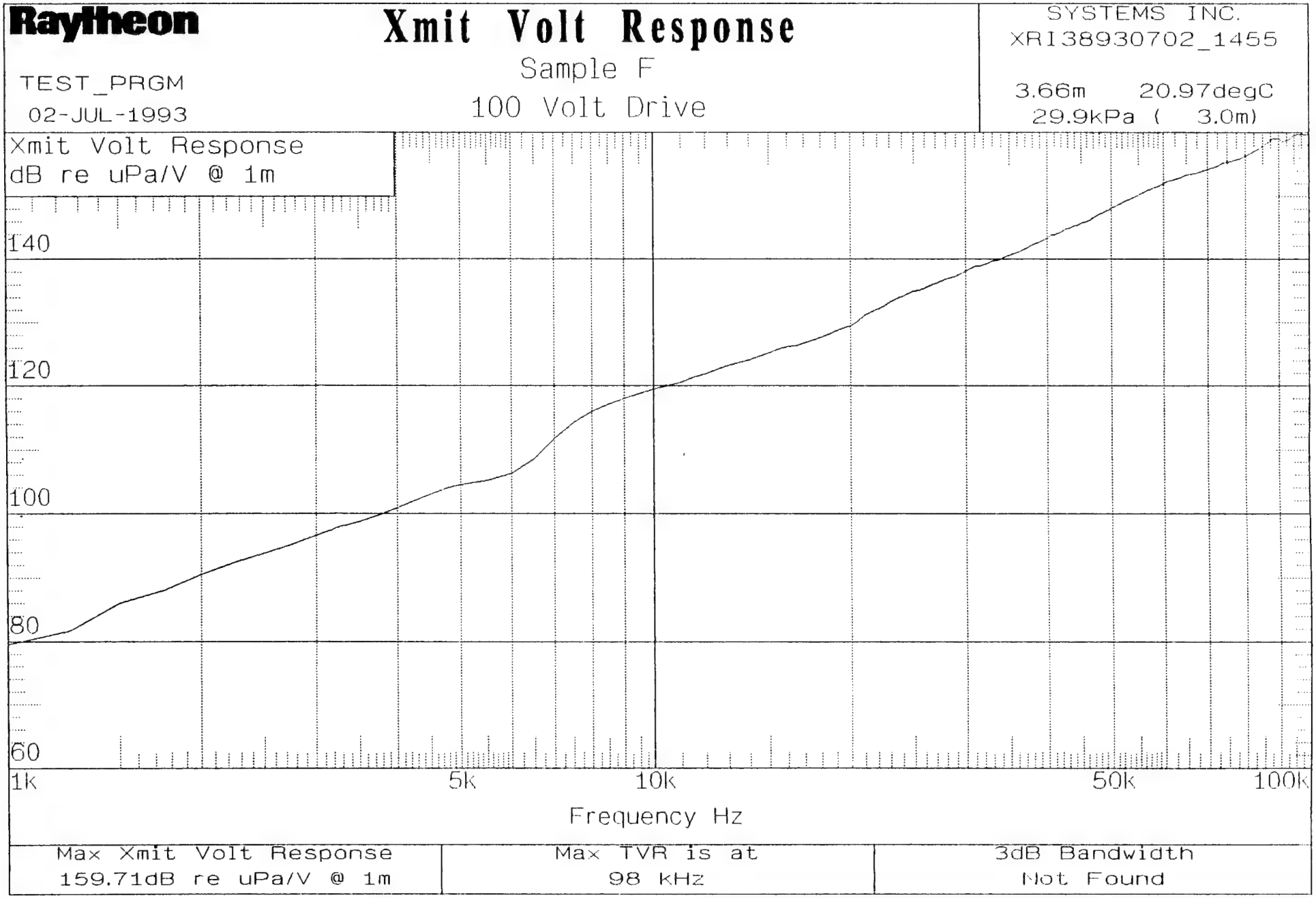
Raytheon
Xmit Volt Response
Sample F
100 Volt Drive
SYSTEMS INC.
XRI38930702_1455
TEST_PRGM
02-JUL-1993
3.66m 20.97degC
29.9kPa (3.0m)
Xmit Volt Response
dB re uPa/V @ 1m
140
120
100
80
60
1k
5k
10k
50k
100k
Frequency Hz
Max Xmit Volt Response
159.71dB re uPa/V @ 1m
Max TVR is at
98 kHz
3dB Bandwidth
Not Found

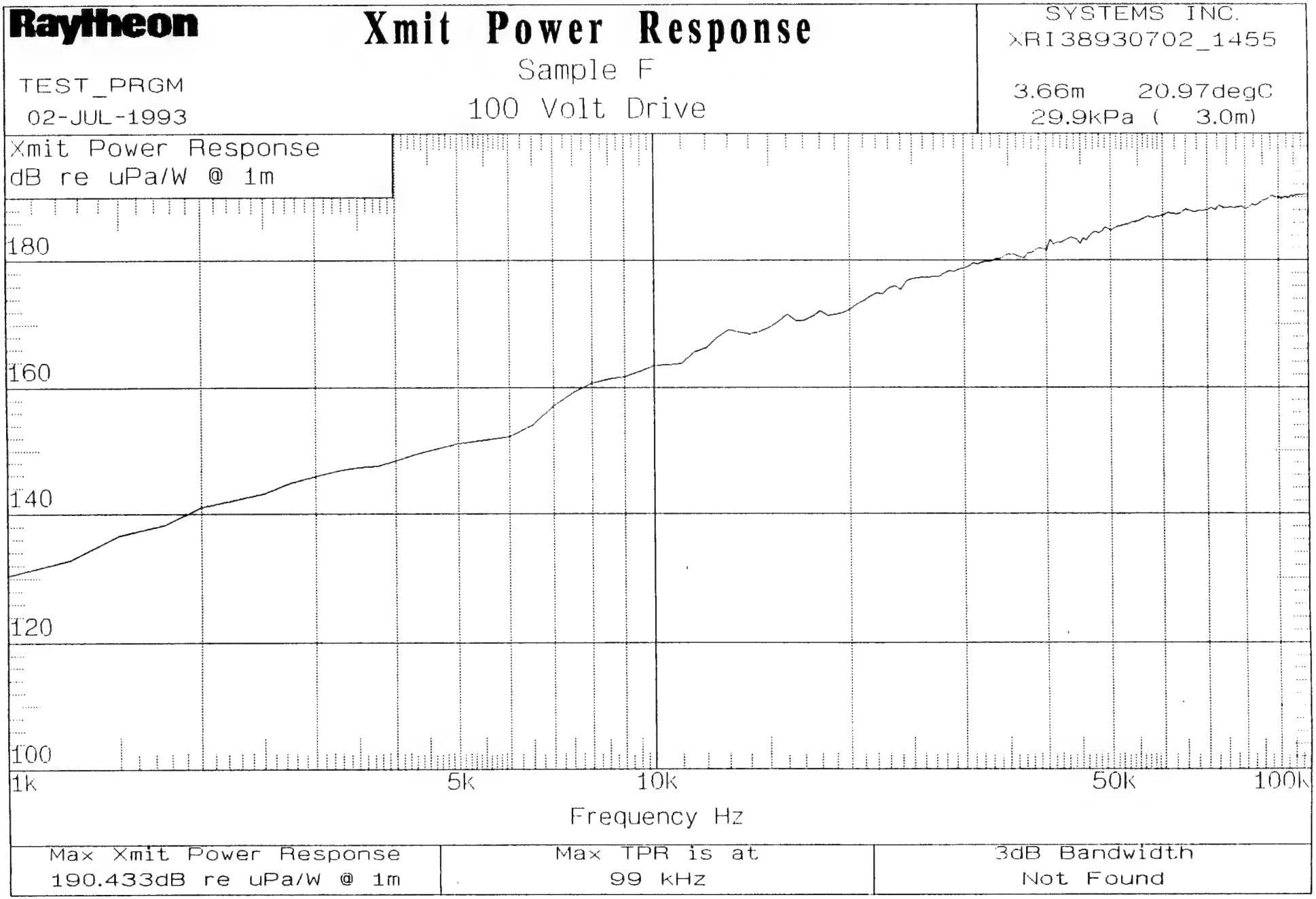
Raytheon
Xmit Power Response
Sample F
100 Volt Drive
SYSTEMS INC.
XRI38930702_1455
TEST_PRGM
02-JUL-1993
3.66m 20.97degC
29.9kPa (3.0m)
Xmit Power Response
dB re uPa/W @ 1m
180
160
140
120
100
1k
5k
10k
50k
100k
Frequency Hz
Max Xmit Power Response
190.433dB re uPa/W @ 1m
Max TPR is at
99 kHz
3dB Bandwidth
Not Found

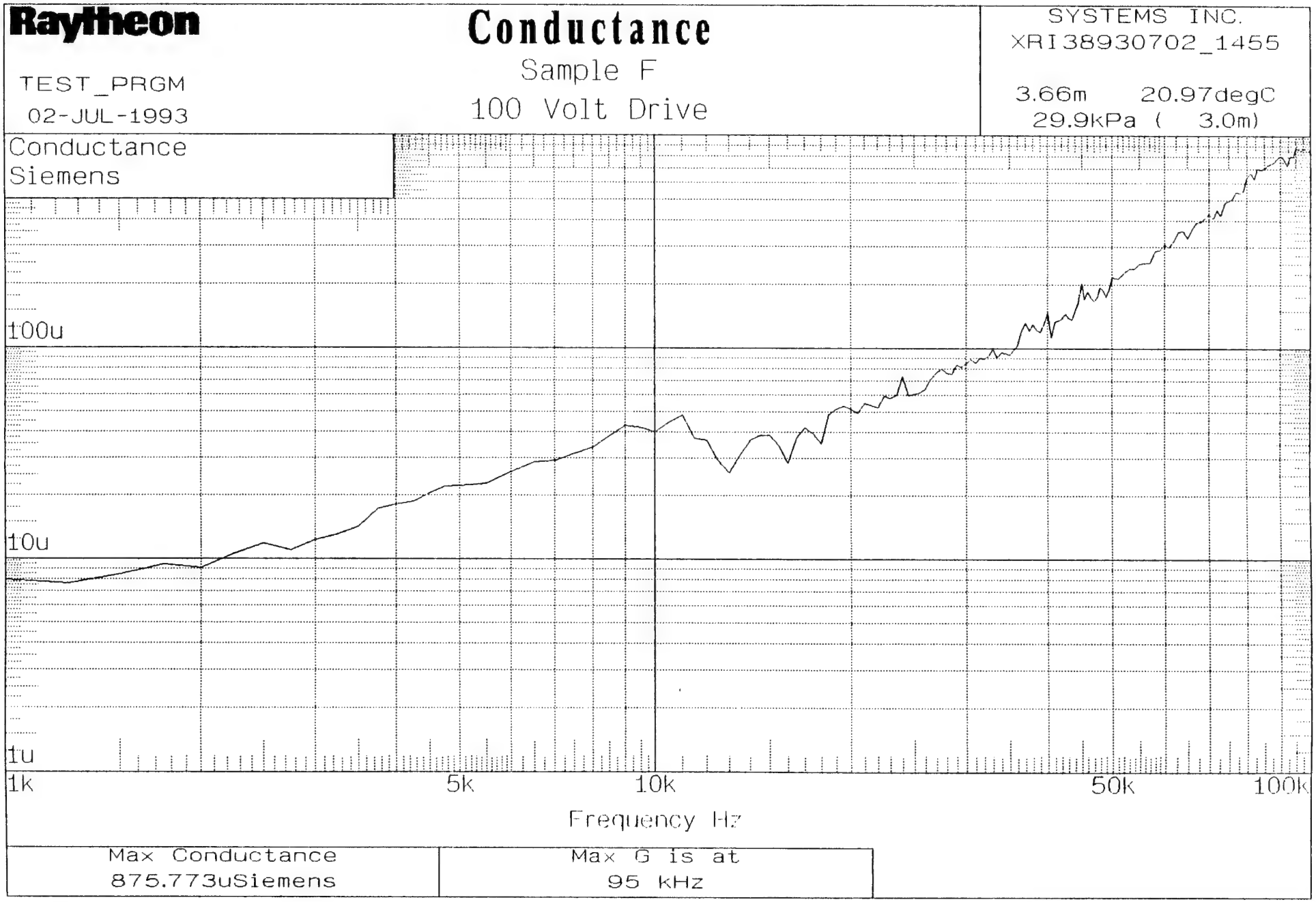
Raytheon
Conductance
Sample F
100 Volt Drive
SYSTEMS INC.
XRI38930702_1455
TEST_PRGM
02-JUL-1993
3.66m 20.97degC
29.9kPa (3.0m)
Conductance
Siemens
100u
10u
1u
1k
5k
10k
50k
100k
Frequency Hz
Max Conductance
875.773uSiemens
Max G is at
95 kHz

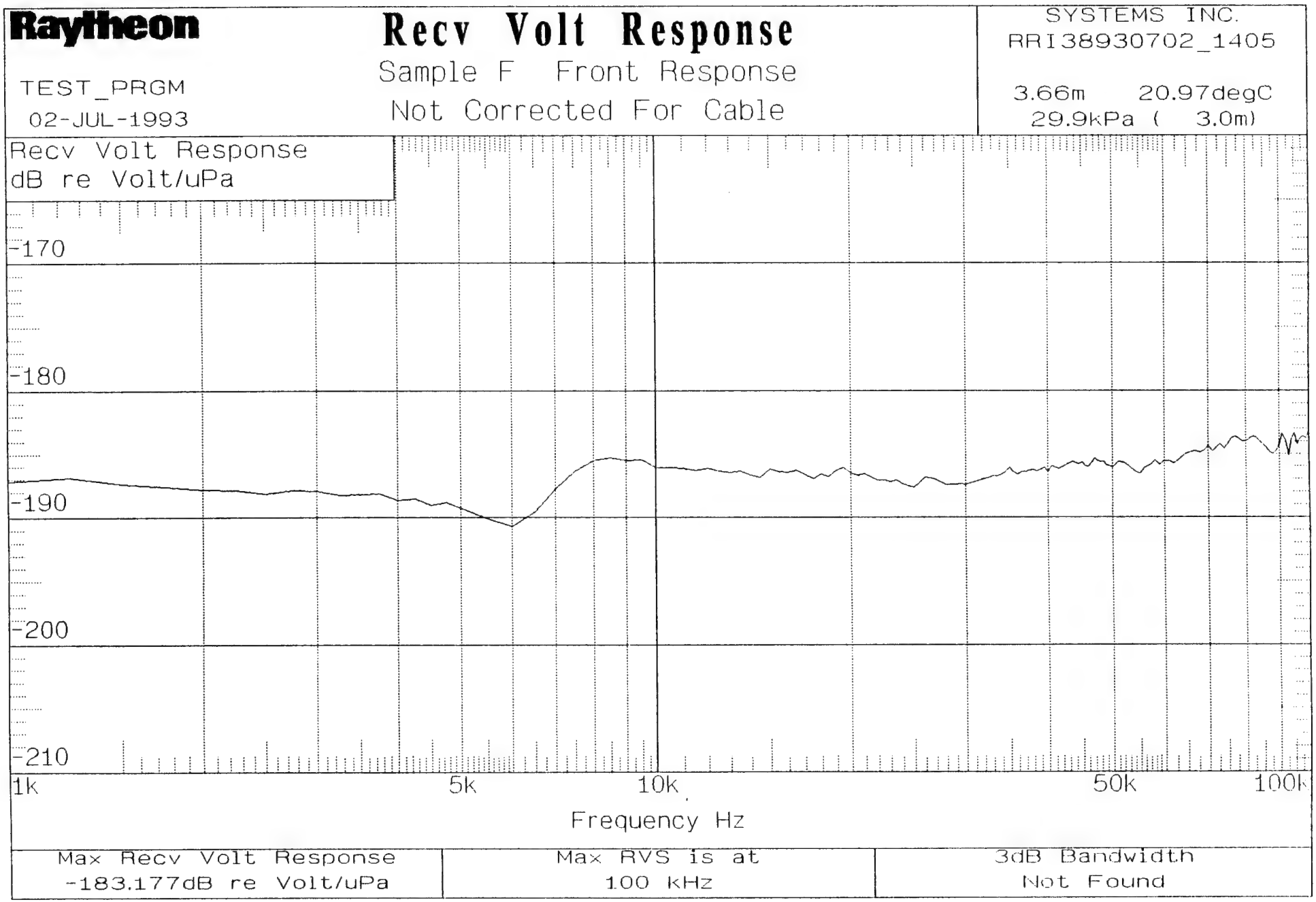
Raytheon
Recv Volt Response
Sample F Front Response
Not Corrected For Cable
SYSTEMS INC.
RRI38930702_1405
TEST_PRGM
02-JUL-1993
3.66m 20.97degC
29.9kPa (3.0m)
Recv Volt Response
dB re Volt/uPa
-170
-180
-190
-200
-210
1k
5k
10k
50k
100k
Frequency Hz
Max Recv Volt Response
-183.177dB re Volt/uPa
Max RVS is at
100 kHz
3dB Bandwidth
Not Found

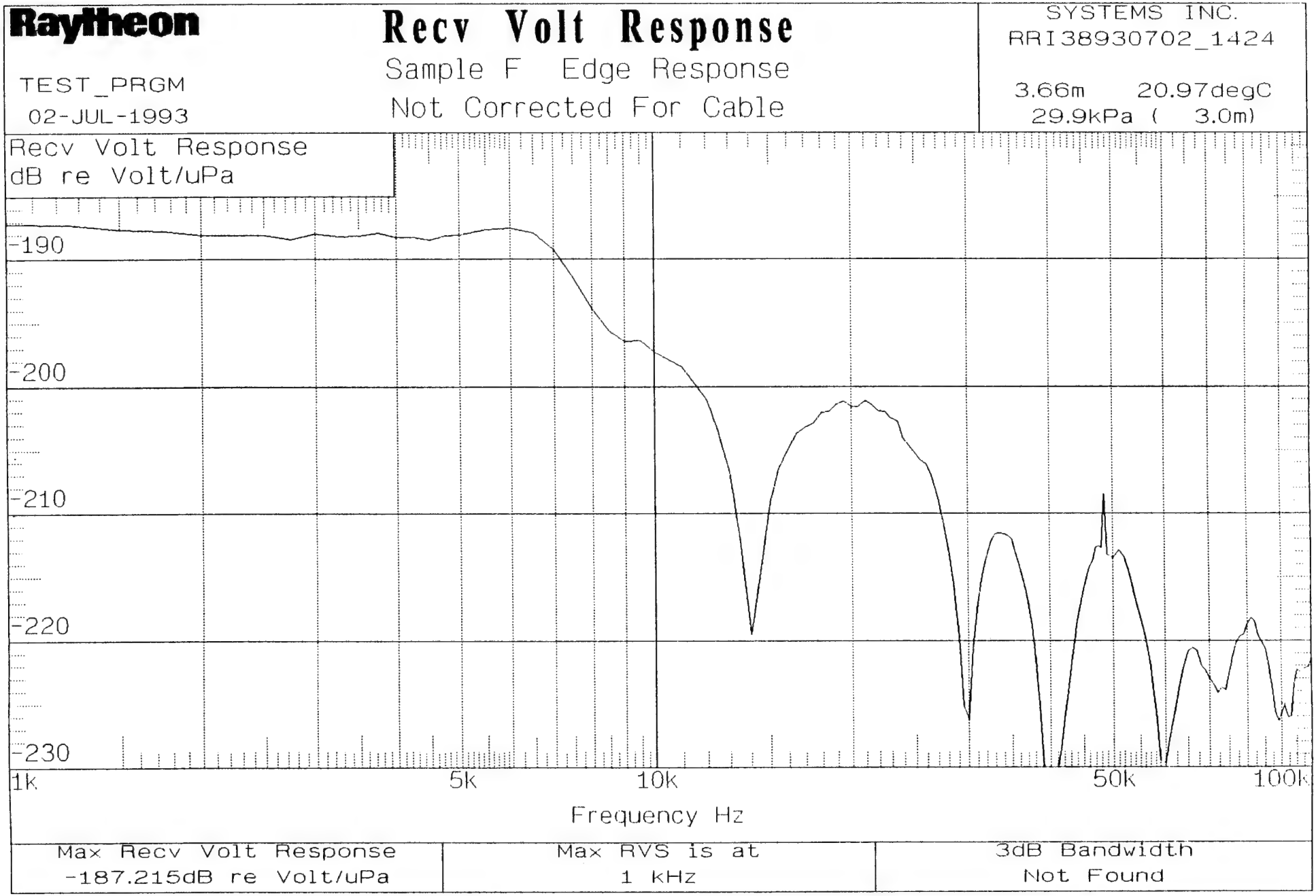
Raytheon
Recv Volt Response
Sample F Edge Response
Not Corrected For Cable
SYSTEMS INC.
RRI38930702_1424
TEST_PRGM
02-JUL-1993
3.66m 20.97degC
29.9kPa (3.0m)
Recv Volt Response
dB re Volt/uPa
-190
-200
-210
-220
-230
1k
5k
10k
50k
100k
Frequency Hz
Max Recv Volt Response
-187.215dB re Volt/uPa
Max RVS is at
1 kHz
3dB Bandwidth
Not Found

Raytheon

TRANSMIT PATTERN

Sample F

X/Y Plane

TEST_PRGM
02-JUL-1993

SYSTEMS INC.
XBI38930702_1503
Frequency 6k
3.66m 20.97degC
29.9kPa (3.0m)

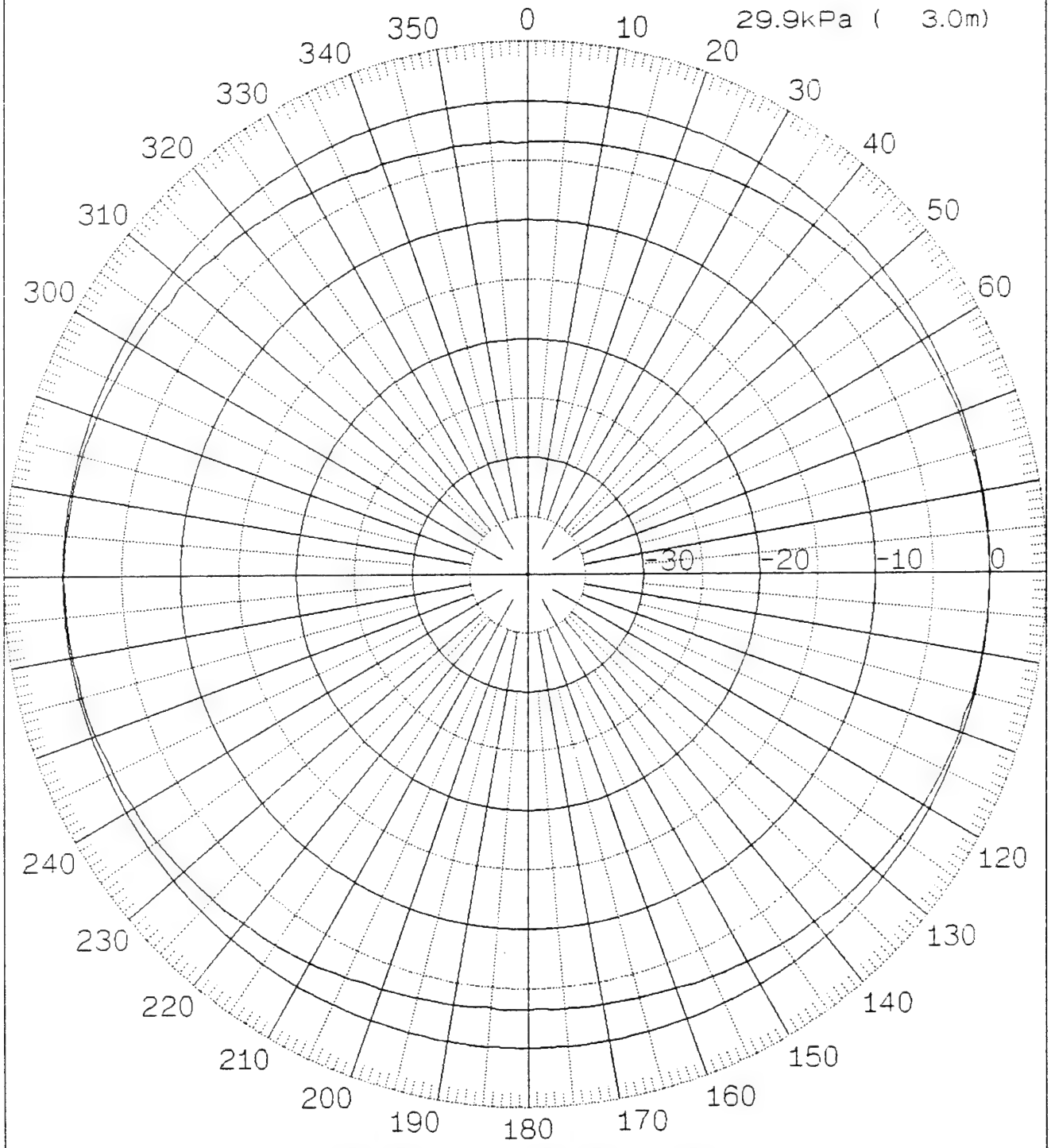

Relative Response in dB

Maximum Response Angle	Maximum Response Value	Beam Width	DI
91.11 Degrees	109.31 dB re uPa/V @ 1m	149.41 Deg	2.00 dB

Raytheon

RECEIVE PATTERN

Sample F

X/Y Plane

TEST_PRGM
02-JUL-1993

SYSTEMS INC.
RBI38930702_1341
Frequency 100k
3.66m 20.97degC
29.9kPa (3.0m)

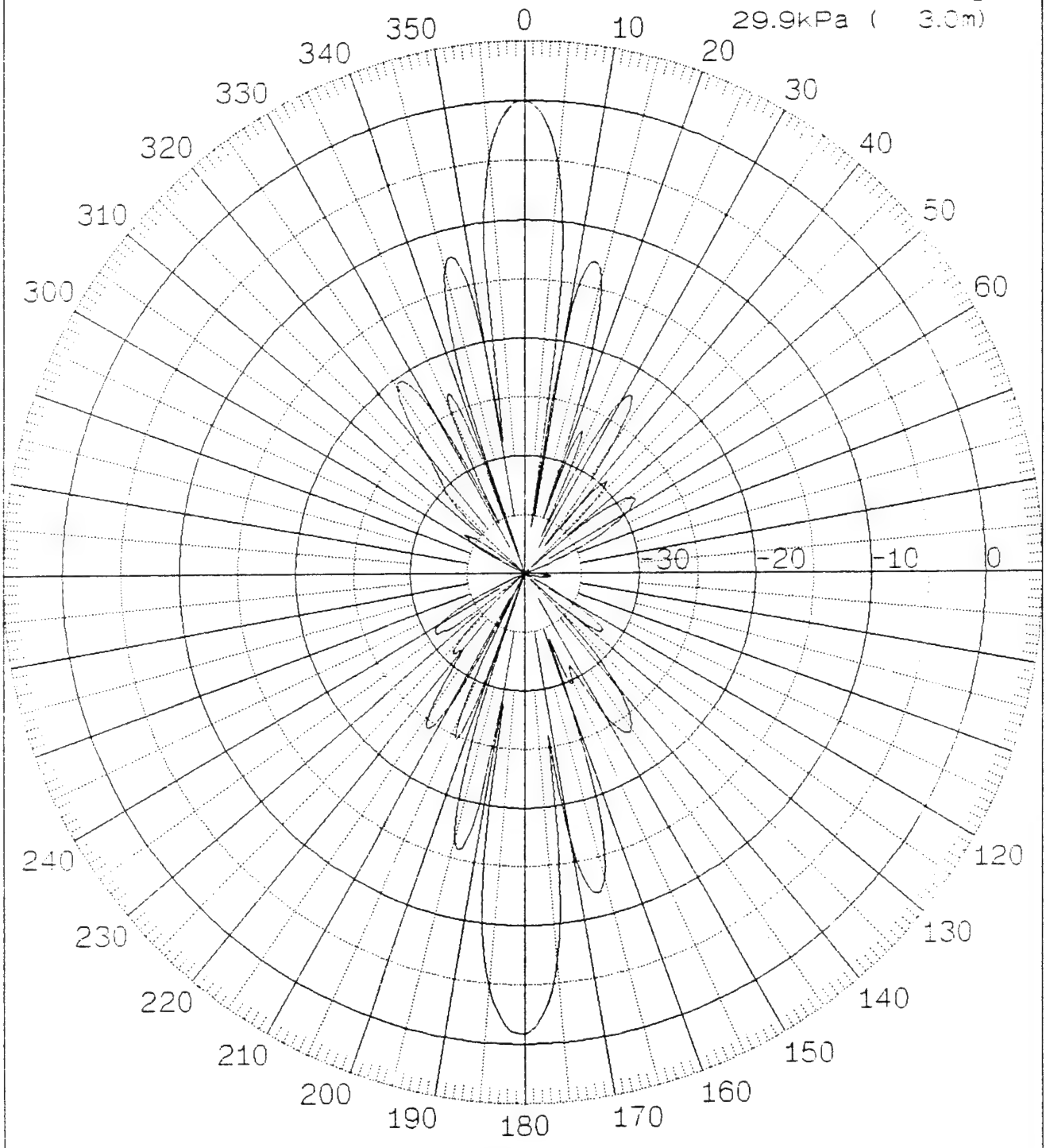

Relative Response in dB

Maximum Response Angle	Maximum Response Value	Beam Width	DI
-178.17 Degrees	-183.14 dB re V/uPa	Not Found	23.27 dB

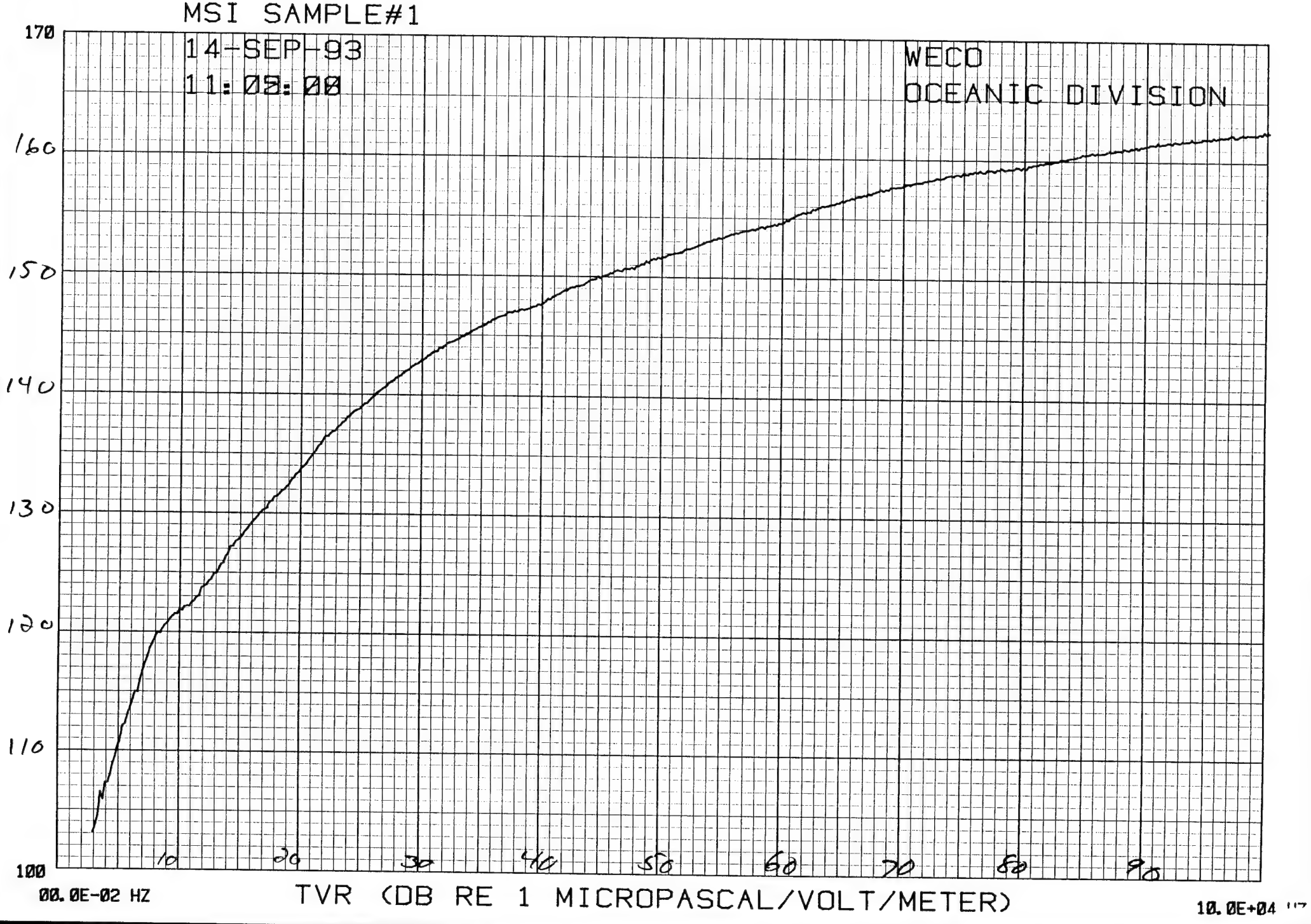

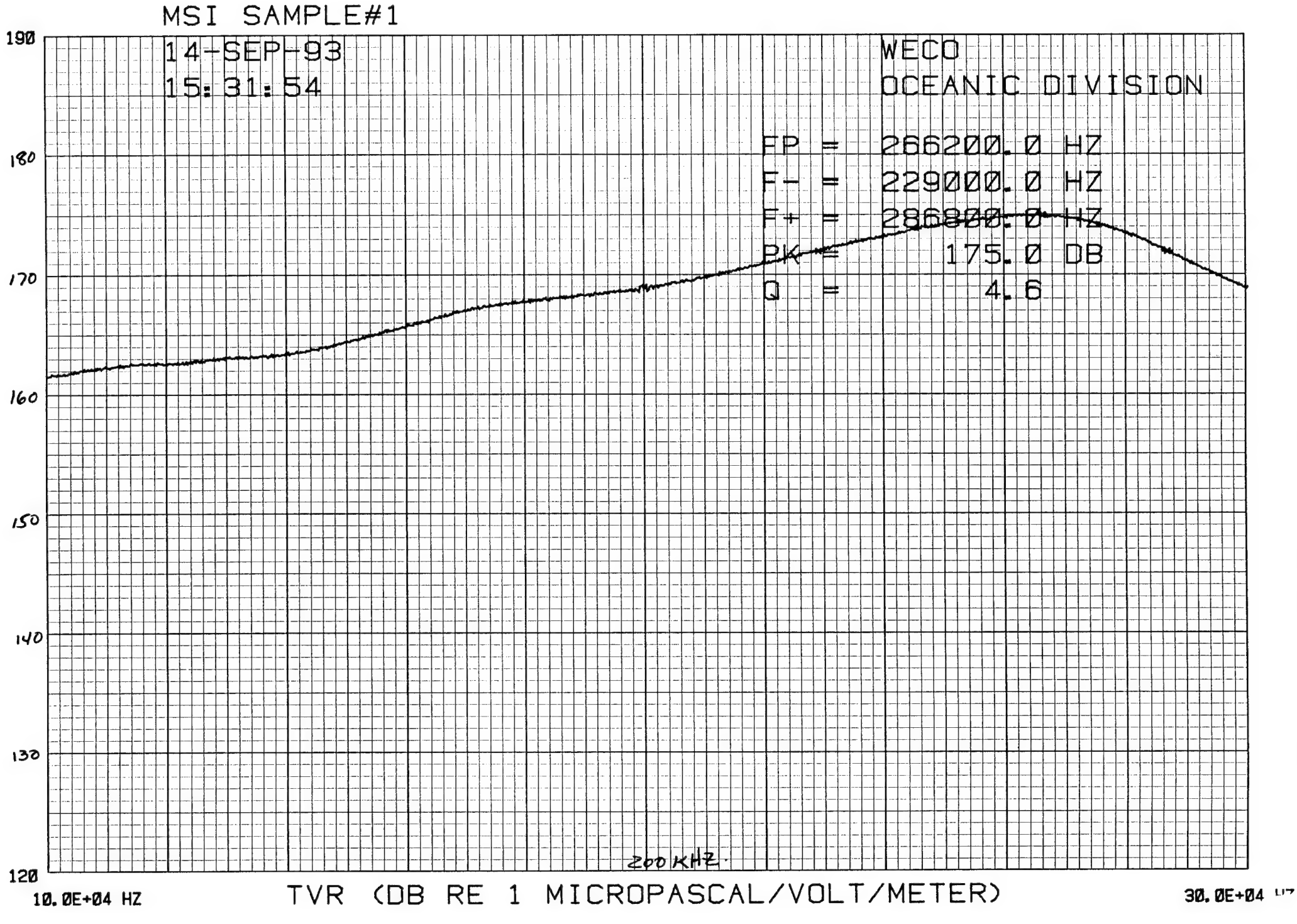

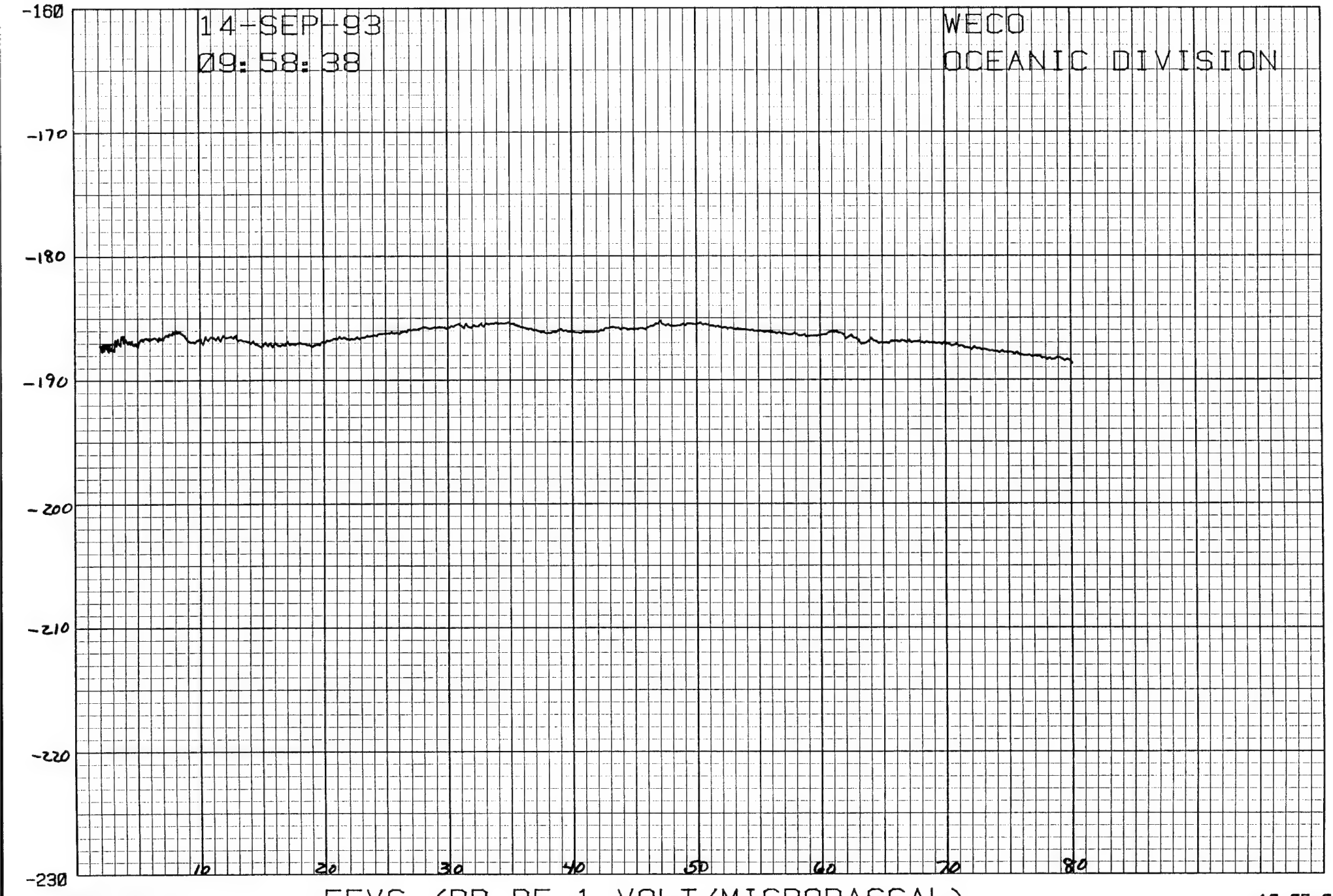

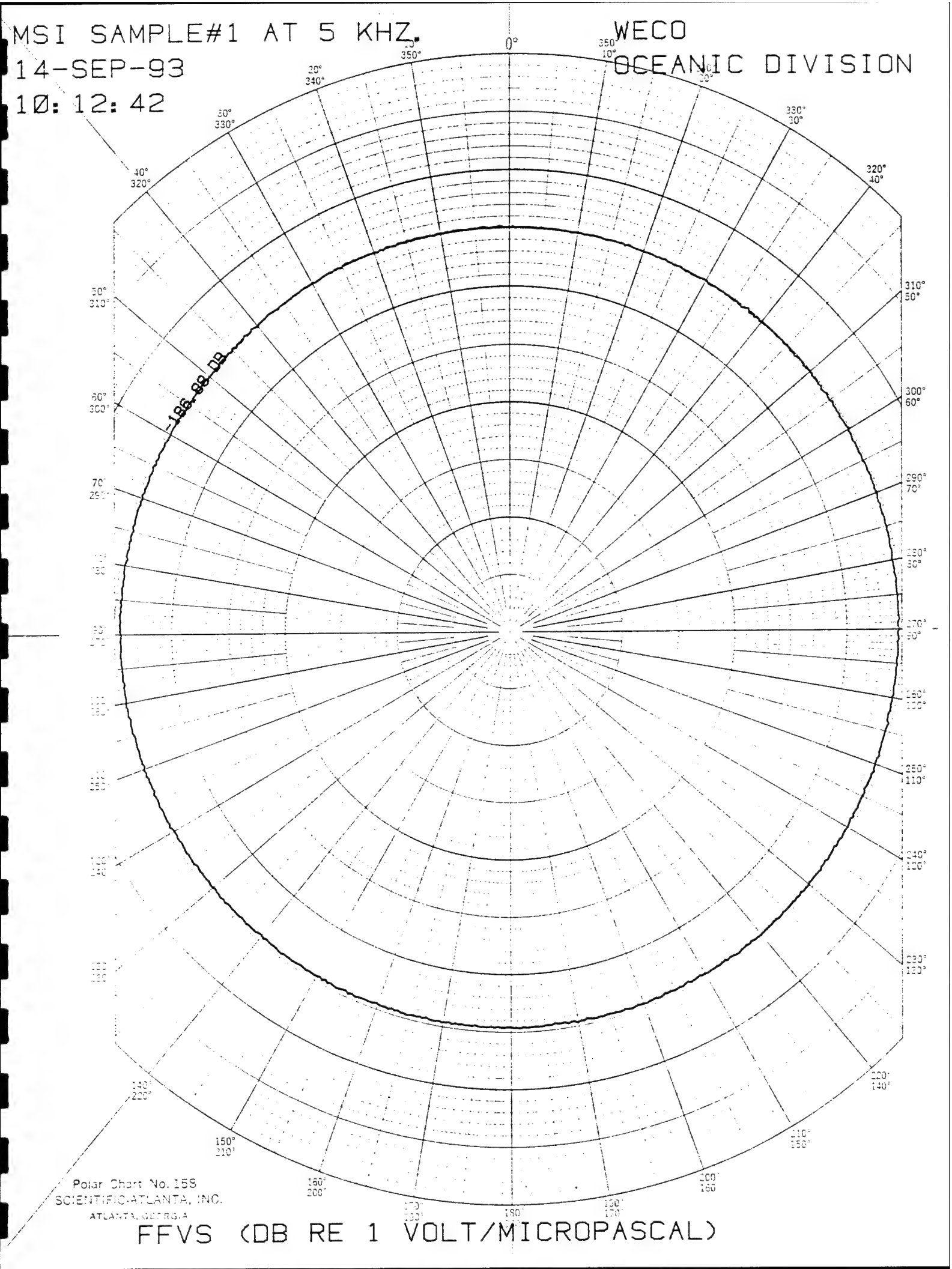
MSI SAMPLE#1 AT 5 KHZ.
14-SEP-93
10: 12: 42
WECO
OCEANIC DIVISION
-186.98 DB
Polar Chart No. 158
SCIENTIFIC-ATLANTA, INC.
ATLANTA, GEORGIA
FFVS (DB RE 1 VOLT/MICROPASCAL)

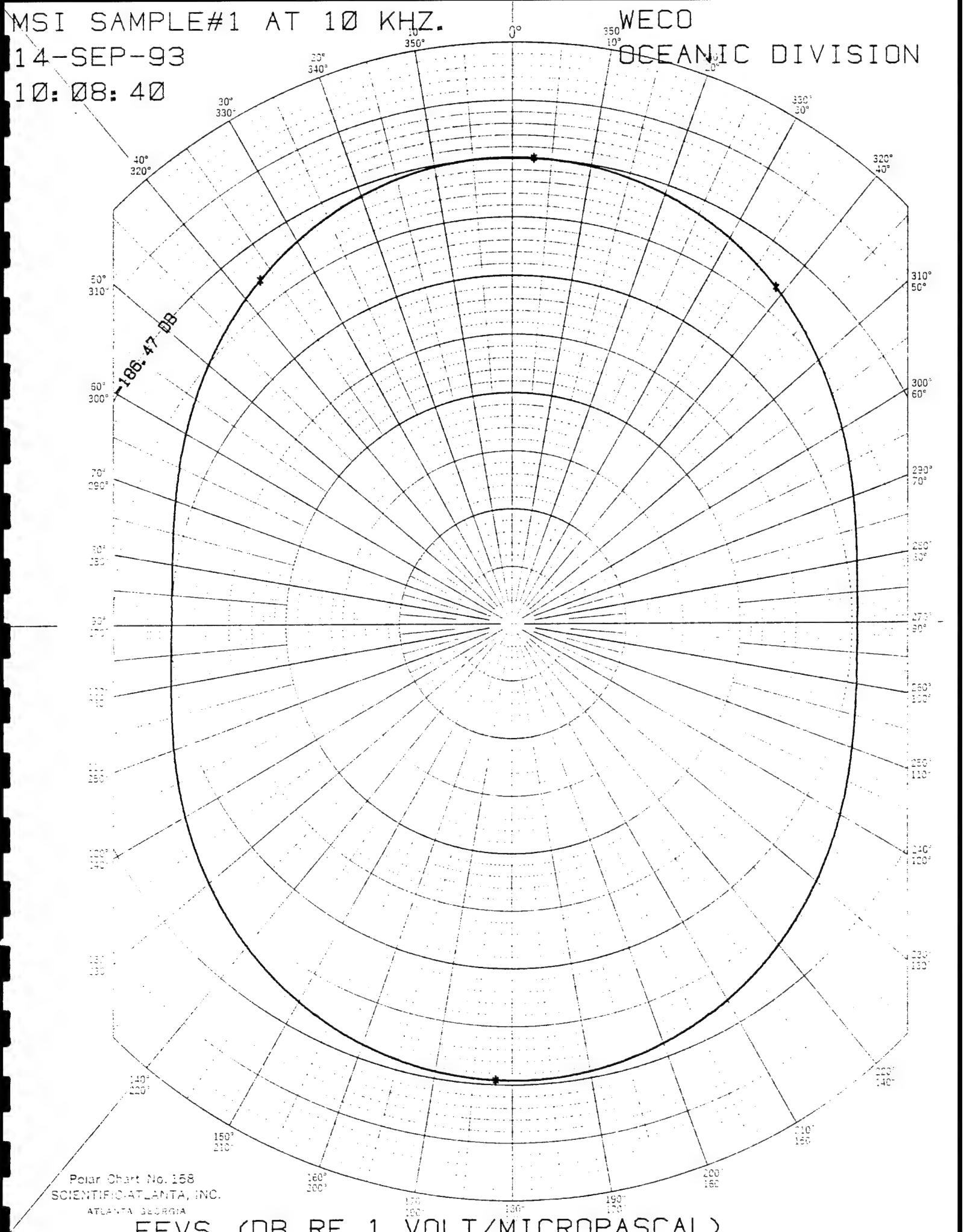
MSI SAMPLE#1 AT 10 KHZ.
14-SEP-93
10:08:40
WECO
OCEANIC DIVISION
-186.47 DB
Polar Chart No. 158
SCIENTIFIC-ATLANTA, INC.
ATLANTA GEORGIA
FFVS (DB RE 1 VOLT/MICROPASCAL)

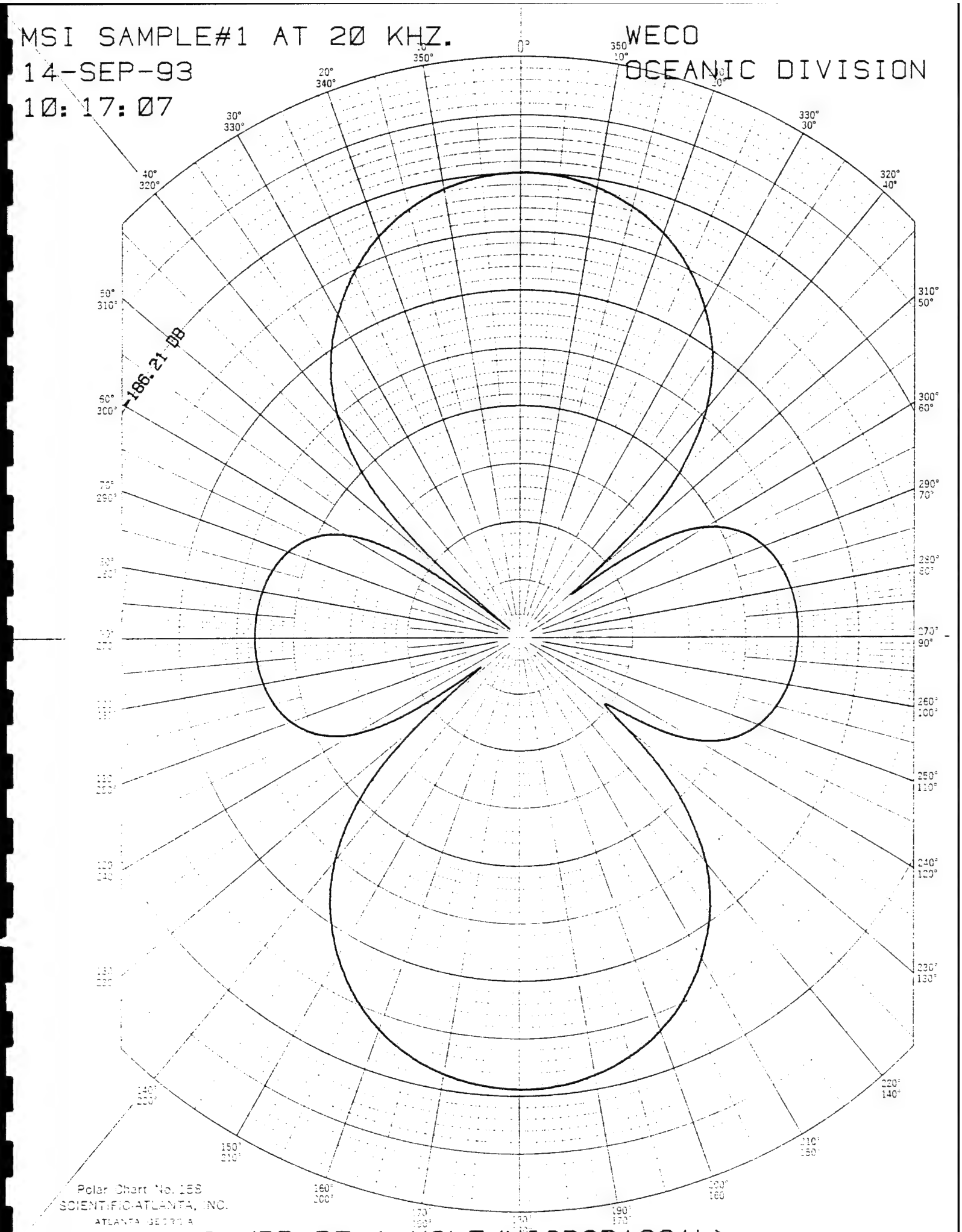
MSI SAMPLE#1 AT 20 KHZ.
14-SEP-93
10:17:07
WECO
OCEANIC DIVISION
-186.21 DB
Polar Chart No. 1SS
SCIENTIFIC-ATLANTA, INC.
ATLANTA GEORGIA
FFVS (DB RE 1 VOLT/MICROPASCAL)

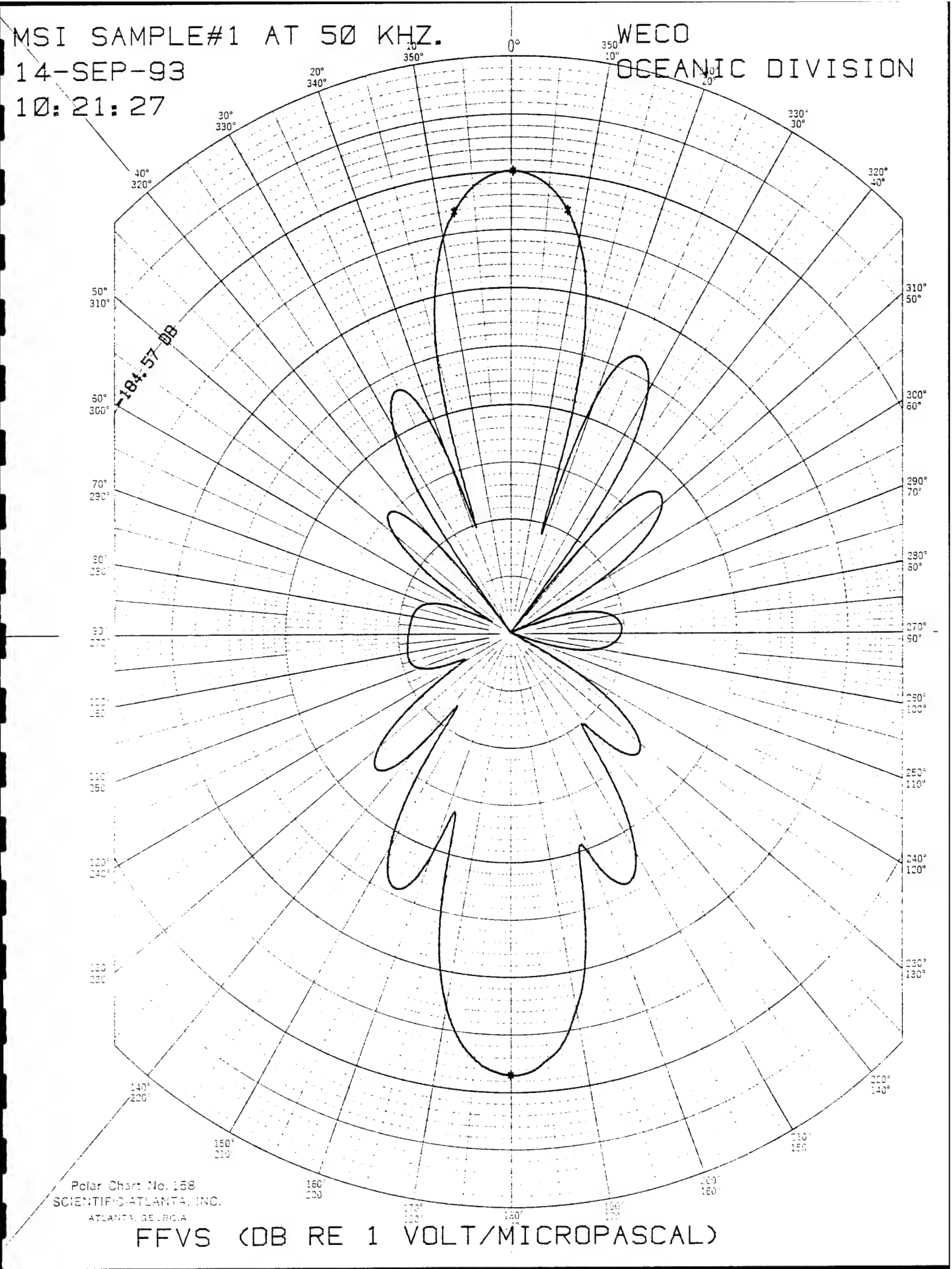
MSI SAMPLE#1 AT 50 KHZ.
14-SEP-93
10:21:27
WECO
OCEANIC DIVISION
-184.57 DB
Polar Chart No. 168
SCIENTIFIC-ATLANTA, INC.
ATLANTA, GEORGIA
FFVS (DB RE 1 VOLT/MICROPASCAL)

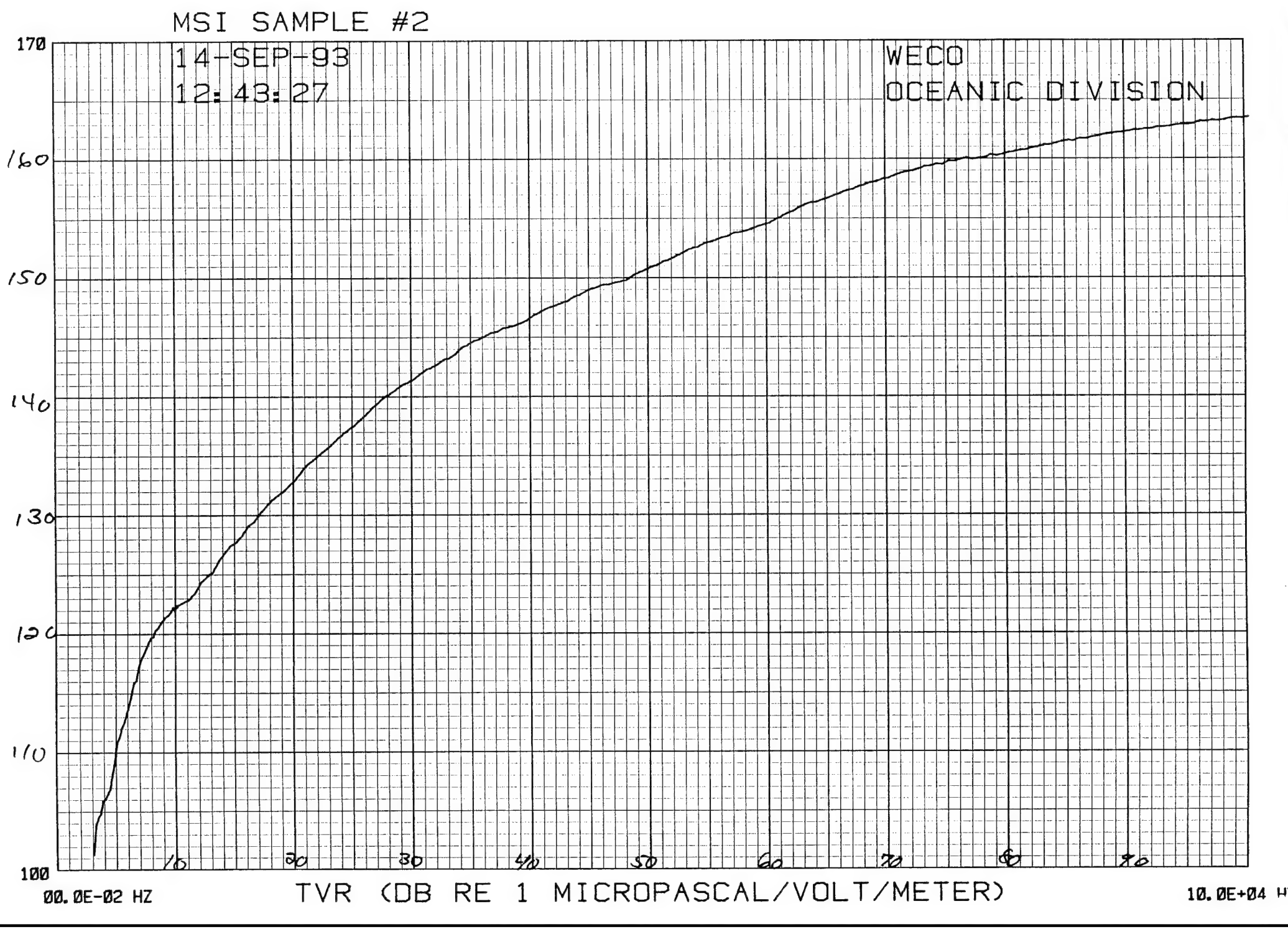

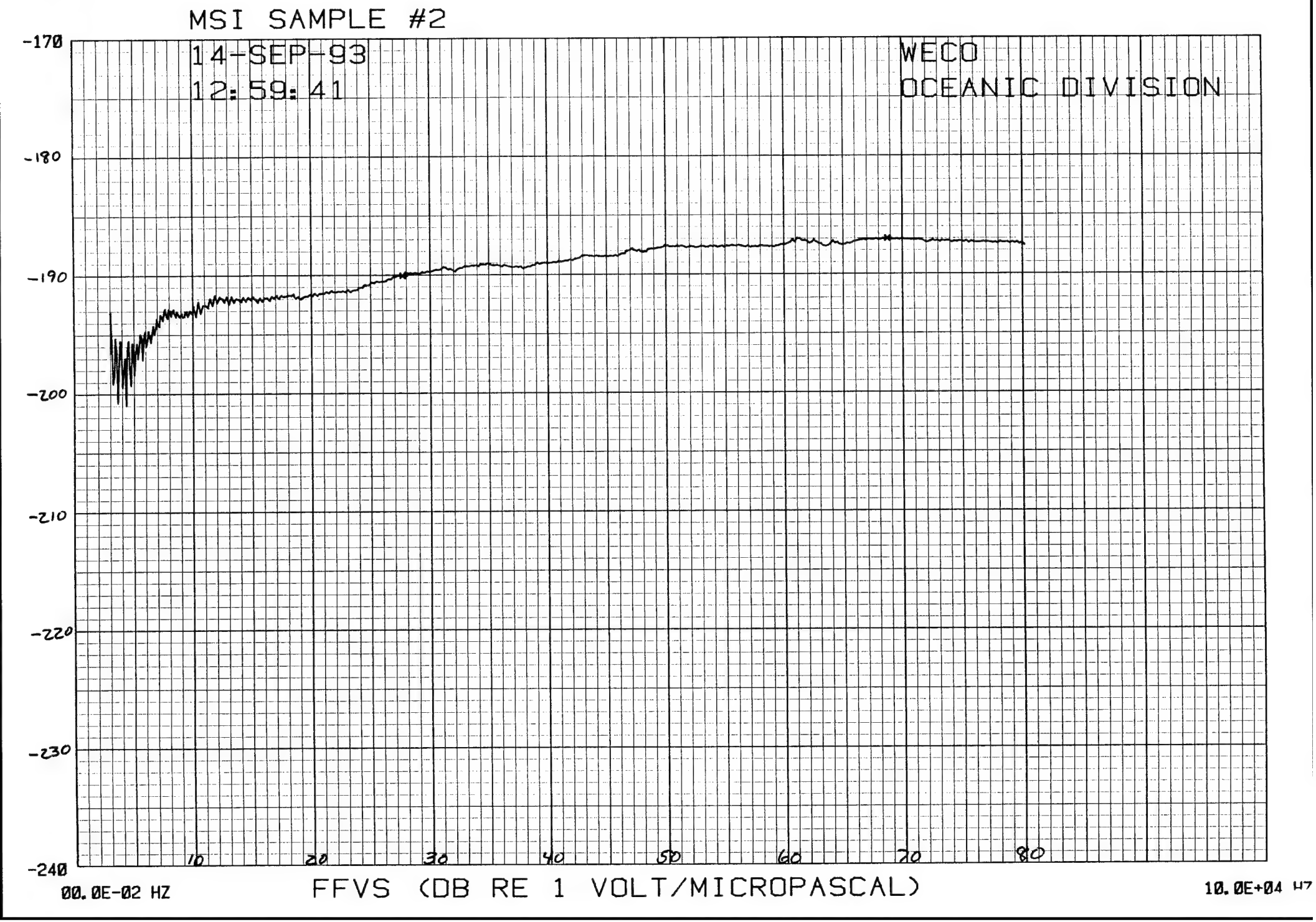

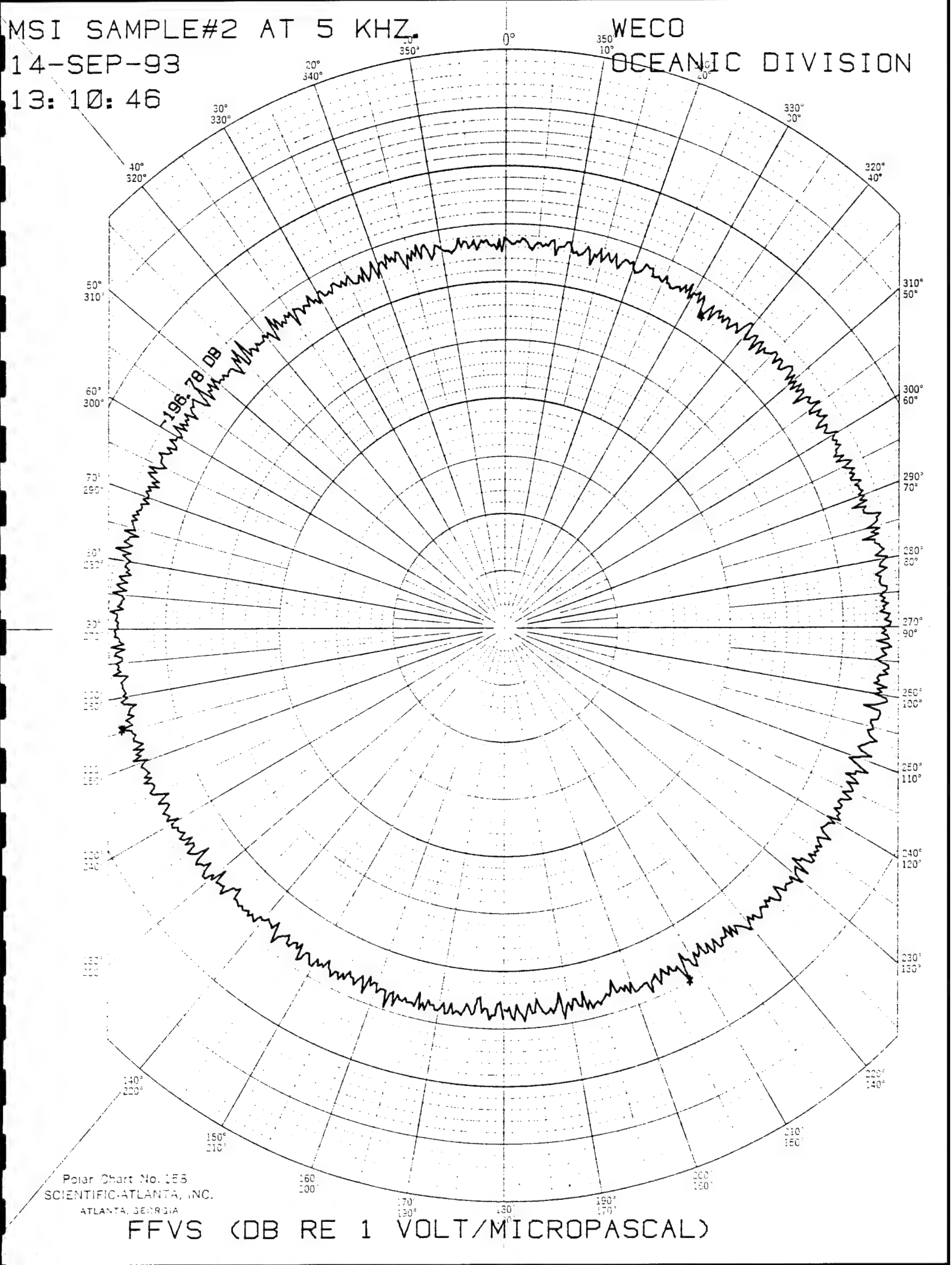
MSI SAMPLE#2 AT 5 KHZ.
14-SEP-93
13:10:46
WECO
OCEANIC DIVISION
-196.78 DB
Polar Chart No. 155
SCIENTIFIC-ATLANTA, INC.
ATLANTA, GEORGIA
FFVS (DB RE 1 VOLT/MICROPASCAL)

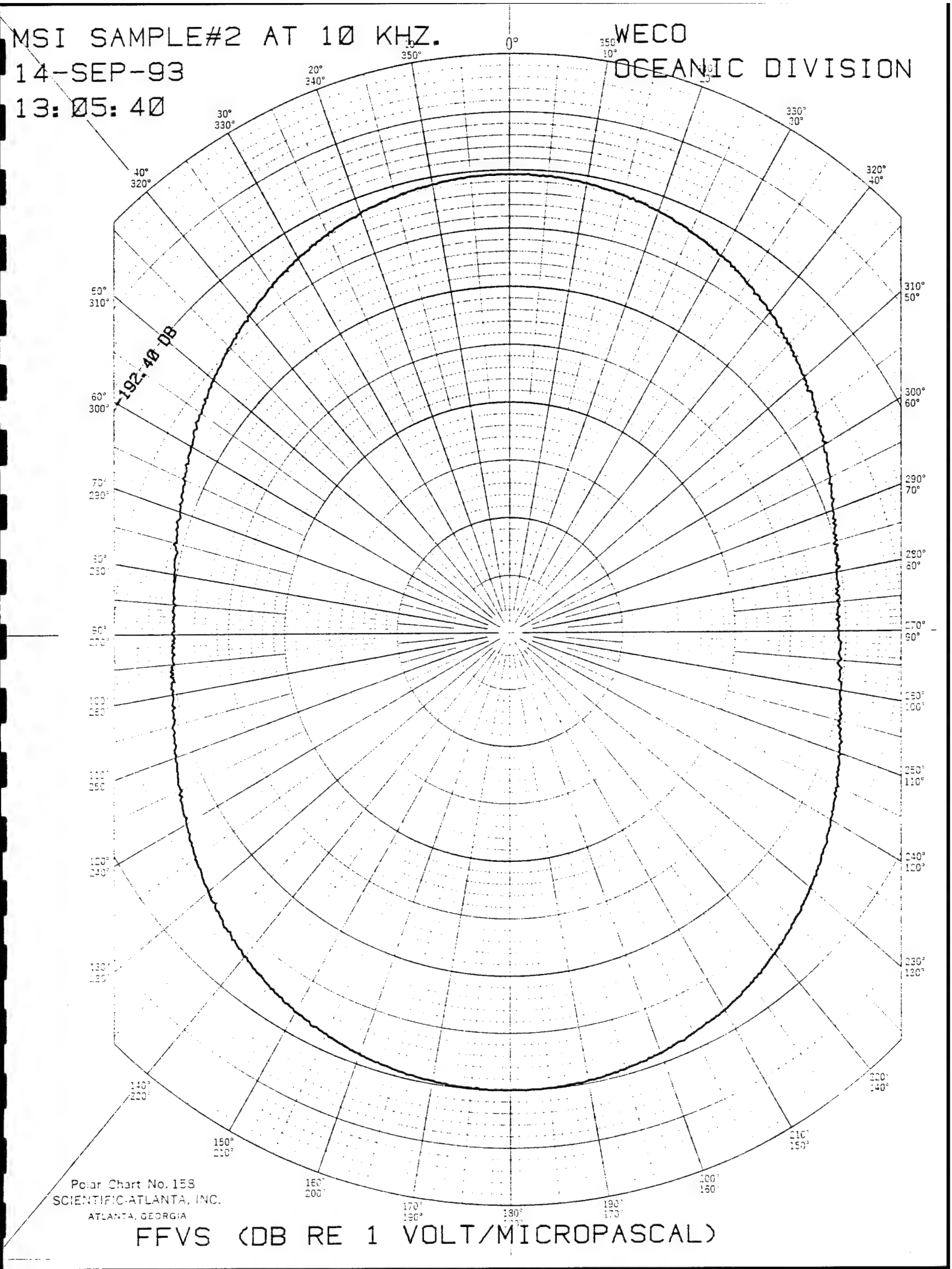
MSI SAMPLE#2 AT 10 KHZ.
14-SEP-93
13:05:40
WECO
OCEANIC DIVISION
-192.40 DB
Polar Chart No. 158
SCIENTIFIC-ATLANTA, INC.
ATLANTA, GEORGIA
FFVS (DB RE 1 VOLT/MICROPASCAL)

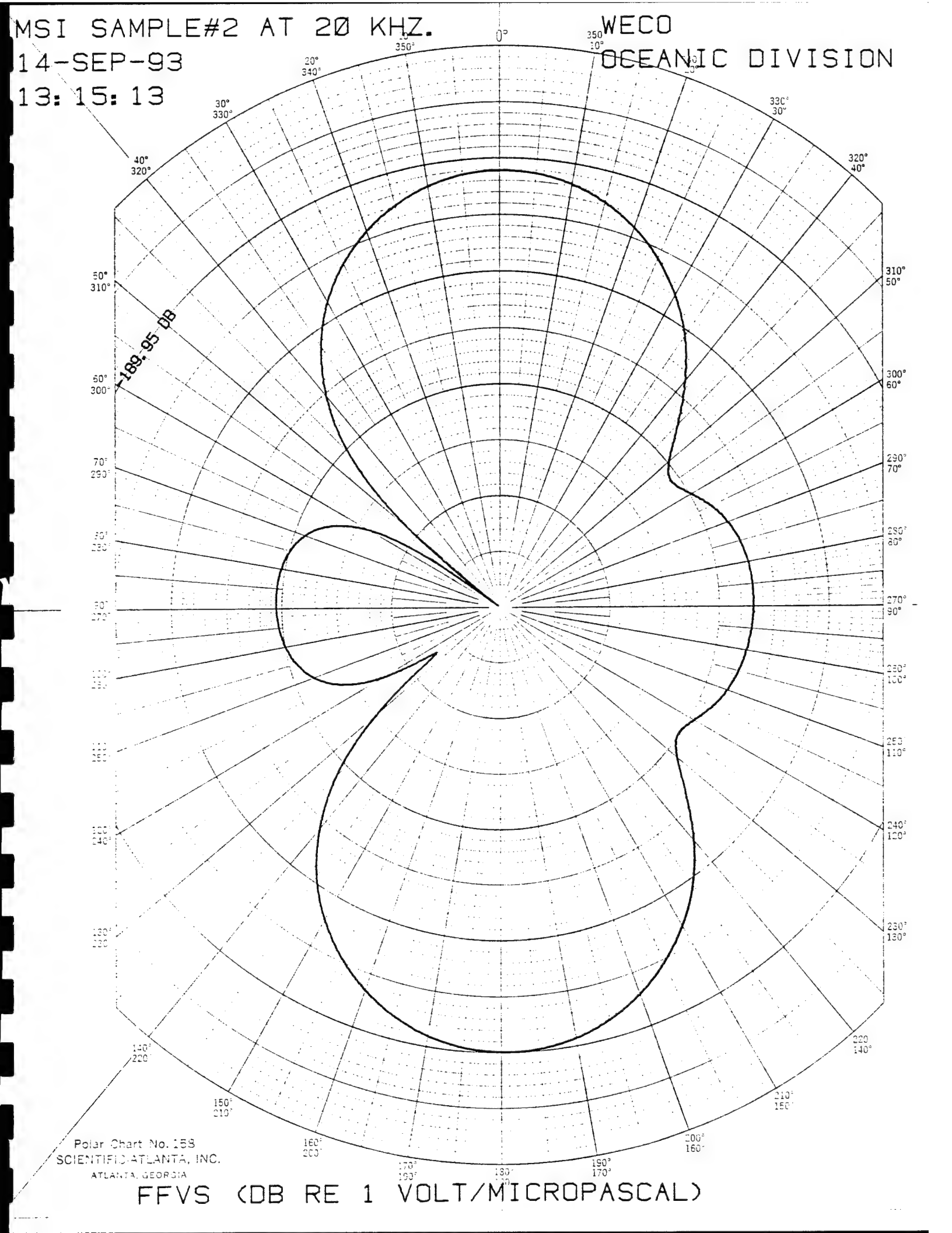
MSI SAMPLE#2 AT 20 KHZ.
14-SEP-93
13:15:13
WECO
OCEANIC DIVISION
-189.95 DB
Polar Chart No. 158
SCIENTIFIC-ATLANTA, INC.
ATLANTA, GEORGIA
FFVS (DB RE 1 VOLT/MICROPASCAL)

APPENDIX C

250 mm TRANSDUCER TEST DATA

SONOPANEL # 10-13

Measurements made by:

Raytheon Company
Portsmouth, RI

SUMMARY

Receiving voltage sensitivity (RVS) and receive beam patterns of 250 mm square SonoPanel™ transducer #10-13 were measured underwater at Raytheon Company in March 1994. These tests were made at no cost to the program. The test results are presented in this appendix.

Company	Date	Transducer	Description	Test Data
Raytheon	Mar-94	10-13	250 x 250 mm Standard SonoPanel	RVS Beam Patterns

Raytheon

Recv Volt Response

10X10 Free Field Shld to Low

TEST_PRGM
11-MAR-1994

8.23m 18.33degC
29.9kPa (3.0m)

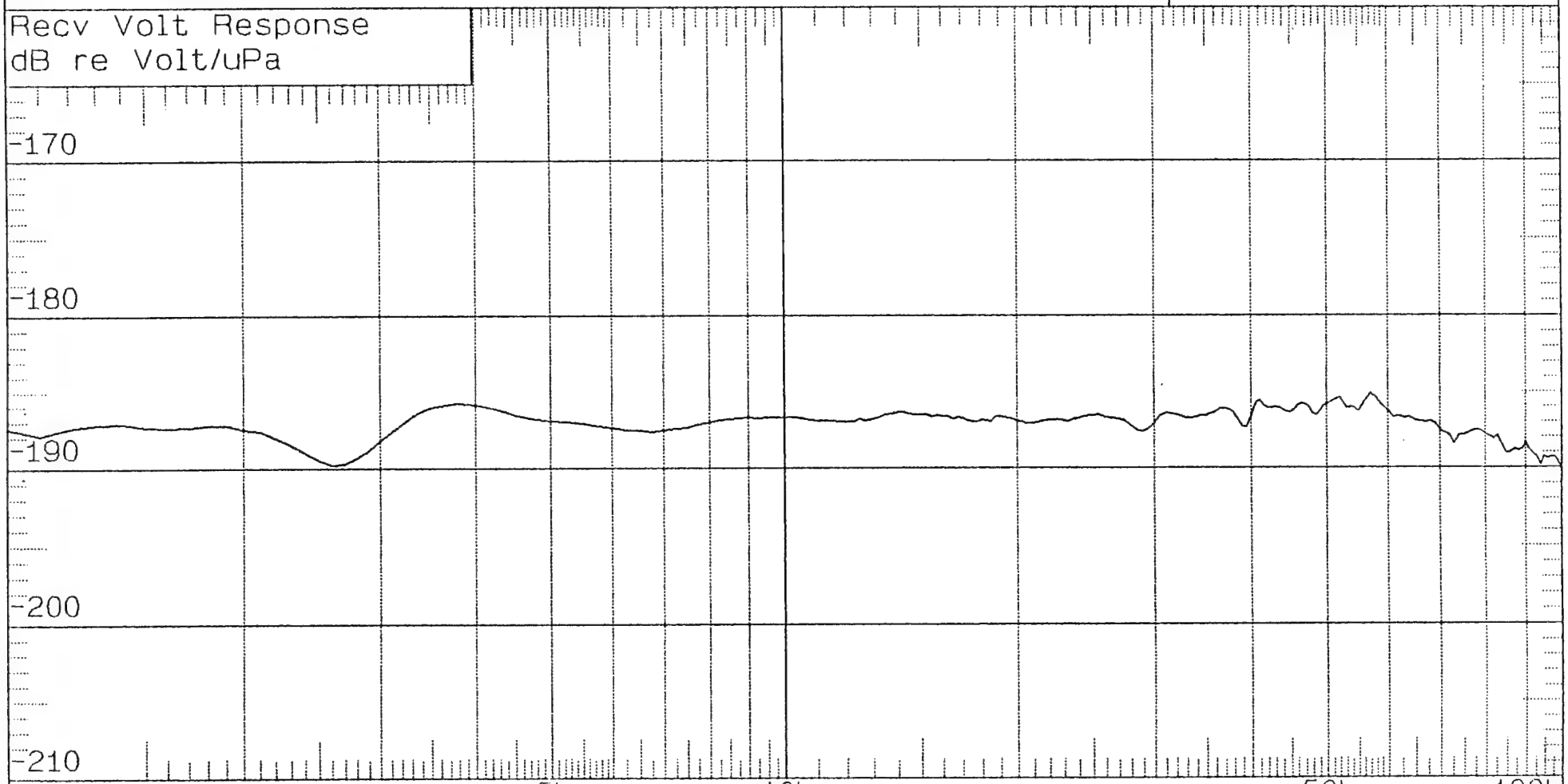

Max Recv Volt Response	Max RVS is at	3dB Bandwidth
-185.132dB re Volt/uPa	57 kHz	69.446kHz

Raytheon

RECEIVE PATTERN

IRP 10X10 (Shld to Low)

X/Y Plane

TEST_PRGM

14-MAR-1994

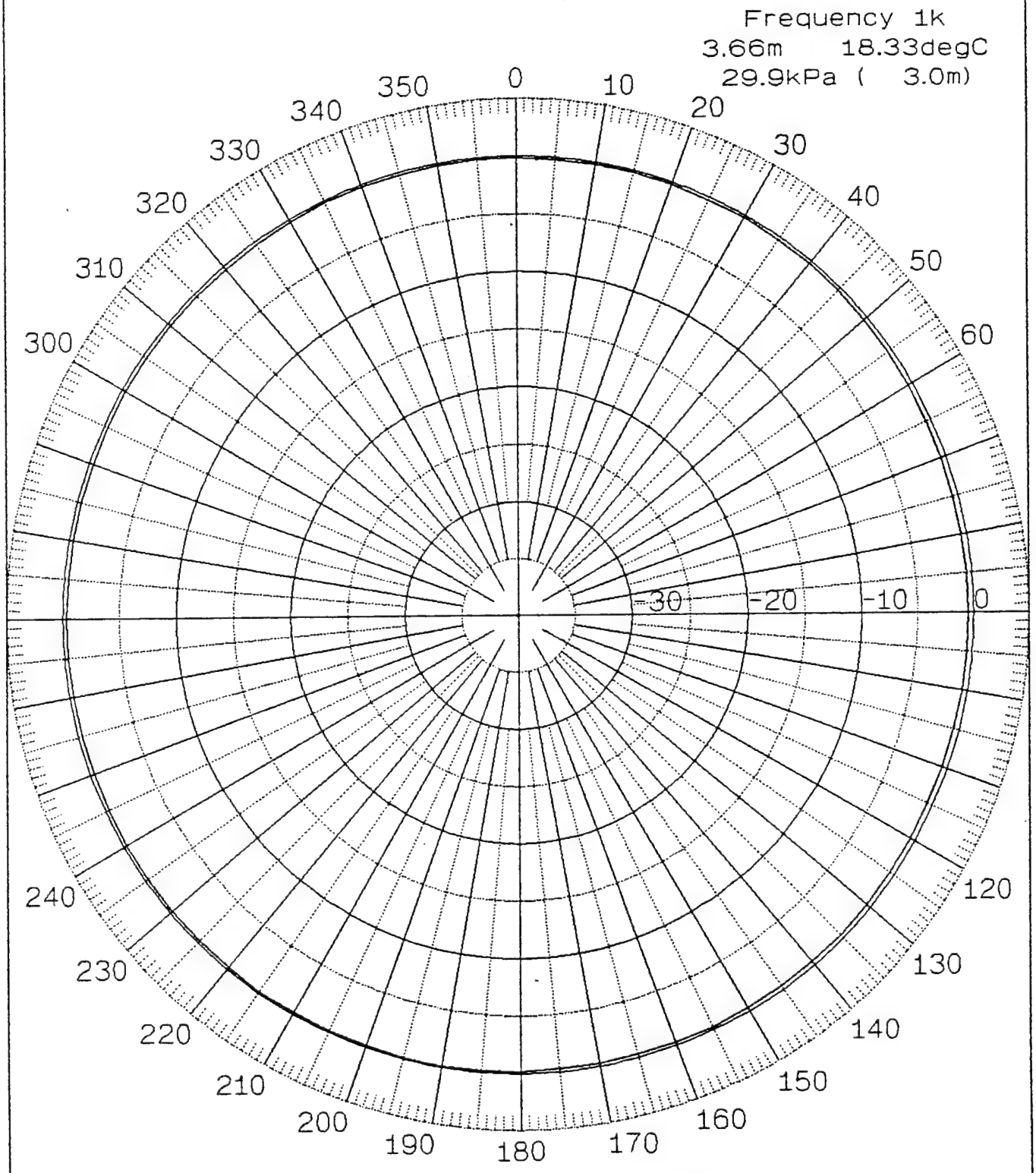

Relative Response in dB

Maximum Response Angle	Maximum Response Value	Beam Width	DI
-170.01 Degrees	-186.81 dB re V/uPa	Not Found	.44 dB

raytheon

RECEIVE PATTERN

IRP 10X10 (Shld to Low)

X/Y Plane

TEST_PRGM

14-MAR-1994

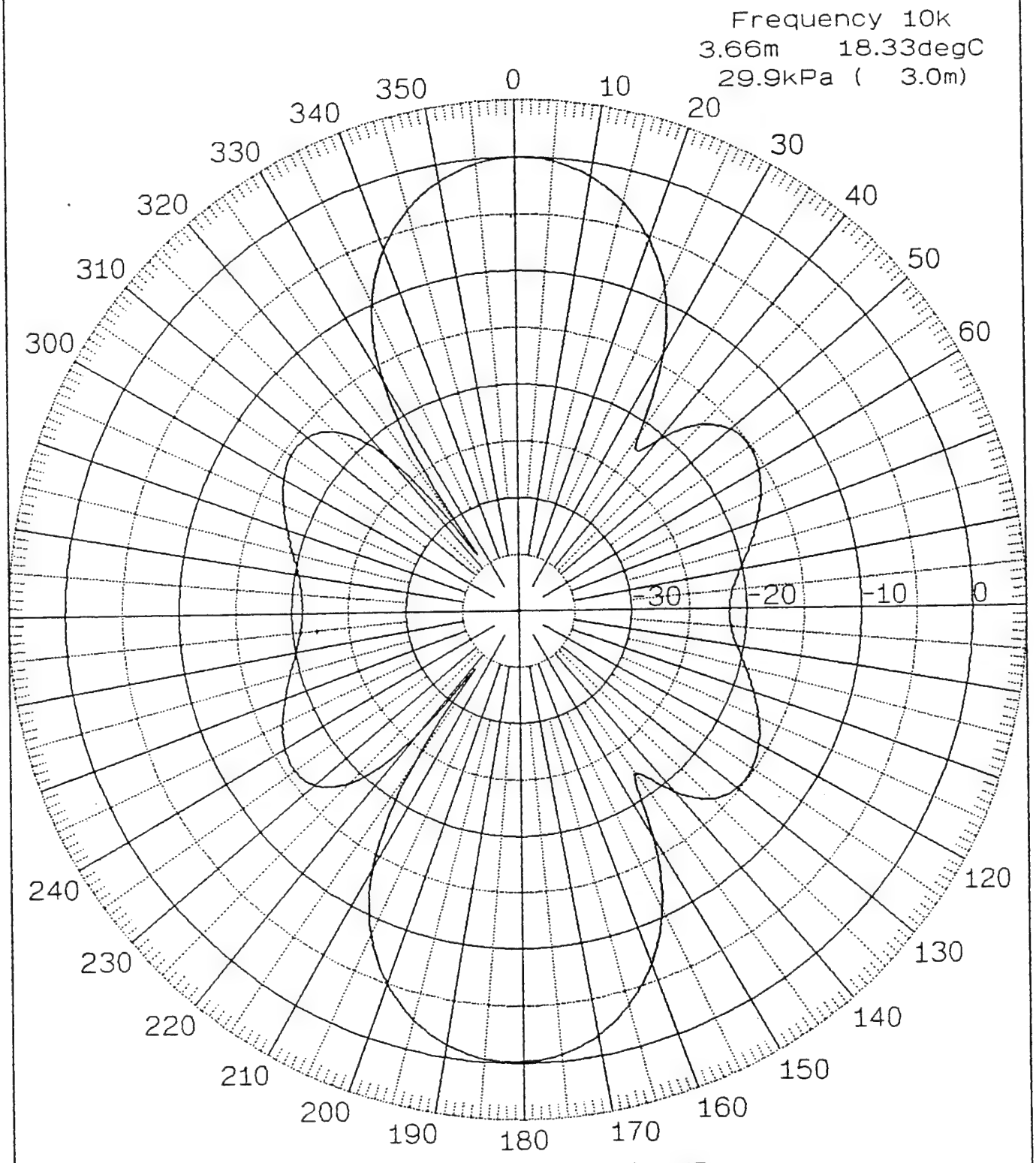

Relative Response in dB

Maximum Response Angle	Maximum Response Value	Beam Width	DI
.65 Degrees	-186.73 dB re V/uPa	29.70 Deg	12.49 dB

Raytheon

RECEIVE PATTERN

IRP 10X10 (Shld to Low)

X/Y Plane

TEST_PRGM

14-MAR-1994

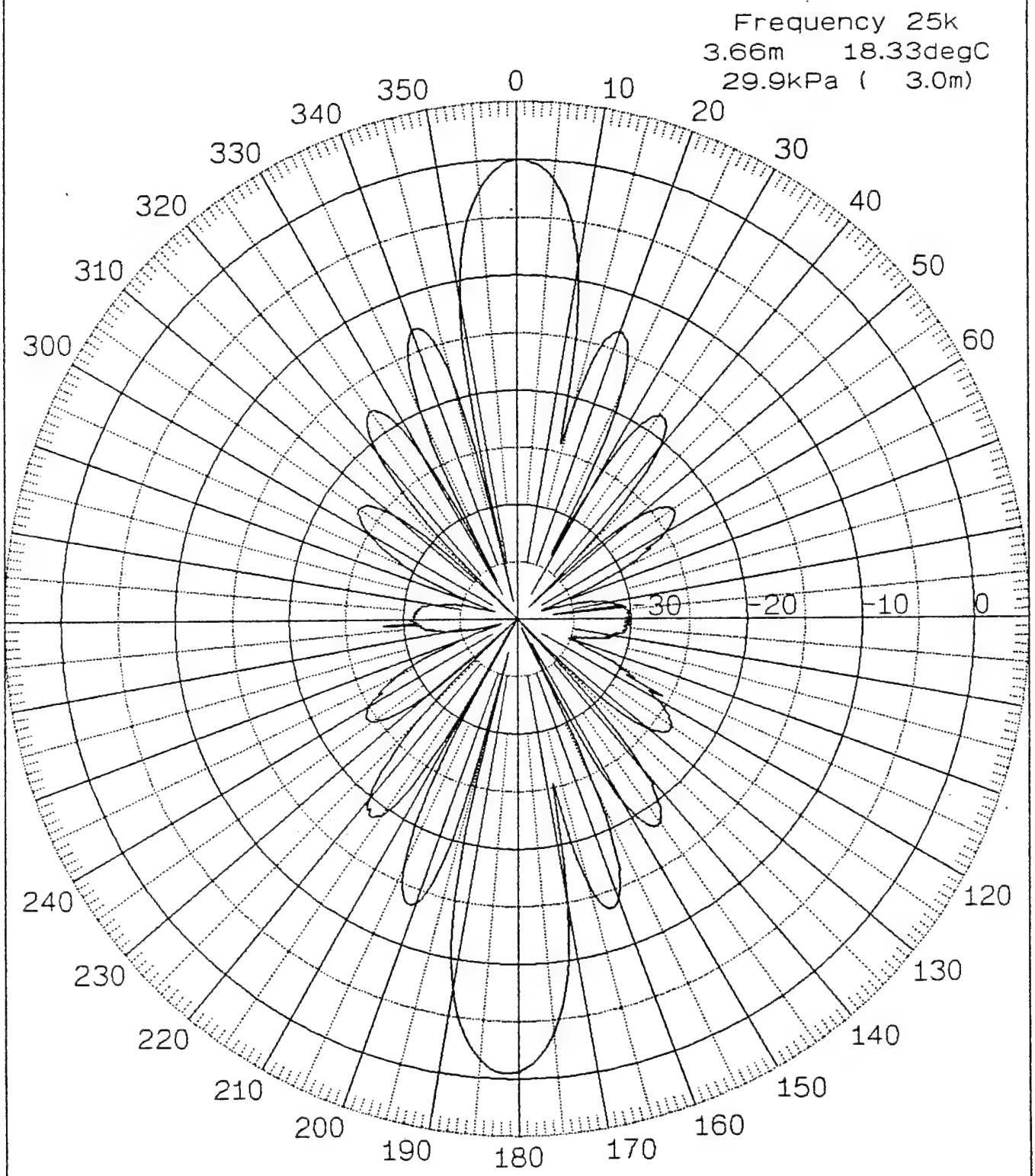

Relative Response in dB

Maximum Response Angle	Maximum Response Value	Beam Width	DI
.23 Degrees	-186.53 dB re V/uPa	11.87 Deg	19.58 dB

Raytheon

RECEIVE PATTERN

IRP 10X10 (Shld to Low)

X/Y Plane

TEST_PRGM

14-MAR-1994

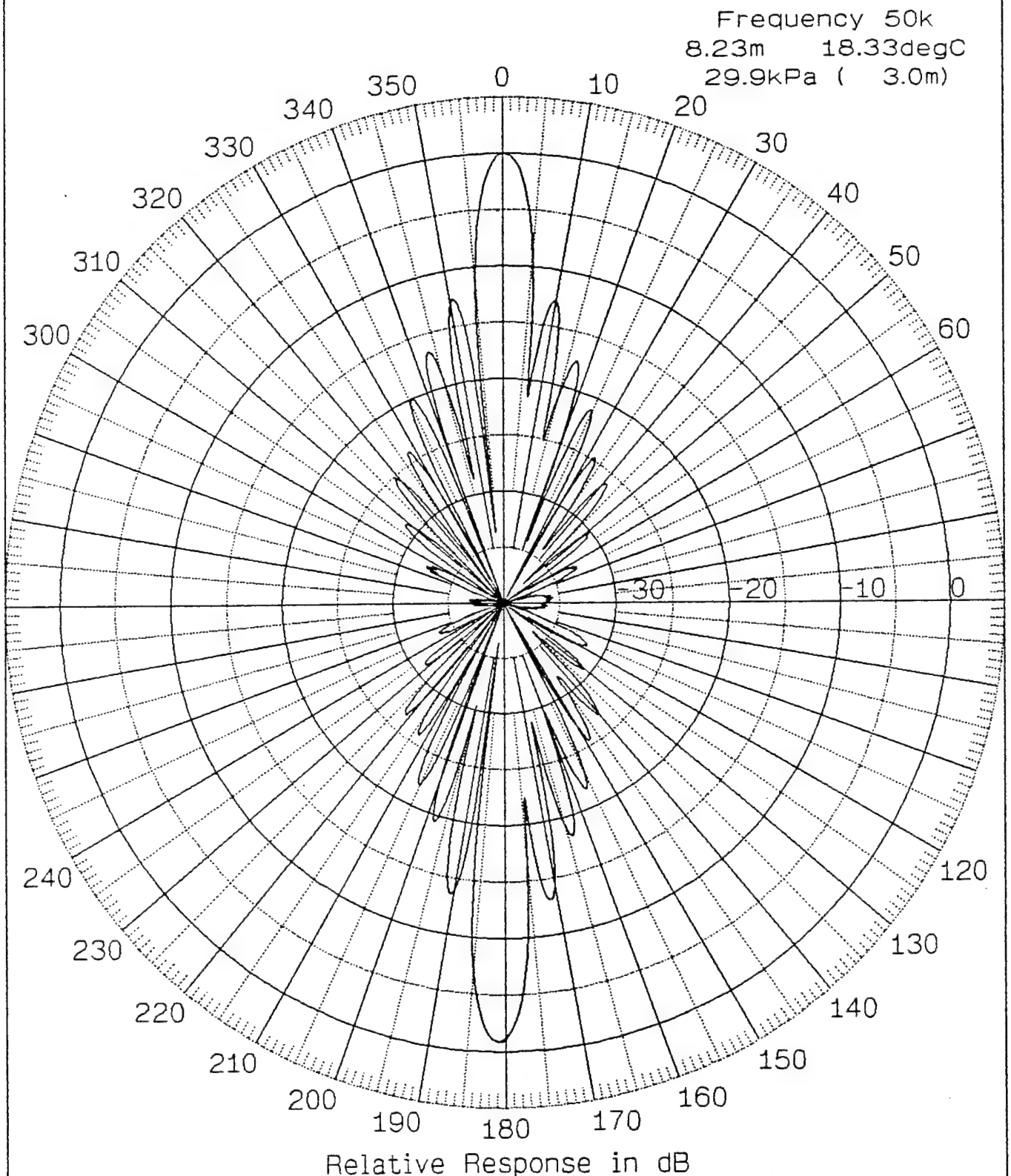

Relative Response in dB

Maximum Response Angle	Maximum Response Value	Beam Width	DI
.16 Degrees	-185.95 dB re V/uPa	5.92 Deg	24.97 dB

Raytheon

RECEIVE PATTERN

10X10 Free Field Shld to Low

X/Y Plane

TEST_PRGM

11-MAR-1994

Frequency 100k

8.23m 18.33degC

29.9kPa (3.0m)

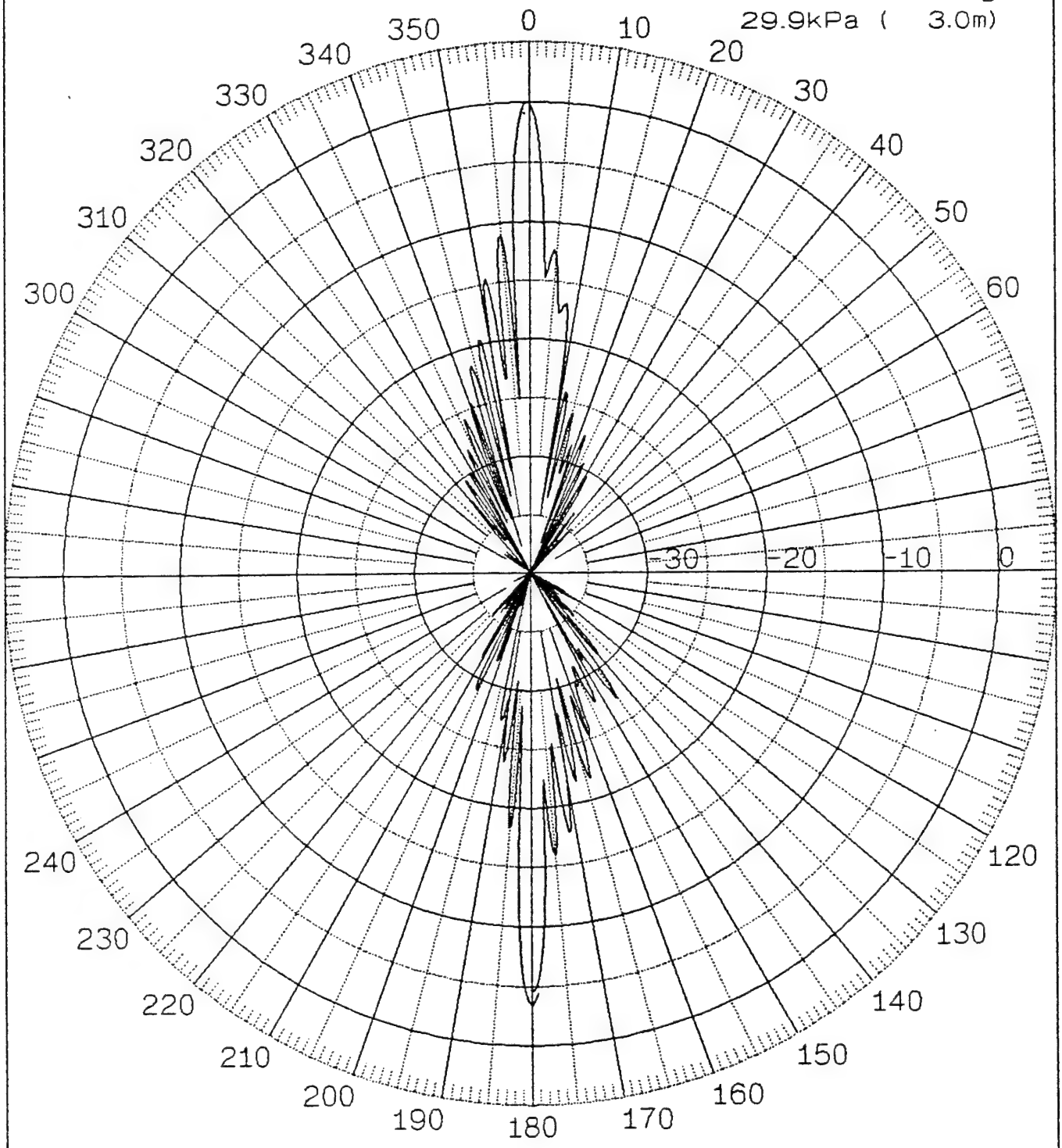

Relative Response in dB

Maximum Response Angle	Maximum Response Value	Beam Width	DI
-.19 Degrees	-190.14 dB re V/uPa	3.02 Deg	30.81 dB

APPENDIX D

250 mm TRANSDUCER TEST DATA

SONOPANEL # 10-40
and
SONOPANEL # 10-43

Measurements made by:

Naval Research Laboratory
Underwater Sound Reference Detachment
Orlando, FL

SUMMARY

Two 250 mm SonoPanel transducer panels (10-40 and 10-43) were tested at NRL-USRD in August 1994. Free-field voltage sensitivity, transmitting voltage response, and sound pressure level were measured for panel 10-43 at the USRD Lake Facility. Receive beam patterns at 5,10, 30, 50, 100, and 200 kHz were measured for panels 10-40 and 10-43. In addition, the free-field voltage sensitivity of panel 10-40 was measured at various pressures up to 6890 kPa in the Anechoic Tank Facility. The test data and related briefing charts from NRL-USRD are presented in this appendix.

Underwater Electroacoustic Evaluations of 1-3 Piezocomposite Panels

Thomas R. Howarth and Robert Y. Ting

Naval Research Laboratory
Underwater Sound Reference Detachment
Orlando, Florida
USA

Underwater Sound Reference Detachment
Orlando, Florida

Specifications of the 1-3 Piezocomposite Panels

- *Transducer Structure (1-3 Panel with Encapsulation)*

  Overall Cross-sectional Area: 27.4 cm by 26.7 cm

  Thickness: 1.47 cm

- *Active 1-3 Panel Structure (Under Cu GRP Board)*

  Cross-sectional Area: 26.4 cm by 25.5 cm

  Thickness: 0.64 cm

- **Piezoceramic fabrication done using injection molding**
- **1.1 mm OD PZT-5H Piezoceramic Rods**
- **Matrix Filler is Voided Polyurethane with 40 % volume of microspheres**
- **25.4 μm Cu foil applied over the edges for EMI shielding**
- **Conductive epoxy used to attach 0.8 mm thick GRP board (with 2 oz Cu electroplated onto board) to both sides**
- **Cable was directly soldered to Cu on GRP board**

Underwater Sound Reference Detachment
Orlando, Florida

Measured Transducer Properties

Load	f_r (kHz)	f_a (kHz)	f_1 (kHz)	f_2 (kHz)	Q_e	Q_m	k_{eff}
vacuum (air)	67.125	72.5	60.25	70.425	0.4	7	53%
water	67.375	74.7	61.25	75.375	0.7	5	47%

C_o = 42 nF @ $2f_a$; tan δ_e = .031; R_o = 560 Ω; G_{max} = 27 mS; G_{air} = 24 mS; G_{wat} = 7 mS

C_c = 2.6 nF; R_c = 3.3 kΩ

η_{ma} = 72 %; η_{em} = 25 %; η_{ea} = 18 %

Underwater Sound Reference Detachment
Orlando, Florida

Transducer Evaluation Expressions

$$k_{eff} = [1 + Q_m Q_e]^{-1/2} \text{ for } 10 < Q_m < 50$$

$$Q_m = f_r / (f_2 - f_1) \text{ and } Q_e = B\ (@\ f_r) / G_{max}$$

f_r occurs at G_{max}; f_a occurs at R_{max}; f_1 and f_2 denote half-power points

$$\eta_{ma} = \text{mechanical-acoustic efficiency} = (G_{air} - G_{wat}) / G_{vac}$$
$$\eta_{em} = \text{electrical-mechanical efficiency} = G_{wat} / G_{max}$$
$$\eta_{ea} = \text{electrical-acoustic efficiency} = \eta_{ma} * \eta_{em}$$

Refs:

1. M. Moffett and W. Marshall, "The importance of coupling factor for underwater acoustic projectors," 127th Meeting of the Acoustical Society of America, Cambridge, MA, June 6-10, 1994.

2. D. Stansfield, Underwater Electroacoustic Transducers, Bath Univ Press, 1991, Ch. 4.

Equivalent Electric Field Network Representation

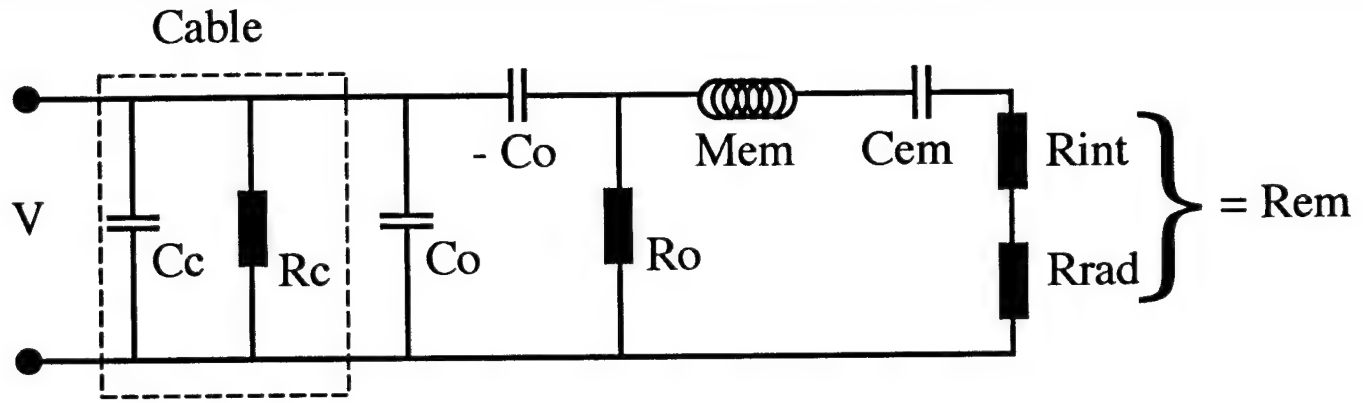

R_c = Cable Resistance

C_c = Cable Capacitance

R_o = Dielectric Losses

C_o = Clamped Capacitance

N = Ideal Electromechanical Turns Ratio (Transformer)

$M_{em} = M_m / N^2$ = Mass Element

$C_{em} = N^2 C_m$ = Compliance Element

$R_{em} = R_m / N^2 = R_{int} + R_{rad}$ = Inherent Mechanical Losses and Acoustic Radiation

Network Element Expressions and Values

$$G_{air} = 1 / R_{int} \text{ and } G_{wat} = 1 / (R_{int} + R_{rad}) \text{ and } R_{em} = R_{int} + R_{rad}$$

$$M_{em} = Q_m * R_{em} / 2\pi * f_r$$

$$C_{em} = 1 / (2\pi * f_r)^2 * M_{em}$$

$C_c = 2.6$ nF

$R_c = 3.3$ kΩ

$C_o = 42$ nF

$R_o = 560$ Ω

$M_{em} = 2.3$ mH

$C_{em} = 2.4$ nF

$R_{int} = 42$ Ω

$R_{rad} = 108$ Ω

$R_{em} = 150$ Ω

Underwater Sound Reference Detachment
Orlando, Florida

Naval Research Laboratory
Underwater Sound Reference Detachment
P.O. Box 568337, Orlando, Florida 32856-8337

USRD No. 0406
Lake Facility
AUG 1994

FREE-FIELD VOLTAGE SENSITIVITY

25.4-cm X 25.4-cm X 1.3-cm Panel Serial 10-43
Open-circuit voltage measured at end of 17.0-m cable; Unbalanced
Water Temp: 30° C
Depth: 3.9-m (38 kPa)

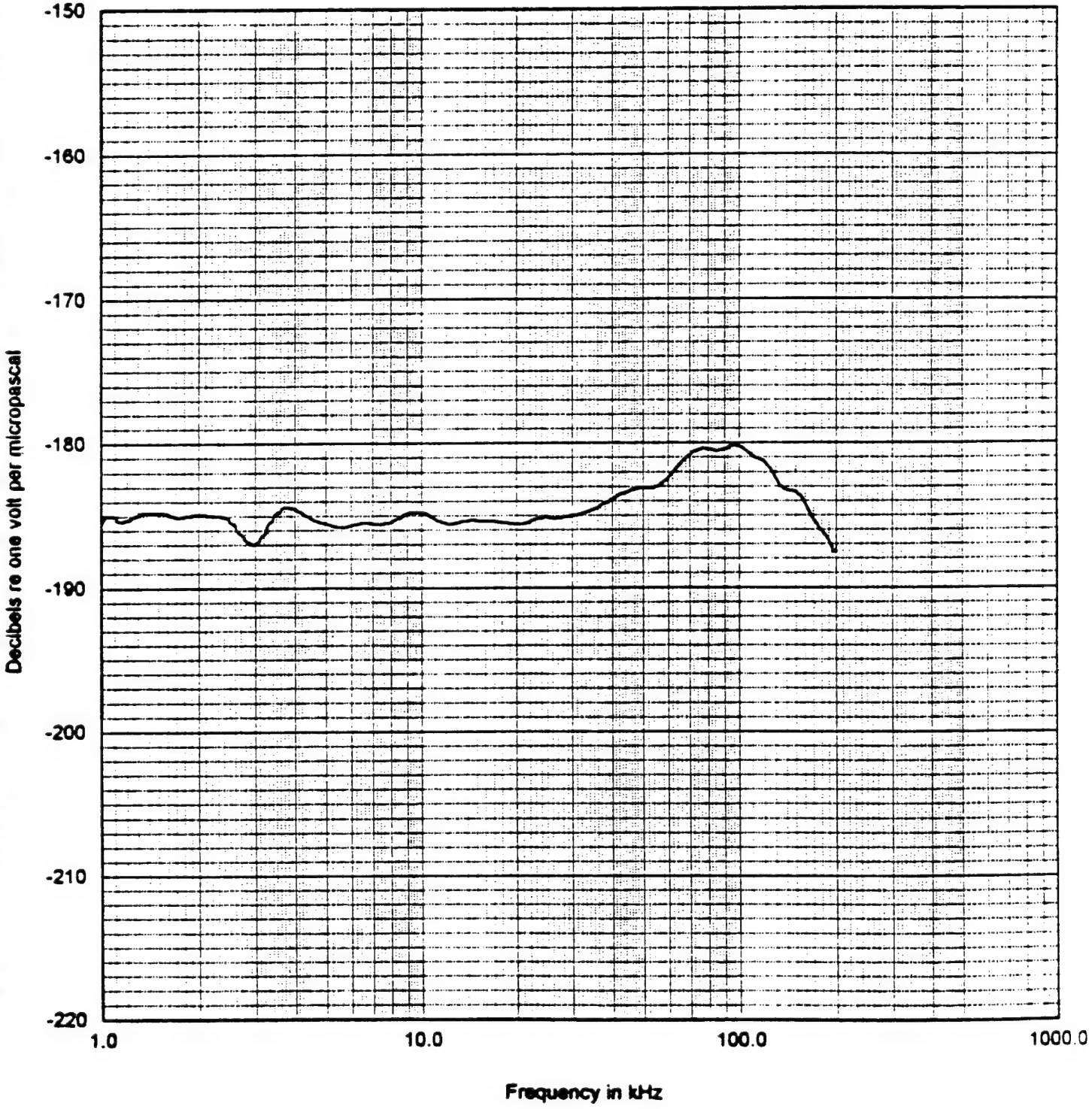

Naval Research Laboratory
Underwater Sound Reference Detachment
P.O. Box 568337, Orlando, Florida 32856-8337

USRD No. 0406
Lake Facility
AUG 1994

TRANSMITTING VOLTAGE RESPONSE

25.4-cm X 25.4-cm X 1.3-cm Panel Serial 10-43
Pressure at one meter per volt applied at end of 17.0-m cable; Unbalanced
Water Temp: 31° C
Depth: 3.9-m (38 kPa)

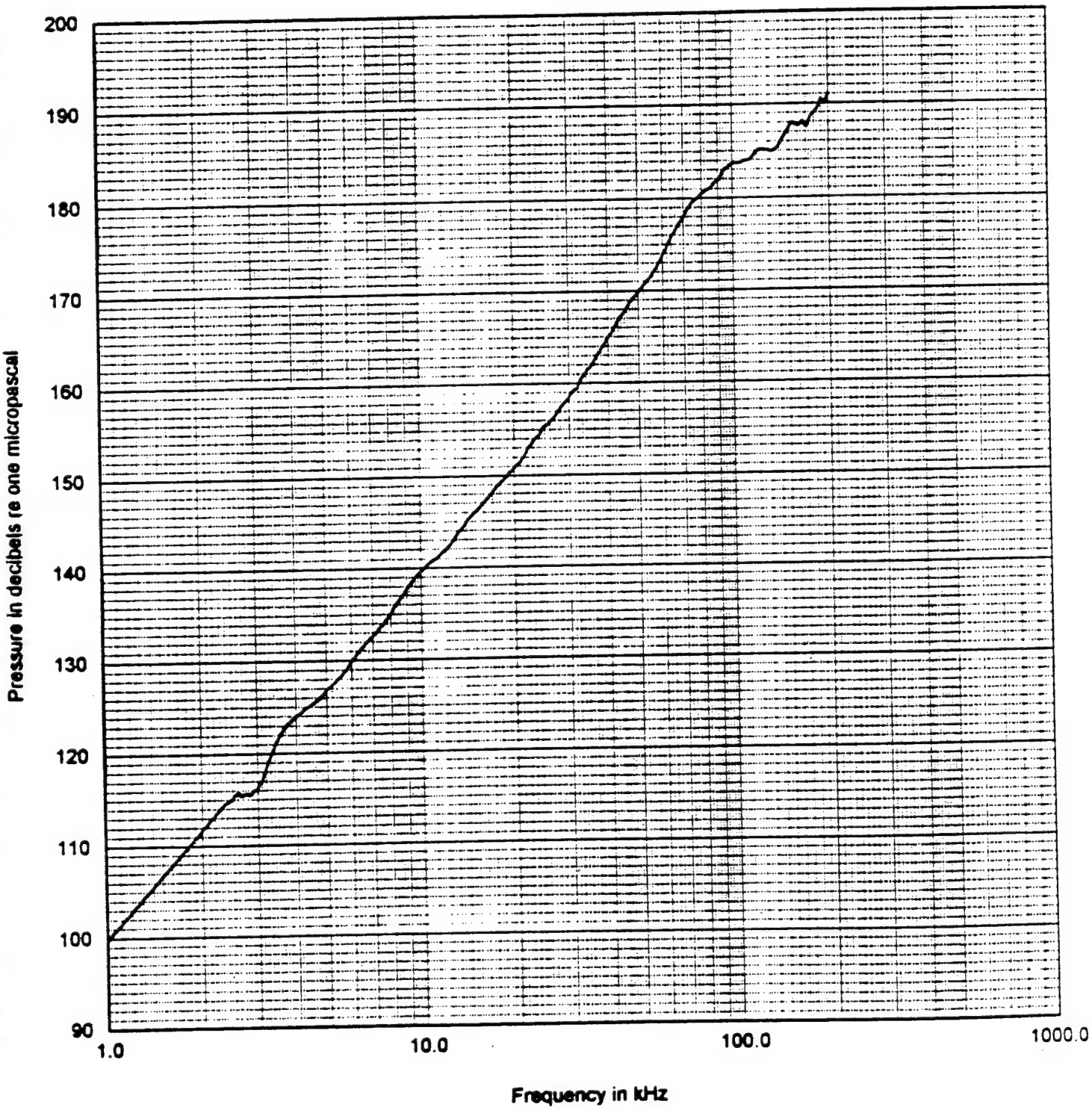

Naval Research Laboratory
Underwater Sound Reference Detachment
P.O. Box 568337, Orlando, Florida 32856-8337

USRD No. 0406
Lake Facility
AUG 1994

SOUND PRESSURE LEVEL

25.4-cm X 25.4-cm X 1.3-cm Panel 10-43
dB re 1uPa at one meter measured at end of 30.0-m cable; Unbalanced
Water Temp: 30° C
Depth: 3.9-m (38 kPa)
Drive Voltage: 100 vrms

15.7 kV/m (0.4 V/mil)

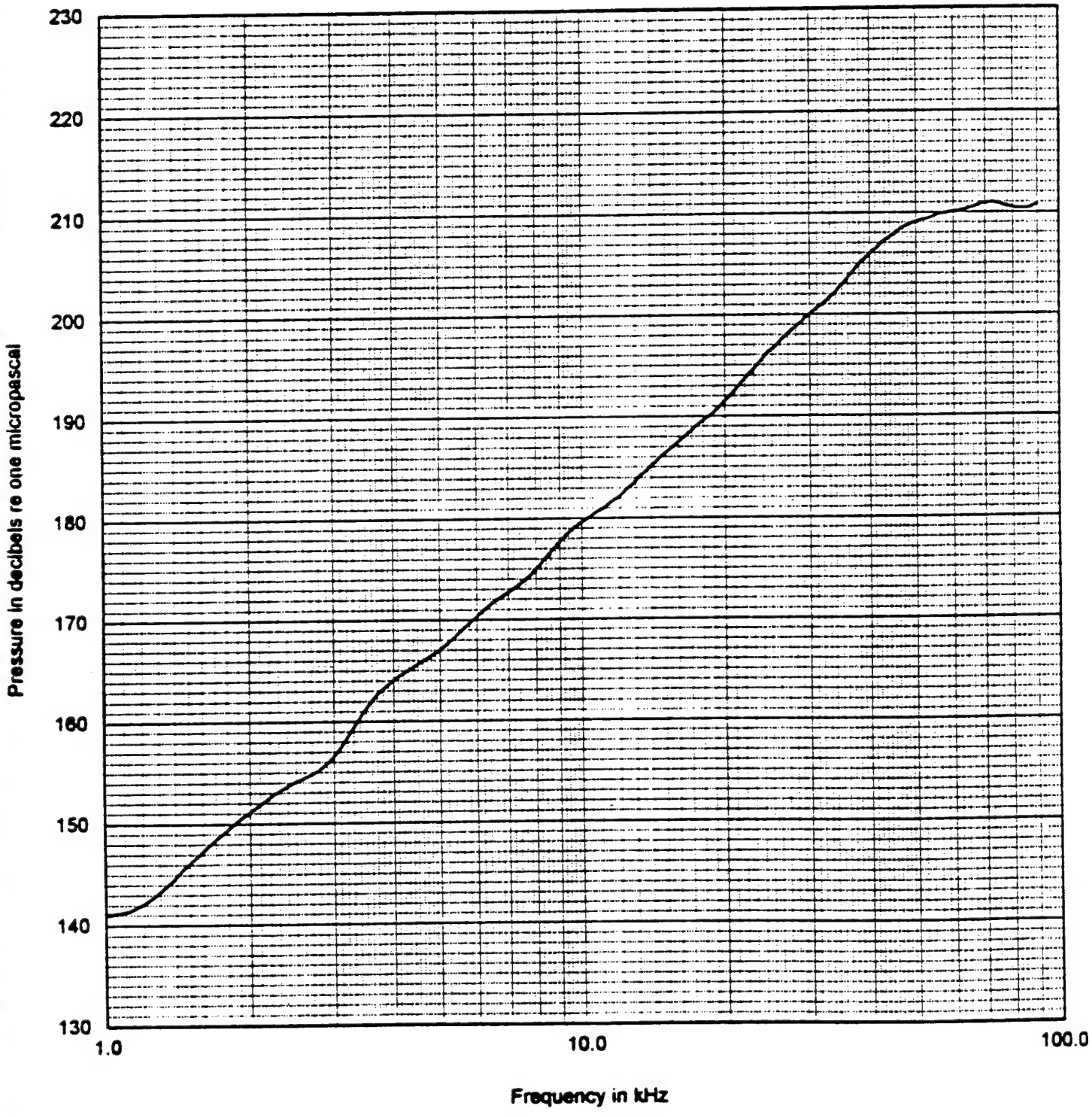

Naval Research Laboratory
Underwater Sound Reference Detachment
P.O. Box 568337, Orlando, Florida 32856-8337

USRD No. 0406
Lake Facility
AUG 1994

SOUND PRESSURE LEVEL

25.4-cm X 25.4-cm X 1.3-cm Panel 10-43
dB re 1uPa at one meter measured at end of 30.0-m cable; Unbalanced
Water Temp: 30° C
Depth: 3.9-m (38 kPa)
Drive Voltage: 200 vrms

31.5 KV/m (0.8 V/m)

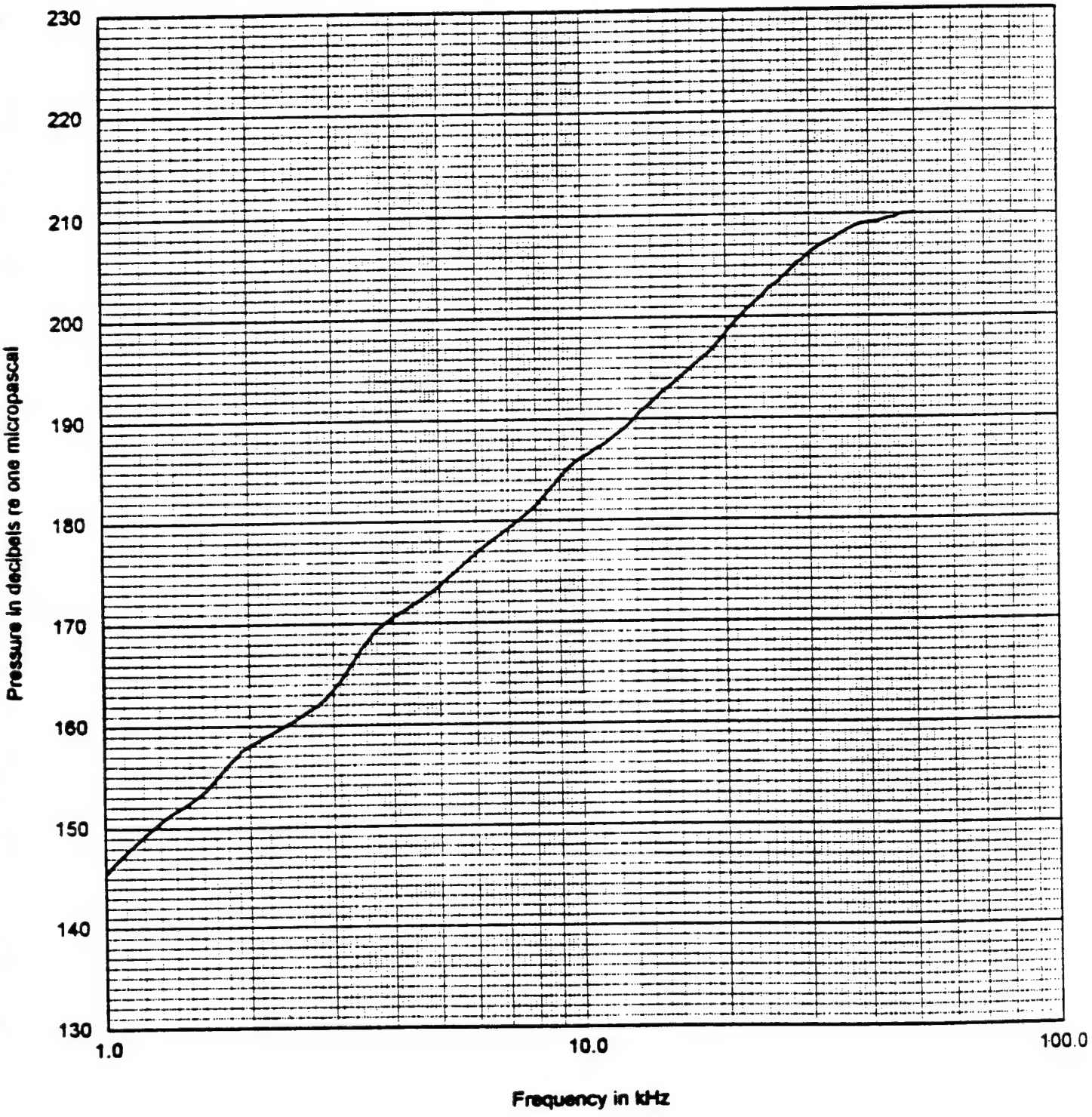

Naval Research Laboratory
Underwater Sound Reference Detachment
P.O. Box 568337, Orlando, Florida 32856-8337

USRD No. 0406
Lake Facility
AUG 1994

SOUND PRESSURE LEVEL

25.4-cm X 25.4-cm X 1.3-cm Panel 10-43
dB re 1uPa at one meter measured at end of 30.0-m cable; Unbalanced
Water Temp: 30° C
Depth: 3.9-m (38 kPa)
Drive Voltage: 500 vrms

79 kV/m (2 V/m:1)

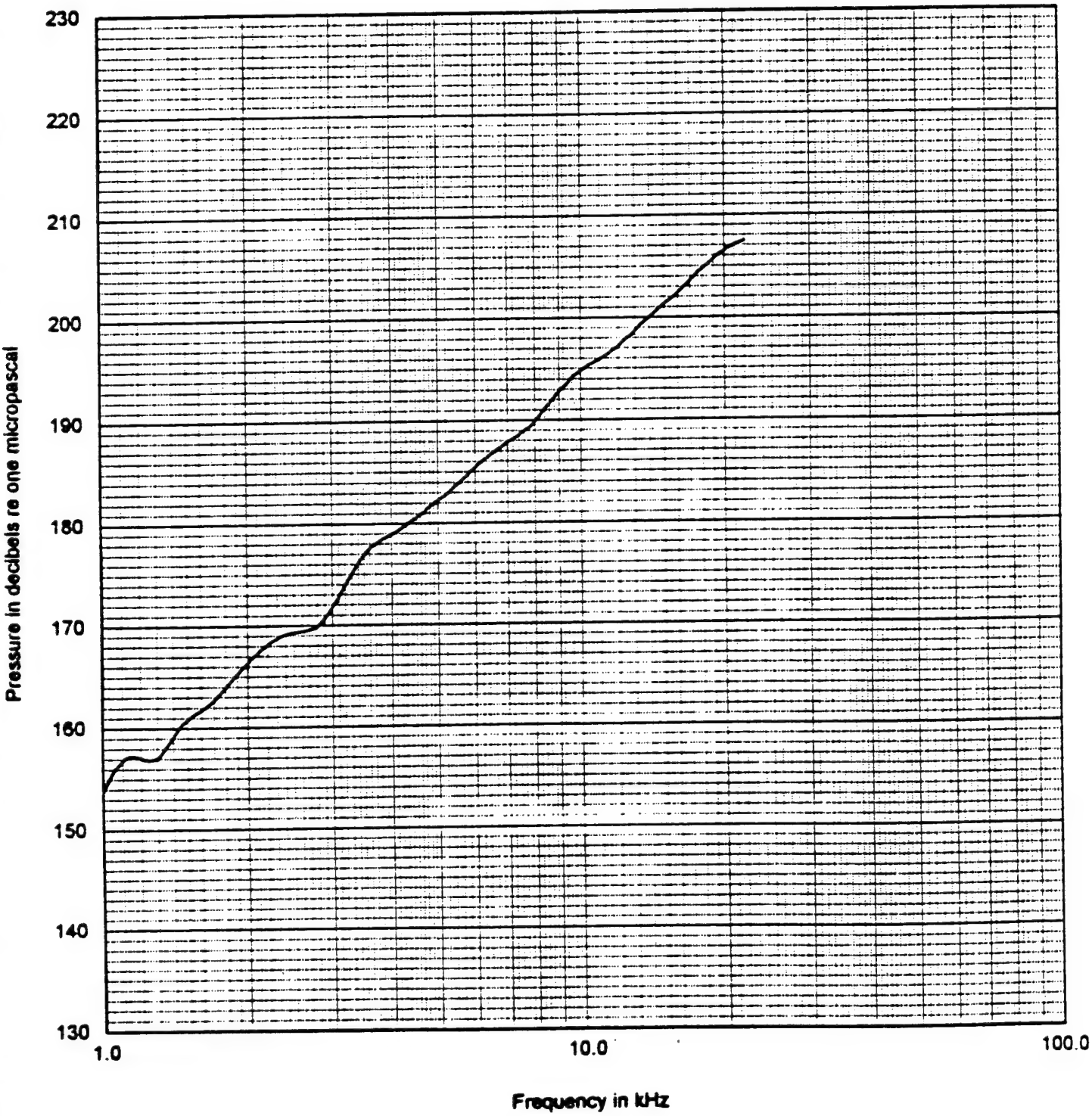

Naval Research Laboratory
Underwater Sound Reference Detachment
P.O. Box 568337, Orlando, Florida 32856-8337

USRD No. 0406
Lake Facility
AUG 1994

SOUND PRESSURE LEVEL

25.4-cm X 25.4-cm X 1.3-cm Panel 10-43
dB re 1uPa at one meter measured at end of 30.0-m cable; Unbalanced
Water Temp: 30° C
Depth: 3.9-m (38 kPa)
Drive Voltage: 700 vrms

70 kV/m (2.8 V/mil)

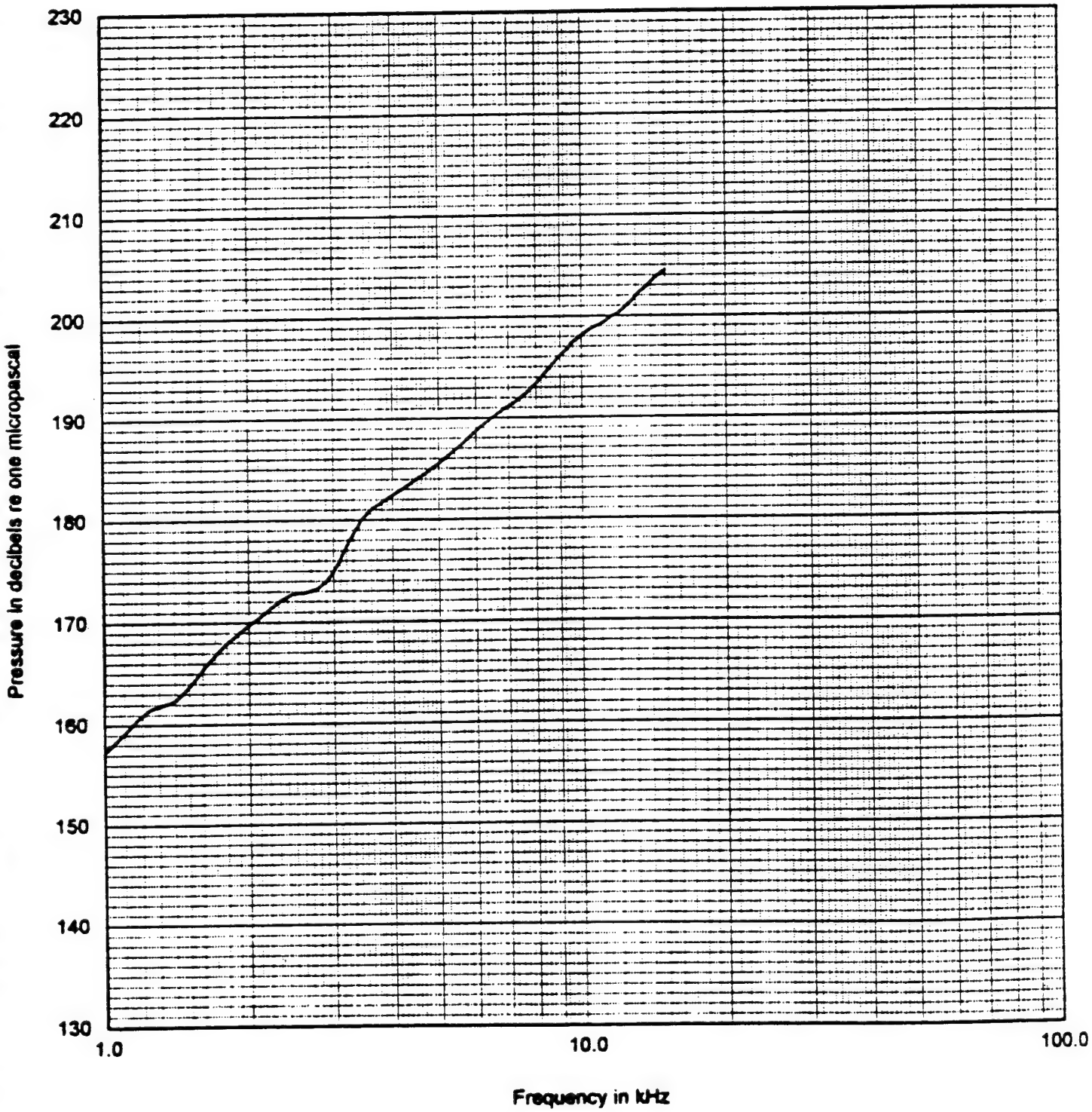

Naval Research Laboratory
Underwater Sound Reference Detachment
P.O. Box 568337, Orlando, Florida 32856-8337

USRD No. 0406
Lake Facility
AUG 1994

SOUND PRESSURE LEVEL

25.4-cm X 25.4-cm X 1.3-cm Panel 10-43
dB re 1uPa at one meter measured at end of 30.0-m cable; Unbalanced
Water Temp: 30° C
Depth: 3.9-m (38 kPa)
Drive Voltage: 900 vrms

142 kV/m (3.6 V/mil)

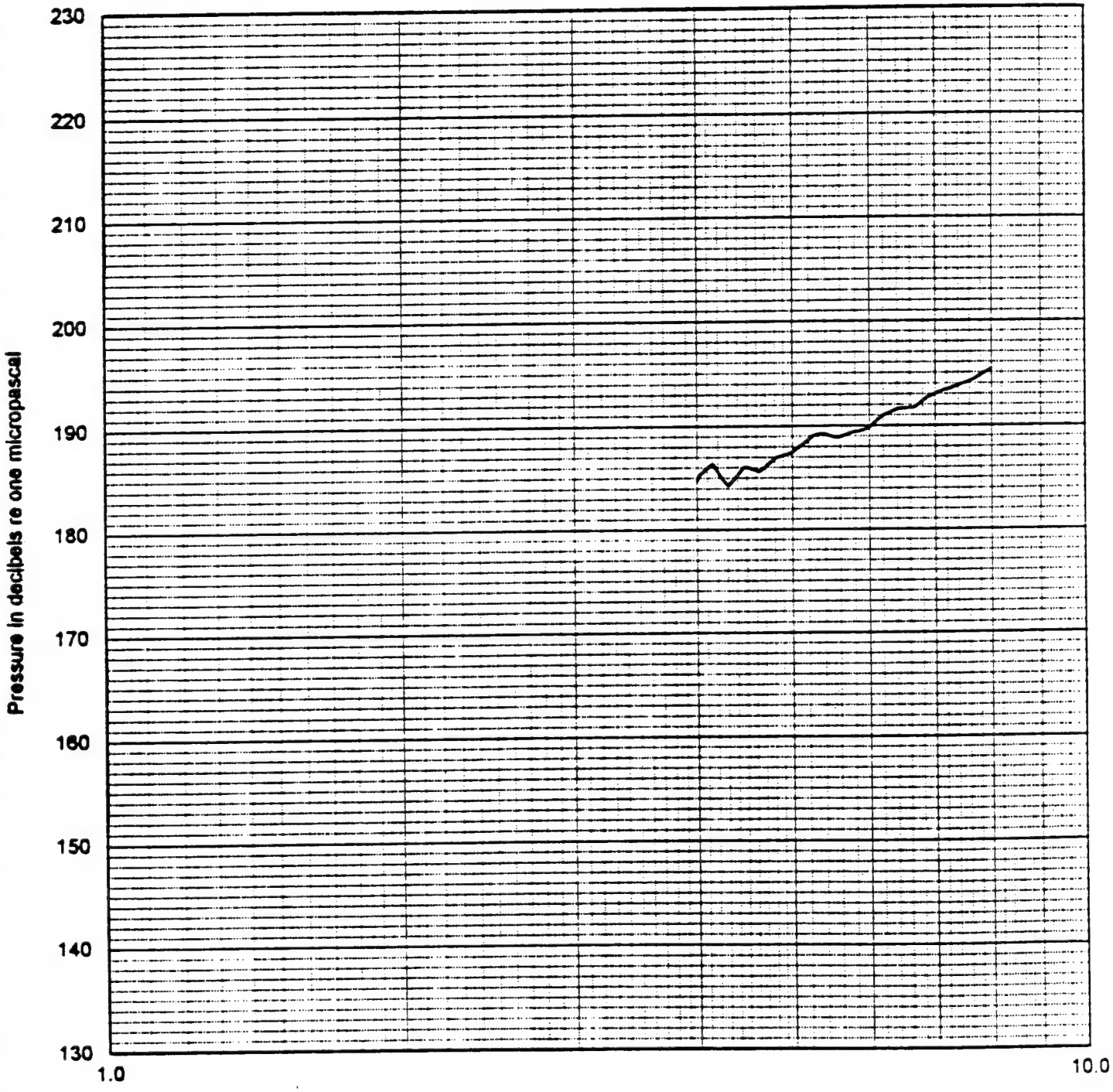

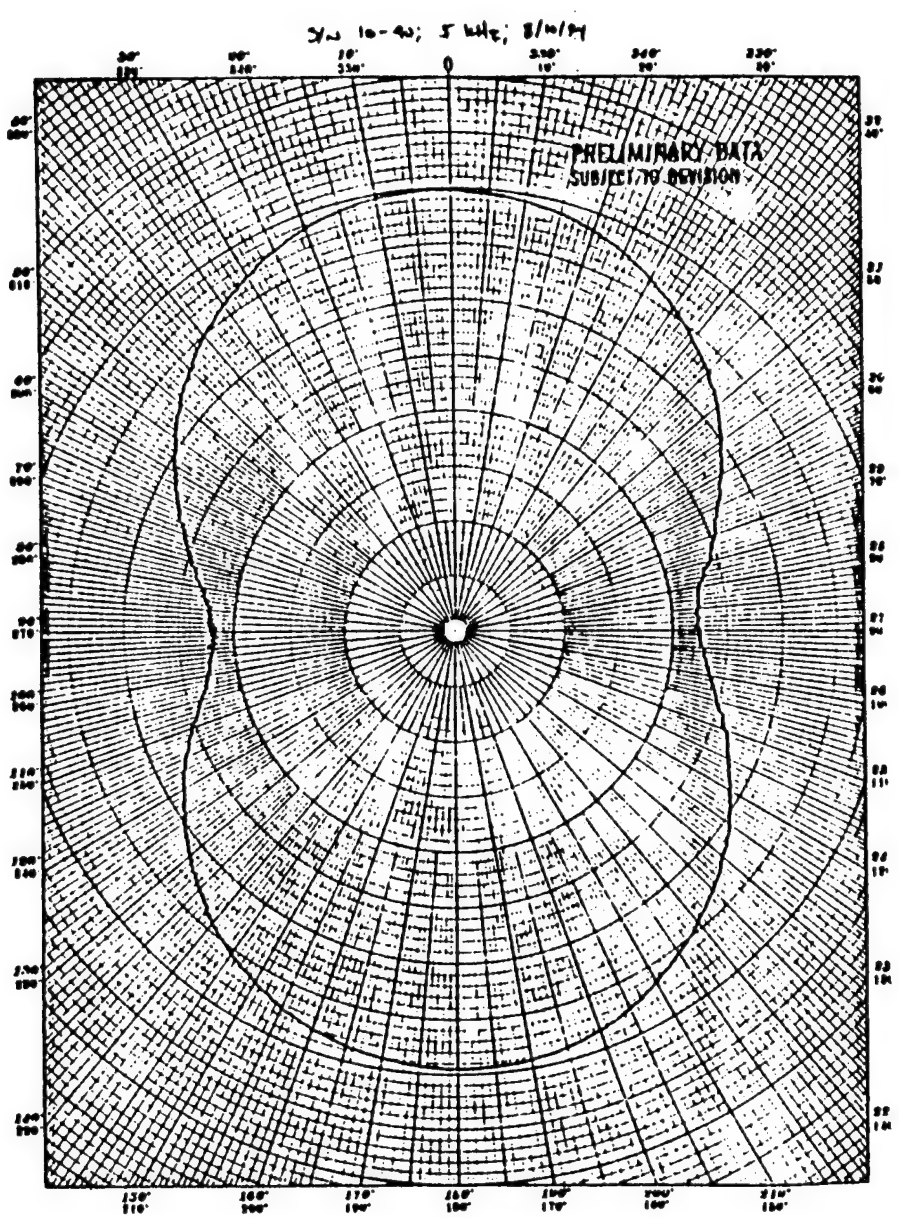
PRELIMINARY DATA
SUBJECT TO REVISION

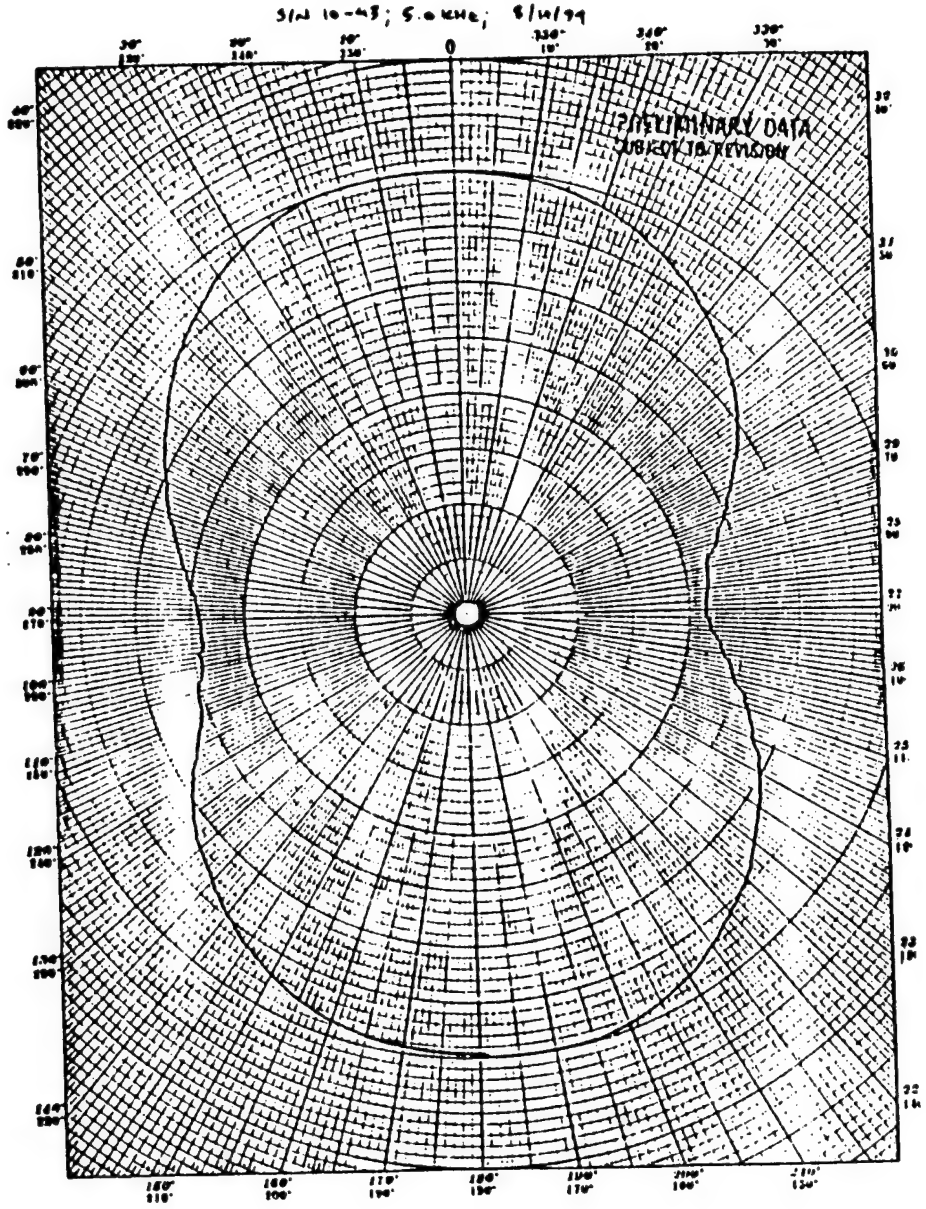
PRELIMINARY DATA
SUBJECT TO REVISION

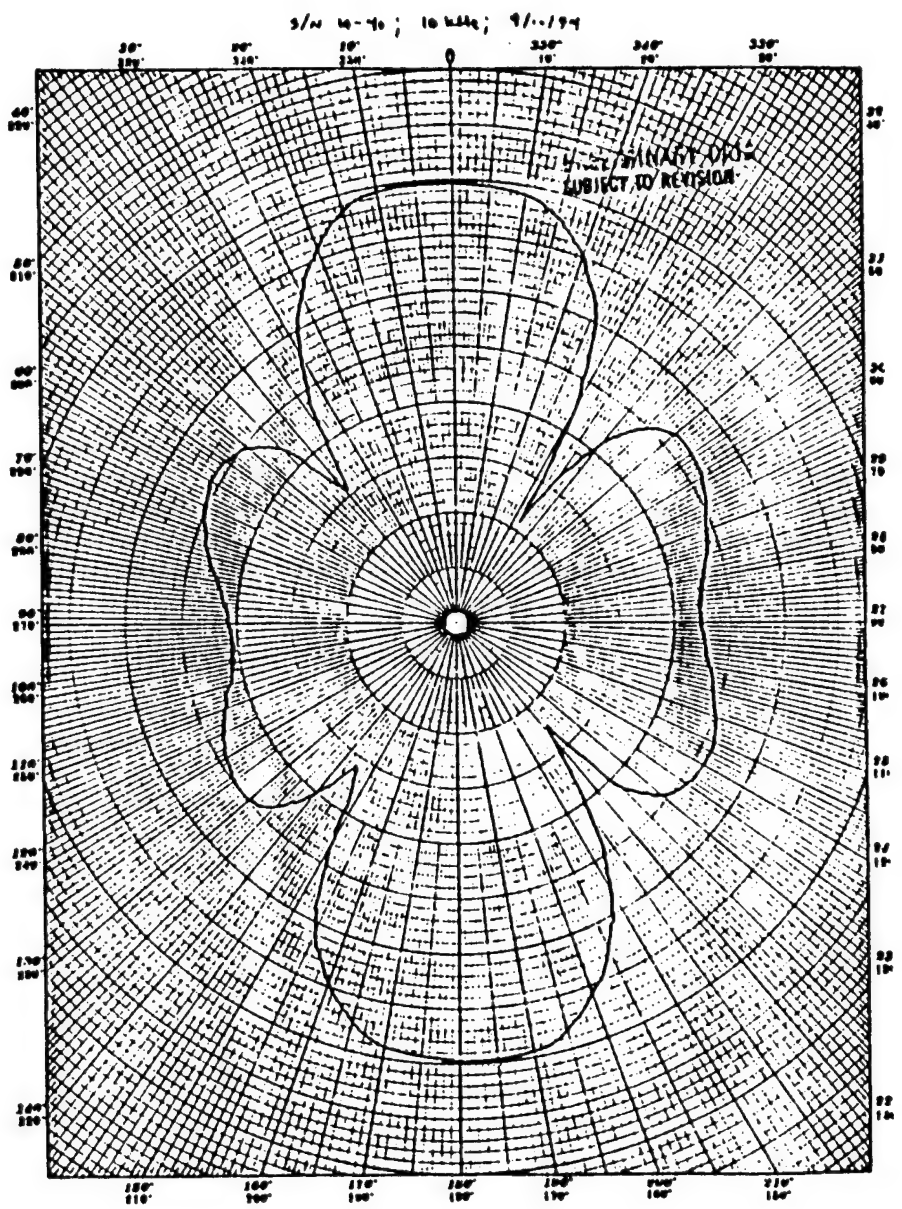
PRELIMINARY DATA
SUBJECT TO REVISION

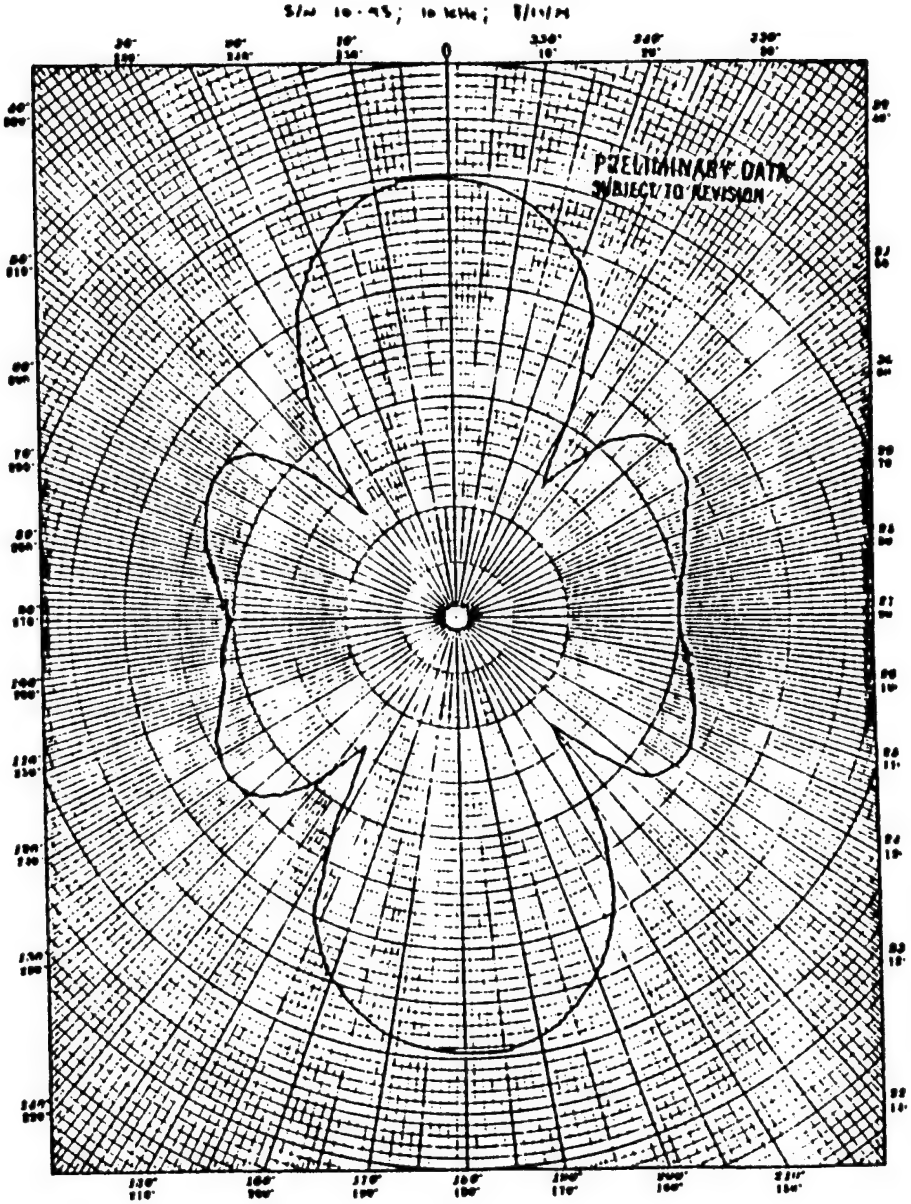
PRELIMINARY DATA
SUBJECT TO REVISION

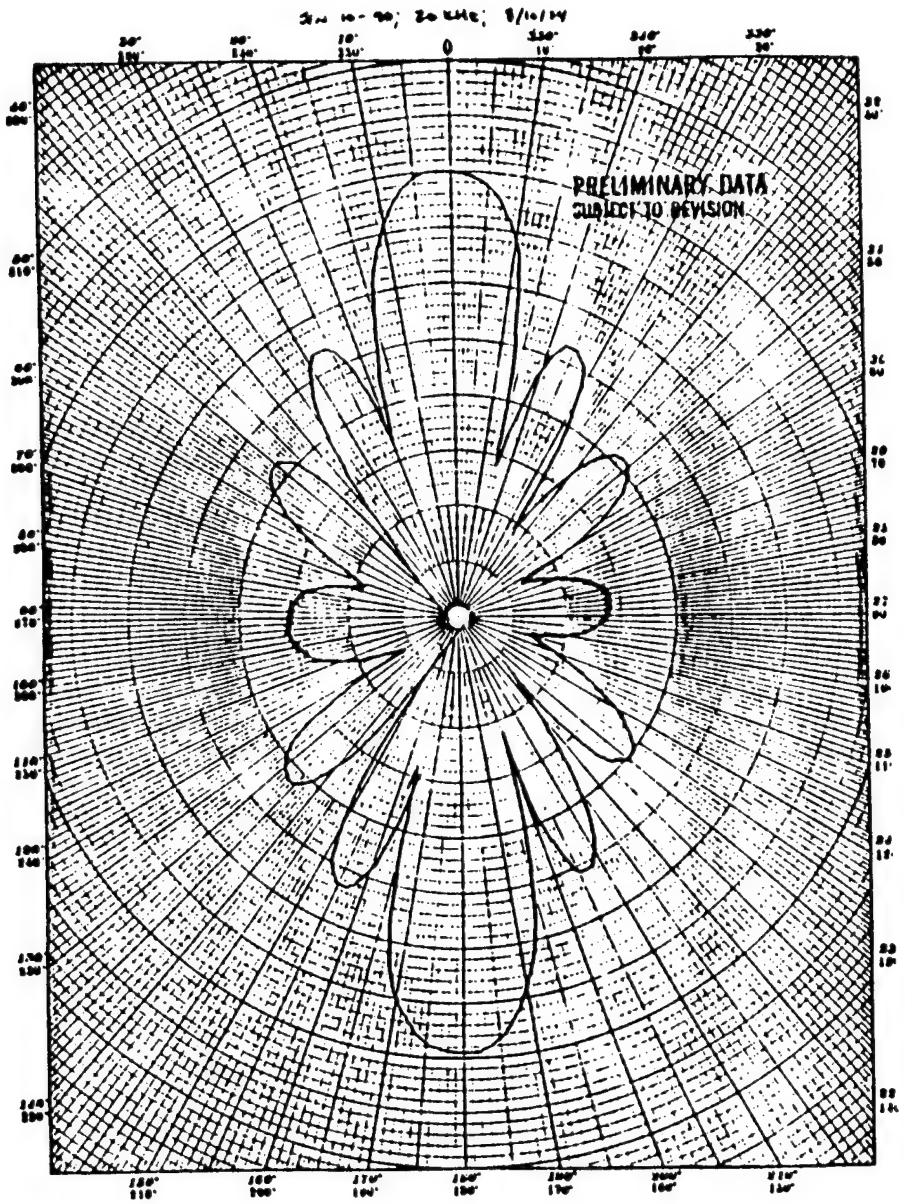
PRELIMINARY DATA
SUBJECT TO REVISION

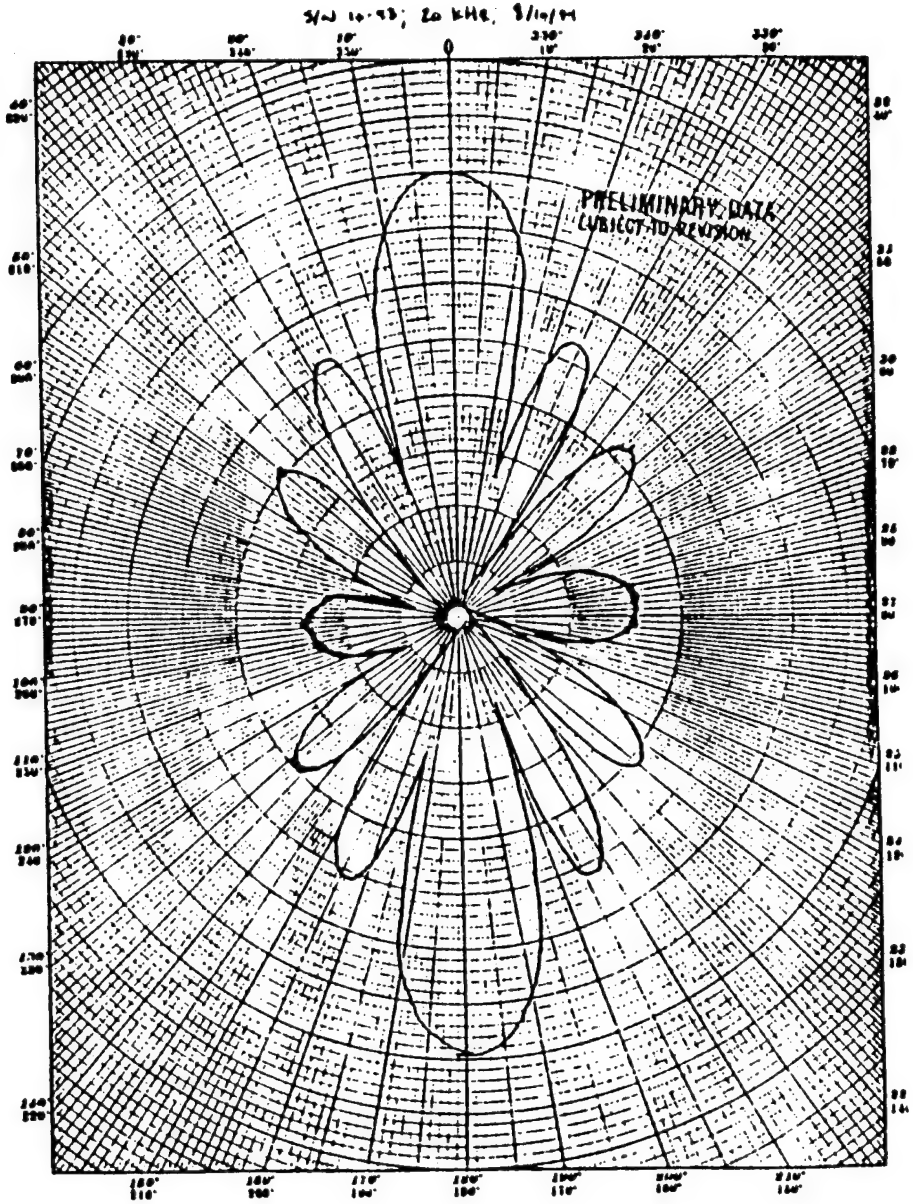
PRELIMINARY DATA
SUBJECT TO REVISION

S/N 10-40; 50 kHz; 8/10/94

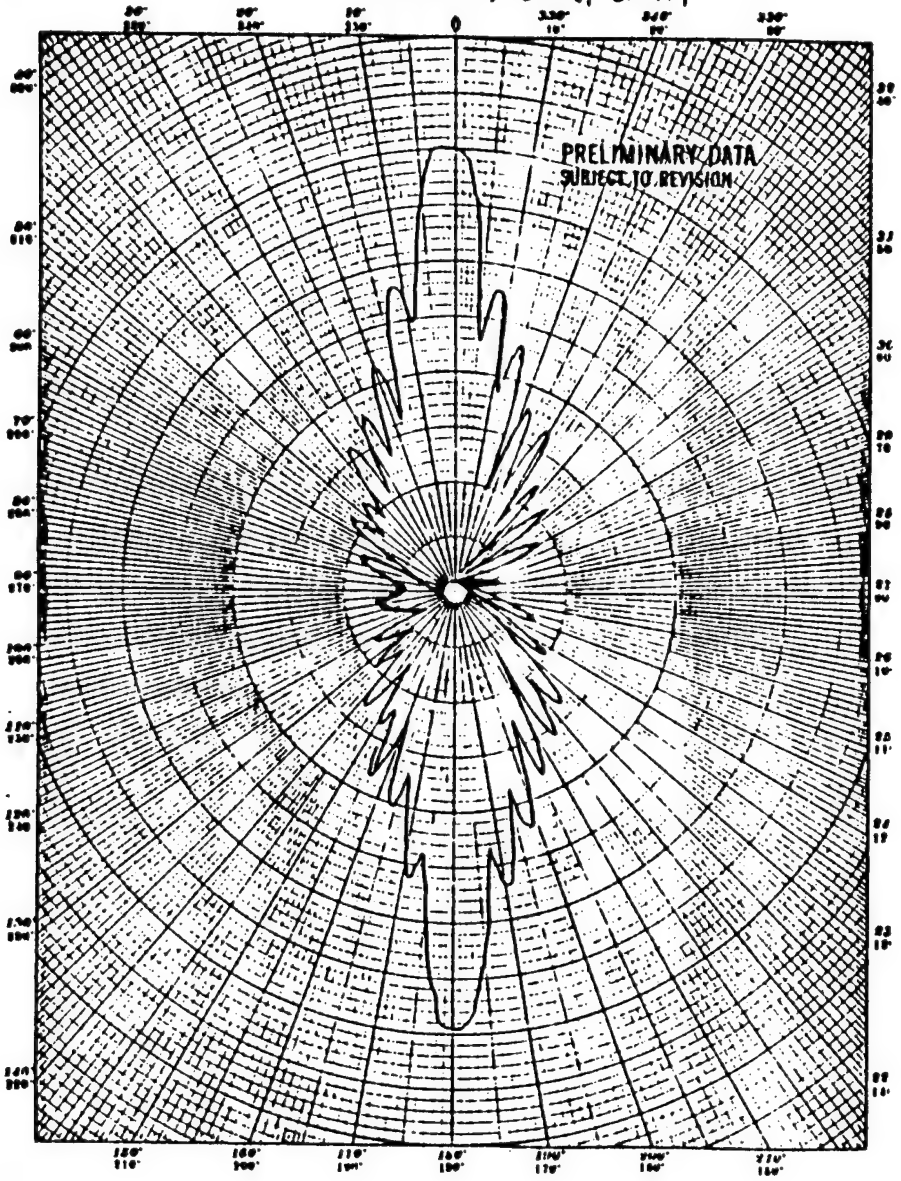

S/N 10-45; 50 kHz; 08/10/94

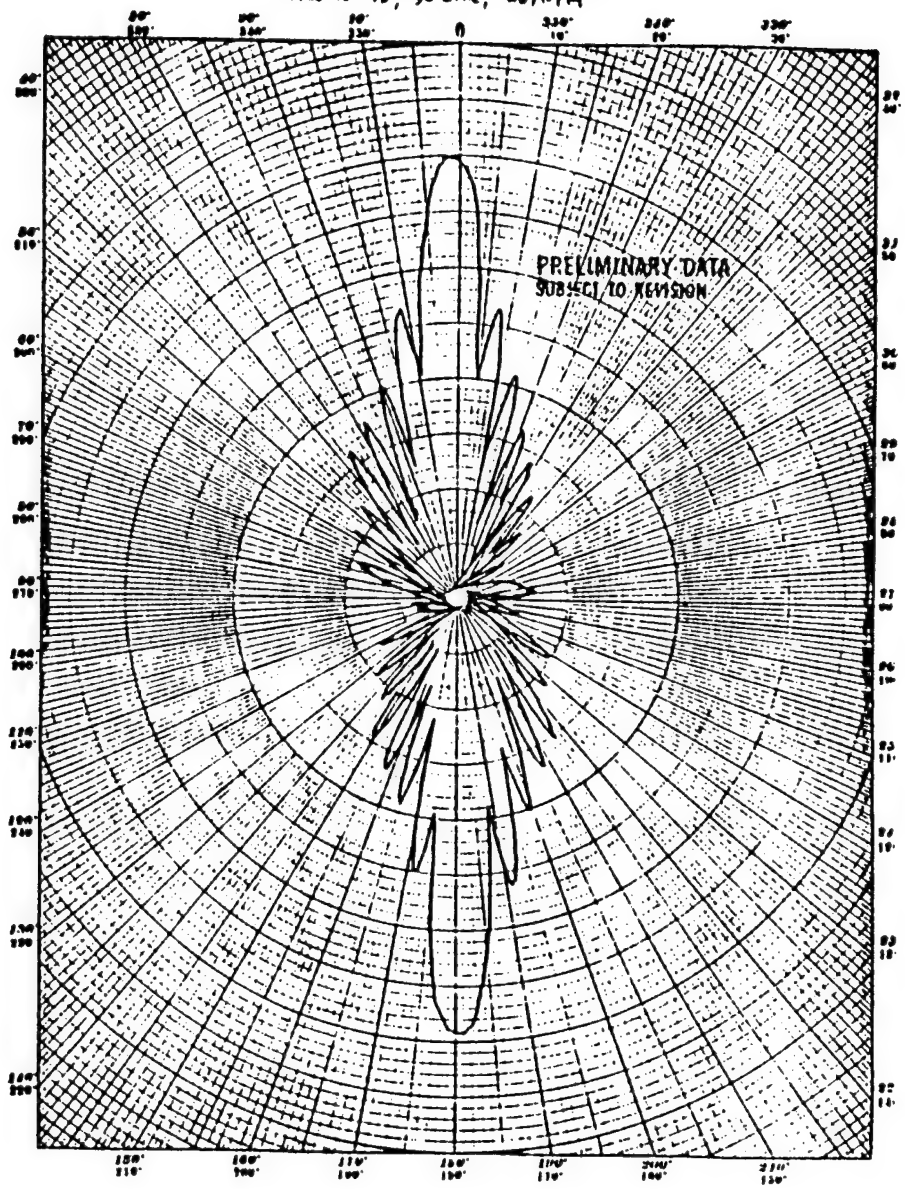

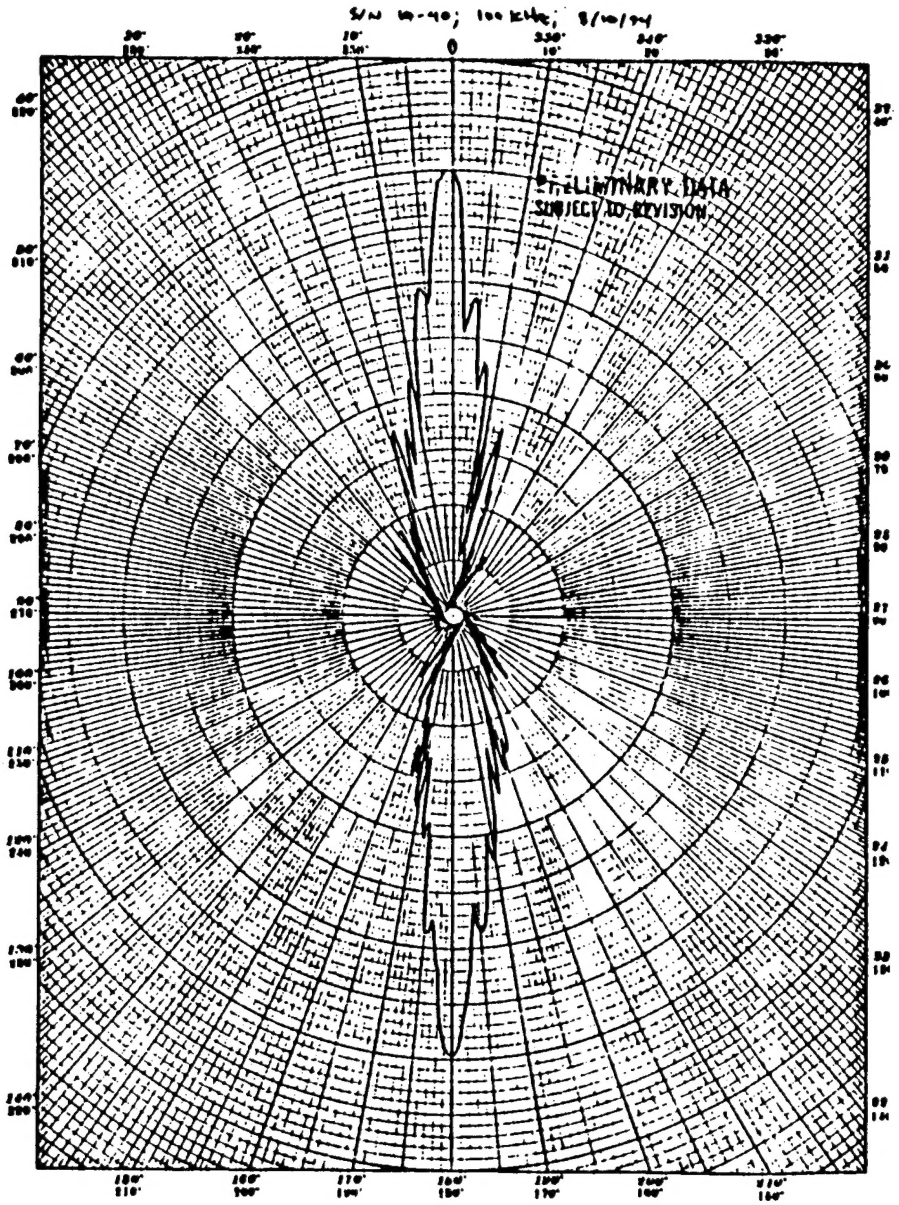
PRELIMINARY DATA
SUBJECT TO REVISION

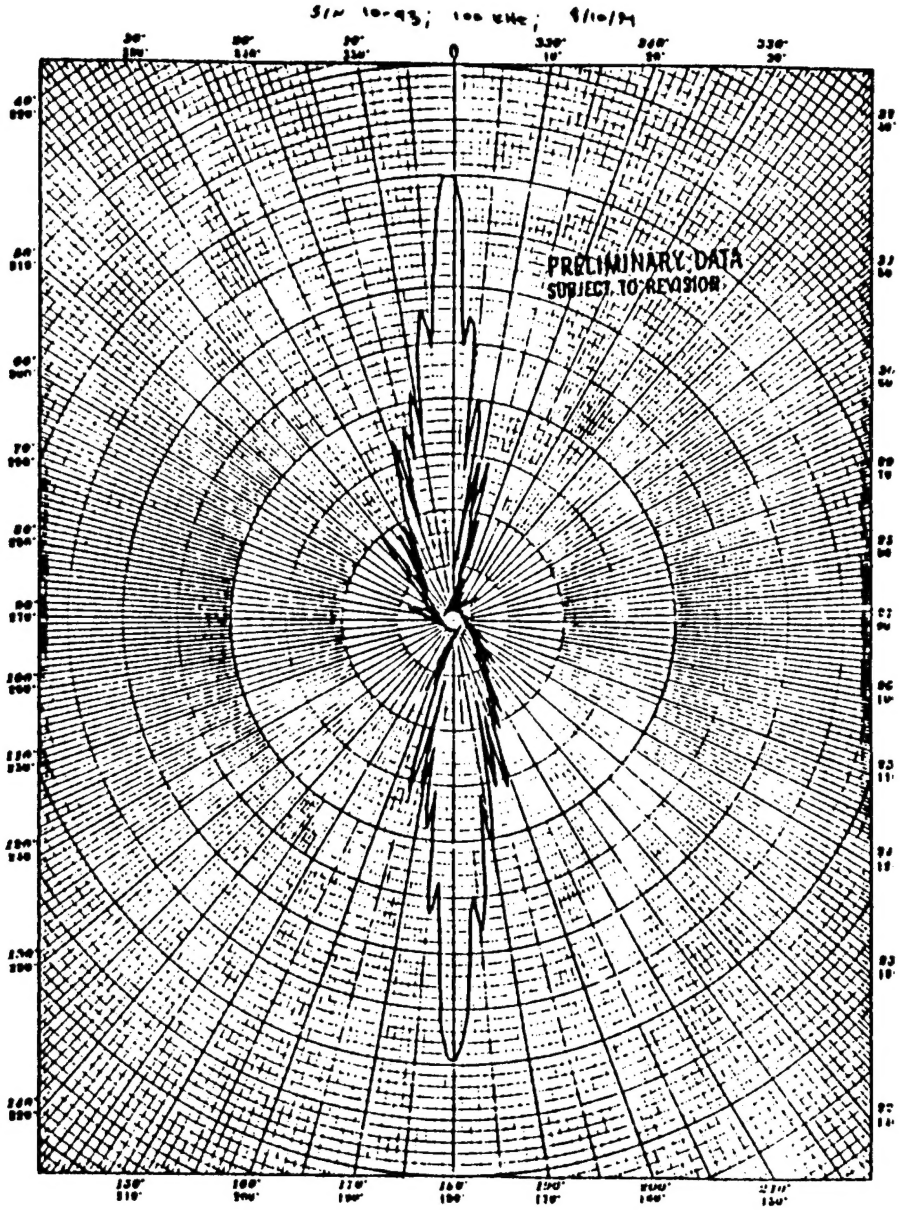
PRELIMINARY DATA
SUBJECT TO REVISION

S/N 20-43; 200 KHz; 20 AUG 94

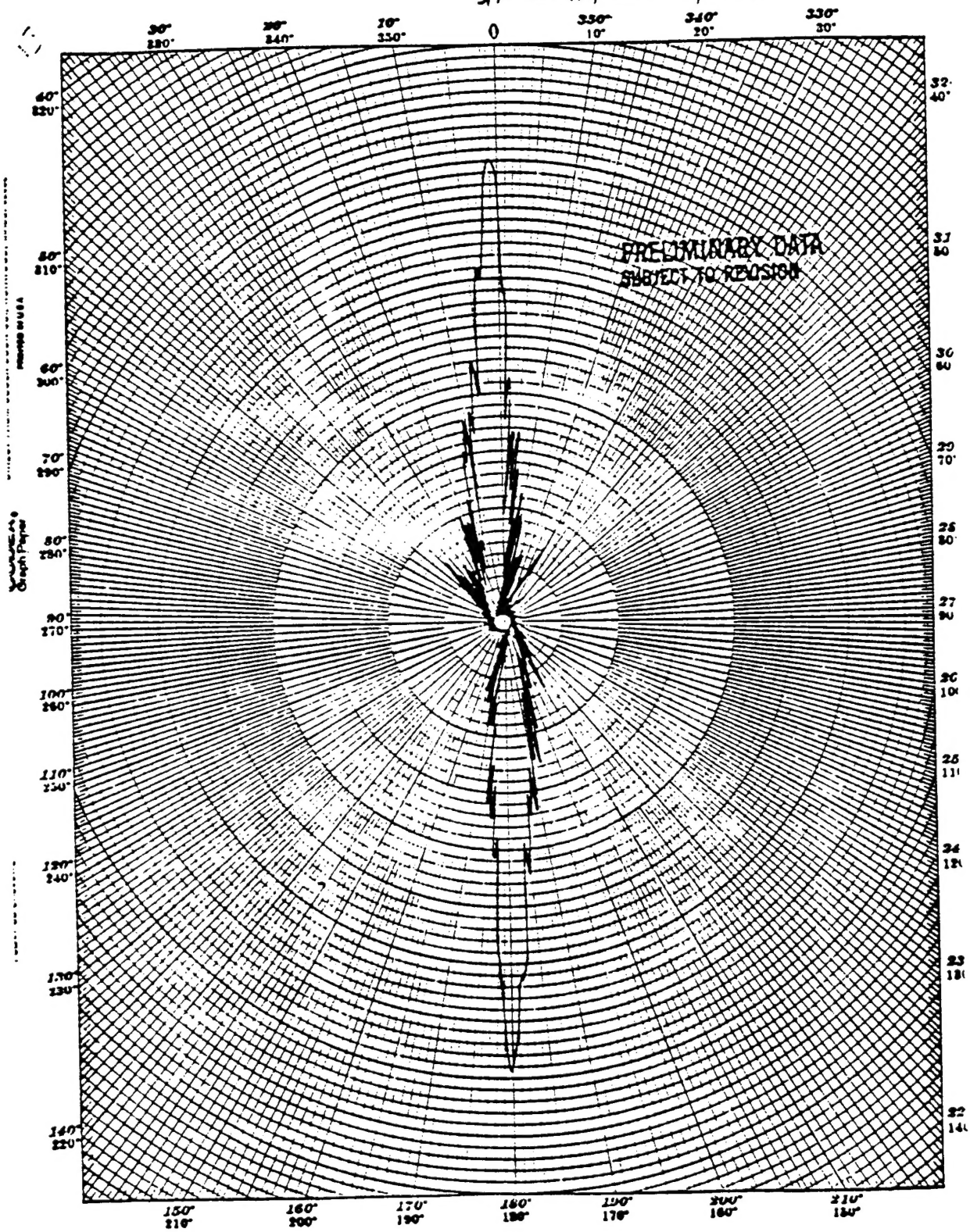

Naval Research Laboratory
Underwater Sound Reference Detachment
P.O. Box 568337, Orlando, Florida 32856-8337

USRD No. 0406
Anechoic Tank Facility
AUG 1994

FREE-FIELD VOLTAGE SENSITIVITY

25.4-cm X 25.4-cm X 1.3-cm Panel Serial 10-40
Open-circuit voltage measured at end of 16.0-m cable; Unbalanced
Water Temp: 4 ° C

——————— 16 kPa (1.6-m)
- - - - - - - - - - - - - - - - 689 kPa (70.3-m)
——————— 3450 kPa (351.2-m)
——————— 6890 kPa (702.6-m)
---------- 16 kPa (1.6-m) After Pressure

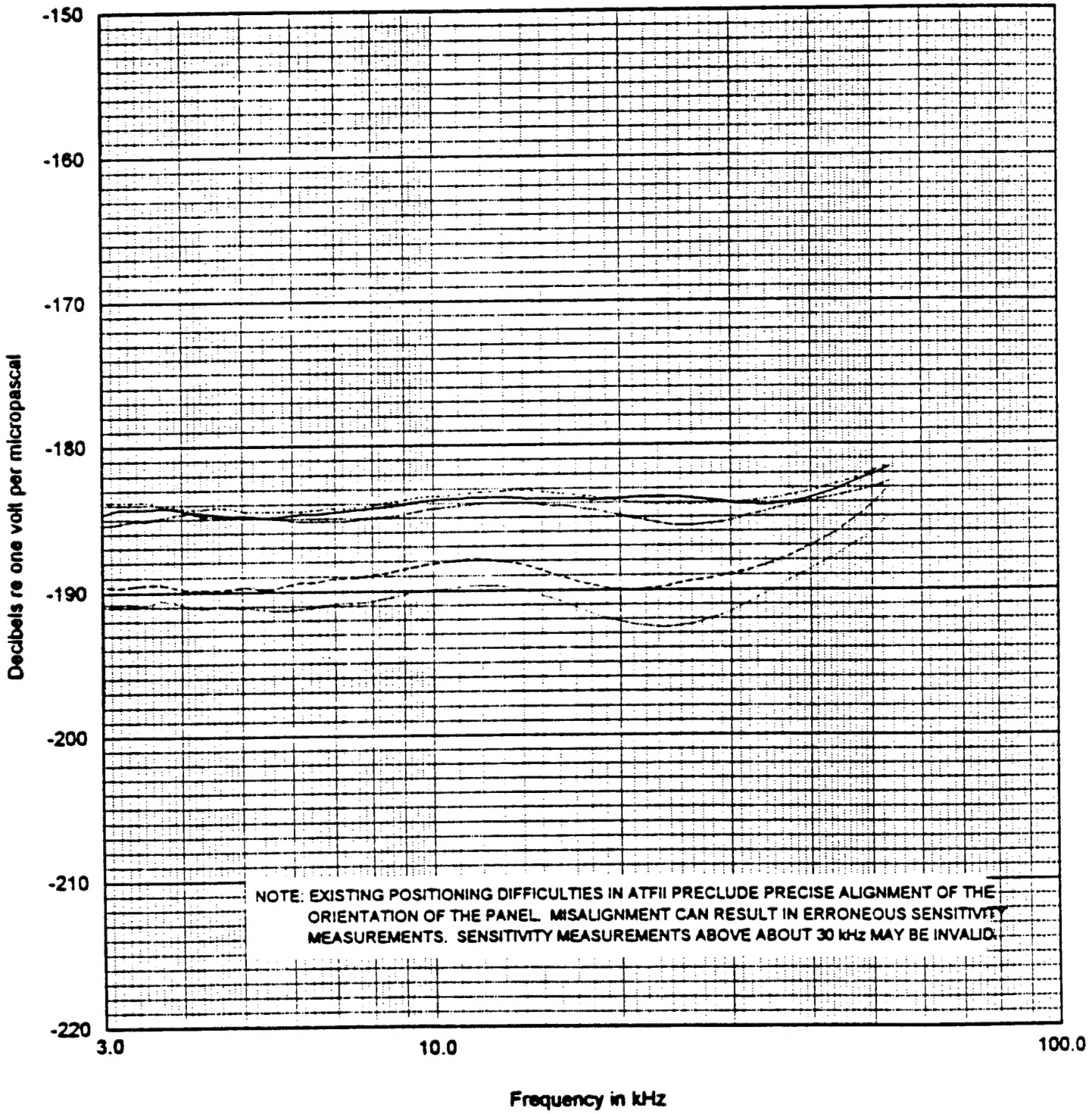

Naval Research Laboratory
Underwater Sound Reference Detachment
P.O. Box 568337, Orlando, Florida 32856-8337

USRD No. 0406
Anechoic Tank Facility
AUG 1994

FREE-FIELD VOLTAGE SENSITIVITY

25.4-cm X 25.4-cm X 1.3-cm Panel Serial 10-40
Open-circuit voltage measured at end of 16.0-m cable; Unbalanced
Water Temp: 22° C

- 16 kPa (1.6-m)
- 689 kPa (70.3-m)
- 3450 kPa (351.2-m)
- 6890 kPa (702.6-m)
- 16 kPa (1.6-m) After Pressure